5-2017

Development of a Tissue Engineered Mitral Valve

Christopher Patrick deBorde
Clemson University, cdebord@g.clemson.edu

DEVELOPMENT OF A TISSUE ENGINEERED MITRAL VALVE

A Dissertation
Presented to
the Graduate School of
Clemson University

In Partial Fulfillment
of the Requirements for the Degree
Doctor of Philosophy
Bioengineering

---

by
Christopher Patrick deBorde
May 2017

Accepted by:
Dr. Agneta Simionescu, Committee Chair
Dr. Dan Simionescu
Dr. Naren Vyavahare
Dr. Christopher Wright

ABSTRACT

Heart valve diseases affect nearly 8 million people every year in the United States. Of these patients, 72% are affected by mitral valve diseases. Stenosis, regurgitation, and prolapse of the mitral valve are the primary pathologies affecting valve function resulting in atrial fibrillation, arterial thromboembolism, pulmonary edema, pulmonary hypertension, cardiac hypertrophy and heart failure. Surgical options to repair or replace the mitral valve are only palliative, especially for children with congenital defects, and do not exclude the need for reoperation. A tissue-engineered option is feasible and holds great potential through the combination of decellularized scaffolds, patient stem cells, and heart valve bioreactors. Development of living tissue engineered mitral valves have not been reported in the recent literature. The primary focus of my research was threefold: 1) develop an acellular ECM scaffold which is mechanically robust, and allows for sufficient bioactivity for cellular seeding and signaling by use of a non-toxic matrix-binding polyphenolic antioxidant, pentagalloyl glucose (PGG); 2) confirm this scaffold to be biologically compatible with future hosts and limiting inflammatory responses in vivo by virtue of PGG's antioxidant properties; 3) achieve recellularization of the mitral valve scaffold and direct differentiation and maturation through bioreactor preconditioning.

First, a complete decellularization of porcine mitral valves was established and optimized to remove all cellular and nuclear material from the scaffolds while still preserving ECM components and basal lamina proteins. Treatment with PGG recovered lost mechanical integrity due to the decellularization process. Seeded cells were able to grow and proliferate on and in the acellular scaffold confirming cytocompatibility.

An in vivo rat study was conducted to evaluate the scaffolds' biocompatibility. In comparing non-treated and PGG-treated groups, PGG –treatment regularly and significantly showed increased resistance to degradation, polarization of macrophages to the pro-healing M2 phenotype, discouragement of inflammatory markers, and no limitations towards cell infiltration.

Lastly, PGG-treated acellular scaffolds were recellularized with pre-differentiated fibroblasts and endothelial cells and placed in a newly developed mitral valve bioreactor. Design of the bioreactor required a full understanding and appreciation for the four tissue types present in the mitral apparatus. Preconditioning of the seeded constructs yielded a mitral construct similar to a native valve.

The overarching goal of this research was to develop a stable mitral valve construct. It is expected that the progress made by this project will have a positive impact on those that suffer from mitral valve pathologies. Our translatable approach towards this tissue engineered mitral valve should allow clinicians to readily adopt this regenerative replacement and contribute as a whole to the field of cardiovascular tissue engineering.

DEDICATION

This dissertation is dedicated to my family and friends who supported me, without whom I would not be where I am today. To my family, those with us and those who have passed, you are my rock, my foundation, my inspiration, and words cannot describe how much your support, love, and encouragement have driven me forward and molded me into the person I am today. To my friends, please know that I would not have made it through this process without you. Your support has not gone unnoticed and I greatly appreciate the times we spent both in and out of the lab. You all have instilled in me a drive for excellence, you have shaped my character for the better, and established a level of effort I will always strive to achieve.

I will carry these lessons with me forever, as you have all carried me, through this amazing chapter of my life. Thank you.

ACKNOWLEDGMENTS

I must first acknowledge and give great thanks to my advisor and mentor, Dr. Agneta Simionescu. Your mentorship not only as a scientific advisor but also as an individual has sincerely shaped me for the better. Your drive, passion, and your care for your students led me to commit to this PhD. Your passion and continued amazement at the miracles of science have been an inspiration to me and to others in the lab. Similarly, thank you Dr. Dan Simionescu for your continued support. You have helped me to establish a bar of excellence that I will always strive to achieve. Thank you for your mentorship and continued support of my research.

I also must thank my other committee members Dr. Christopher Wright and Dr. Naren Vyavahare. I cannot tell you how much your advice and suggestions shaped this project and shaped me as a researcher. You were able to think outside of the box when I could not see solutions. Without the time you sacrificed to contribute to and support this project, I would not have made the strides I made over the last 5 years.

It is also important that I acknowledge Aptus Bioreactors for their design support for the mitral valve bioreactor system. Without their knowledge and expertise for creating custom bioreactors, this process would have been much more difficult. Thank you for your consultation and support throughout this process.

Last but certainly not least, I have to thank those that spent so many hours with me in and out of the lab. Thank you to my fellow BTRL and CTERM graduate student past and present. To Lee Sierad, James Chow, Jason Schulte, Mike Jaeggli, George Fercana, Allison Kennamer, Tasha Topoluk, Grace Dion, Anna Lu Carter, Laura McCallum, Megan

Casco, Jhilmil Duhlekar, Eric Wright, Harrison Smallwood, Clayton Compton, Margarita Portilla, Spencer March, Nick Rierson, Brady Culbreth, Chris Ferreira, Jessica Canavan, Elizabeth Fontaine, Harleigh Warner, and Sarah Stafford, I cannot thank you enough. Each of you in some way greatly affected my experience as a student and taught me so much.

Thank you to Snow Creek Meat Processing for their generosity as well as Godley-Snell Research Center for their hard work on our animal studies. There are so many others in the Bioengineering department that had an enormous impact on my research and success out of the lab – it was a privilege to work with you, learn from you, and to be friends with you. I would also like to acknowledge Dr. Agneta Simionescu's funding sources NIH and COBRE.

TABLE OF CONTENTS

Page

Table of Contents (Continued) Page

Table of Contents (Continued) Page

LIST OF TABLES

Page

LIST OF FIGURES

Page

List of Figures (Continued) Page

List of Figures (Continued) Page

CHAPTER ONE: REVIEW OF LITERATURE

1.1 Anatomy of the Mitral Valve:

1.1.1 Introduction:

The mitral valve, named so due to its likeness to that of a Bishop's miter, is an intricate atrioventricular valve located on the left side of the heart. The mitral valve prevents backflow from the left atrium to the ventricle during systole. Housing a complicated anatomy, the mitral valve is built from four different tissue groups each performing different functions for this valvular apparatus. In its open state, the valve resembles a funnel extending from the hinge line at the atrioventricular junction and the ends of its two leaflets. Proper function of the valve not only requires normally functioning leaflets but also their coordinated interaction with the annulus, chordae tendinae, and the papillary muscles. Due to its placement within the heart, the effectiveness and function of the mitral valve is closely tied to its surrounding environment, namely the aortic valve and the left ventricular wall. Integrity of the valve is critical for the maintenance of normal left ventricle size and function.

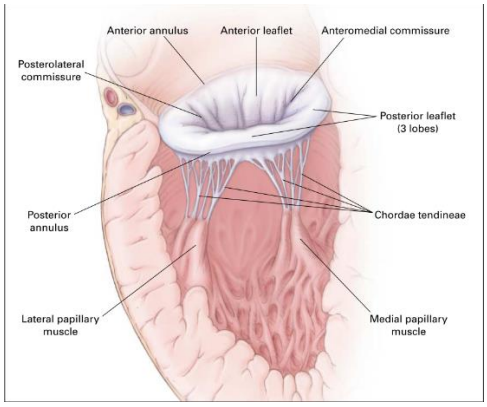

Figure 1.1: Anatomy of the mitral valve including its four major components, the mitral annulus, leaflets, chordae tendinae, and papillary muscles.[1]

1.1.2 Mitral Annulus:

The foundation for proper mitral valve shape and function is established by the annulus, a thin, nonconductive, fibro-fatty transition region from the myocardia of the atrium (posteriorly) and fibrous aortic annulus (anteriorly) to the valve leaflets[2]. The term annulus implies a solid ring-like fibrous cord to which the leaflets are attached; however, this is not the case. The mitral annular region is indistinct since the fibrous continuity is an extensive sheet[3]. Some in literature distinguish the annulus as a tissue plane at the confluence of adjacent structures as opposed to a separate anatomical entity[4]. The annulus, like the leaflets, is split into two regions, the anterior and posterior annulus. Each of these portions is different in size and purpose. The anterior annulus, which constitutes one-third of the annular surface area, is anatomically coupled with the aortic annulus and is flanked by the left and right trigones[2,4]. This connection with the aortic annulus is termed the aorto-mitral curtain or intervalvular fibrosa[2]. This attachment elevates this portion of the annulus as the aortic-mitral continuity comes up to meet the lower edges of the left and non-coronary sinuses and the interleaflet fibrous triangle[5]. The posterior leaflet comprises the other two-thirds of the annular area and is externally related to the musculature of the left ventricle inflow region and internally to the left atrium where it merges with the leaflet[2]. This area tends to be "weaker" due the lack of a formed fibrous cord[3].

The geometric shape of the annulus approximates to that of a hyperbolic paraboloid[2,4,6–8]. More simply, this shape resembles a saddle with peaks("riding horns") located anteriorly and posteriorly and valleys located medially and laterally at the commissures[9]. Computational modeling has shown that as annular height (measured at

the peaks) increases relative to width of the valve (at the commissures), peak leaflet stress decreases, becoming maximally attenuated once this height to width ratio exceeds 0.2[4,6,7,10,11]. A higher ratio implies that the annulus is more saddle-shaped, while a lower ratio infers a flatter annulus. Although this nonplanar shape's origins are not fully described in literature, it is understood that this shape is the determinant of optimal force distribution in the leaflets and chordae tendinae[4,8,12]. Changes in annular shape and dynamics have been observed in patients with functional mitral regurgitation, acute ischemic mitral regurgitation, and different types of cardiomyopathies[8]. Therefore, when anatomically correct, the annulus provides an optimal foundation for the remaining components of the valve.

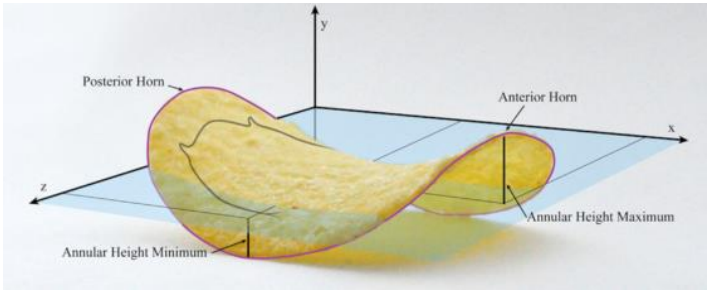

Figure 1.2: The hyperbolic paraboloid shape of the mitral annulus. [13]

Movement of the annulus is heavily influenced by its surrounding environment during atrial and ventricular filling and emptying. The mitral valve however is not entirely passive in its movement, as it contains smooth muscle cells and nerve fibers[14,15]. The atrioventricular conduction bundle passes through the right fibrous trigone[3]. This well-defined network of nerve fibers work to contract the valve tissue. Three types of motion have been described for the annulus, translation between the left ventricular apex, sphincteric contraction, and folding across the intercommissural axis[4]. During diastole,

the annulus acts as a conduit for blood flowing from the left atria into the left ventricle. During this period, when the left atrium is progressively relaxing, the annular area is allowed to increase where it reaches its maximum annular area at the end of diastole. Also during this time, area is increased by movement of the anterior horn towards the aortic annulus. When systole begins, the mitral valve begins to contract and it reaches its narrowest during mid-systole. During this moment, the posterior horn shifts apically, where the anterior horn shifts towards the left atrium. The narrowing of the annulus allows for curvature of the leaflets and therefore optimal coaptation. Note that the annulus is smallest during mid-systole, while contraction of the heart continues, annular circumference progressively increases to allow unobstructed flow from the atria to the ventricle during diastole[13]. Sphincter-like contraction is also key to leaflet coaptation. Contraction of the annulus draws the free margins of the leaflets together in anticipation of the sharp rise in pressure during systole. The annular circumference decreases by 25% during diastole reaching its smallest at the very beginning of systole (end of diastole)[2,13]. Folding of the annulus also occurs during ventricular systole. This conformation promotes normal function without wrinkling or distorting the leaflets. This folding action blunts the rise in leaflet closing stresses during the rise in pressure during left ventricular systole[4].

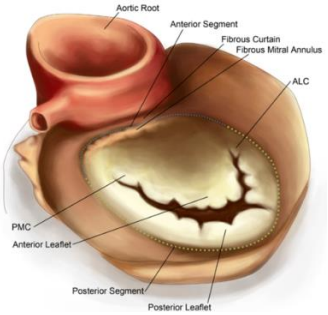

Figure 1.3: Anatomy of the mitral valve leaflets. [13]

1.1.3 Mitral Leaflet:

Similar to the annulus, the mitral valve leaflets are also divided into anterior and posterior positions. Due to the oblique location of the valve, strictly speaking the two leaflets do not technically reside in anterior or posterior positions, therefore these leaflets are also termed "aortic" due to its proximity to the aorta, and "mural" due to its attachment to the ventricular wall[3]. The two leaflets are actually a single continuous structure that become confluent at the commissures[2]. However, each designated leaflet is unique in shape, size, and composition. The anterior, or aortic leaflet, transitioning from the anterior annulus, is much more fibrous in nature and comprises about one third of the annular circumference. It does however make up a majority of the mitral orifice. In terms of pure surface area, the two leaflets are almost equal. The two leaflets meet to form an arc shaped closure line. The posterior, or mural leaflet, takes up a much smaller area of the valve orifice, but comprises about two thirds of the valve's circumference. It is worth noting that the posterior leaflet is often divided into three or more segments (scallops) described as lateral, middle, and medial segments[2,3]. The middle scallop is usually the largest of the three but it can vary. By having three segments, it allows the leaflets to act similarly to how pleats do on clothing, allowing the leaflet to accommodate to the shape of the curved closure[3,16].

In a healthy valve, the leaflets are usually thin, pliable and translucent. Each leaflet is exposed to both the atria and the ventricle. The ventricle side of each leaflet can be dissected into zones designated so by the insertion of tendinous cords. The anterior leaflet has two distinguishable zones, while the posterior leaflet has three zones. Both leaflets have

a clear zone, which has no chordal attachments. This zone is closer to the free margin and because this zone is at the line of closure, it is the thickest part of the valve. Each leaflet by comparison also has a rough zone, where the chordae tendinae attach to the ventricular surface of the leaflets. This zone is broadest at the lowest portions of each leaflet but tapers toward the commissures[3,14,17]. The basal zone, which is specific to the posterior leaflet, has insertions from the basal chordae to its ventricular surface. The anterior leaflet lacks this region due to the distance from the ventricular wall, and therefore lack of basal cords. Closure and function of the leaflets is obviously a product of annular movement and contraction and tension from the chordae, however the mechanics have not been fully defined. Convention holds that the pressures during ventricular systole force the leaflets closed with the chords attached on the ventricular side forbidding prolapse of the leaflets into the atrium. Atrial contraction, and the role it may play in leaflet closure has been debated[2]. Some studies have shown that contraction of the annulus just before systole facilitates closure by approximating the leaflets. The stiffness of the anterior leaflet is influenced by electrical stimulation from the neurally-rich region of aortic-mitral continuity[18]. Myocytes, which occupy a portion of the mitral leaflets are activated after contraction of the left atrium and this may position the leaflets prior to ventricular systole[3]. This provides the basis of a paradigm shift from viewing the leaflets as passive collagenous flaps and as active tissues with a more complex function.

Leaflet coaptation, while simple in function, are some of the most stressed tissues in the body, opening and closing nearly 3 billion times in a lifetime[19]. The biomechanics of the leaflets can be broken down into three loading modes: tension, shear, and flexure.

These are imposed cyclically, the valve opens (flexure), permits blood to pass (shear), closes (flexure), and prevents the reverse flow of blood (tension)[19]. Pressure across the valve (transvalvular pressure) ranges from 100-200 mmHg, usually averaging about 120 mmHg[19,20]. Valves on the left side of the heart experience pressures 5-8 times as large as those on the right[19]. Left side heart valves are about 2 times thicker because of this[19]. These pressures are largely felt during systole on the ventricular side of the valve. Atrial pressures are much lower on average, about 10mmHg for the left atrium. Mechanical data on leaflets, especially in vivo, is especially difficult. Therefore, most studies on valvular mechanics are estimated using some form of computer modeling. For mitral valve leaflets, biaxial testing is used frequently since they are thin and nearly incompressible. Radial and circumferential strains and stresses are applied during these studies. Due to the microstructural makeup of the leaflets and the direction the collagen fibers are aligned, the leaflets act anisotropically, yielding stiffer (lower strain rate) results in the circumferential direction. In fact, in vivo strains of 10.1 and 30.8% in the circumferential and radial directions respectively have been reported[21]. This is because the collagen fibers are aligned in the circumferential direction in the leaflets. Collagen is known to withstand high tensile forces but have low torsional and flexural stiffness[21]. Shear experienced by the valve is determined by the flow rate of blood passing through them. It has been shown that blood flow across the mitral valve is about 5610±620 mL/min[22]. The leaflets are also capable of large deformations, ranging from 10-60% before reaching physiological stress levels[20].

1.1.4 Chordae Tendinae:

The pressures experienced during ventricular systole are too great for the leaflets alone to successfully disallow regurgitant flow back up into the atrium. Tendinous cords descend on the ventricular side of the leaflets and attach to the papillary muscles where they transmit the force necessary to keep the valve closed during systole. In order to perform such functions and endure such pressures, the chordae tendinae must contain a high degree of strength and elasticity. The chordae are largely composed of parallel fibers of collagen and elastin with an outer layer of endothelial cells[23]. This arrangement allows for an efficient transfer of the contraction forces from the papillary muscles to the leaflets.

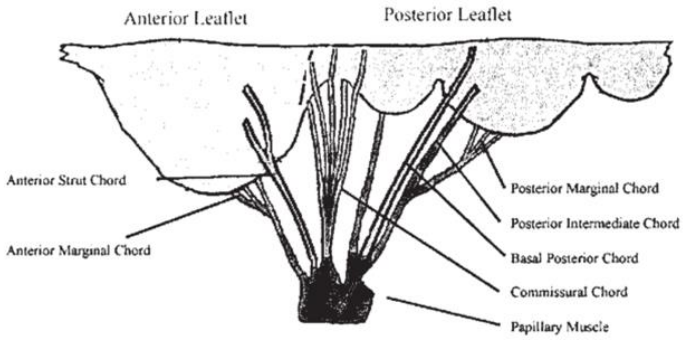

Figure 1.4: Chordae tendinae variety and attachments to corresponding leaflets. [24]

Based on their point of insertion and their size and composition, three types of chords have been delineated: the primary (marginal), secondary (basal) and tertiary[2]. The primary chords attach to the free margins of the leaflets while the secondary chords attach beyond the primaries. Primary or first order chords as they are also called, are numerous and delicate, often forming networks near the edge. Secondary chords are thicker than the primary chords. These two types of chords may rise from the same bifurcating stem however. The tertiary chords arise directly from the side of the left ventricular wall and

insert only into the posterior leaflet. These chords run only a short distance toward the free margin. Some groups have also delineated individual chords such as the commissural chords, strut chords, and the cleft chords[3,23]. Each however have distinct purposes for the valve's coaptation. Primary chords maintain leaflet apposition and facilitate valve closure. The secondary chords help play a role in maintaining normal size in the left ventricle. The thicker and longer of the secondary chords, also known as strut chords, act as the interface between the musculature of the wall and the mitral annulus (connecting at the fibrous trigones)[2]. The strut chords are under continuous tension transmitted to the papillary muscles and trigones.

Chordae tendinae however apparently have a paradoxical size-dependent mechanical behavior. Thinner chordae, such as the primary chords, were less extensible and more stiff than the thicker chordae[14]. Thicker chordae have smaller crimp periods than thinner chordae, meaning that thicker chords could undergo greater strain before collagen was uncrimped. The tensile modulus is also greater in the thinner chordae. It has been reported that thinner chordae have a greater fibril density despite their smaller fibril diameter[25]. Therefore, the smaller chordae, which are responsible for mitral valve competence, with greater interfibrillar interactions explains their greater modulus.

1.1.5 Papillary Muscles:

The last major component of the mitral apparatus are the papillary muscles. While their location can be variable, they are most commonly attached to the middle third of the left ventricle wall[2,3]. In most cases, there are about two papillary muscles where most chordae tendinae are attached. Contraction of the papillary muscles is coordinated with the

left ventricle as a whole. Therefore, function of the papillary muscles is largely affected by the condition of the left ventricle. This coordinated contraction is essential, because were it not for the timely contraction of the papillary muscles, the fixed length of the chordae might otherwise permit the leaflets to prolapse into the atrium. Placement of the papillary muscles also effects the shape of the annulus through chordal attachment[24]. This placement effects chordal forces and therefore coaptation of the valve.

1.1.6 Microstructure:

Interstitially, the extracellular matrix (ECM) of the valve differs within each component, but each is defined by their roles in the valve's coaptation. The matrix is composed of various proteins and polysaccharides that are assembled into a meshwork created, organized, and secreted by the surrounding cells. The relationship between the matrix and the surrounding cells is dependent upon one another. Cells produce and constantly remodel the surrounding matrix. The ECM acts as a ground substance for which cells can exist. Inversely, the ECM exerts powerful influence on the cells. These influences are exerted through transmembrane cell adhesion proteins that act as matrix receptors. These influences can be either mechanical or chemical in nature. The primary membrane receptors that bind to ECM proteins are integrins. Through these matrix receptors, components of the ECM can affect almost any aspect of the cell's behavior. Cells also use integrins to transmit signals from the cells to the matrix as well. Each component of the mitral valve contains a basal lamina or basement membrane, which separates the cells from the underlying connective tissue and forms the mechanical connection between them. Also formed by the surrounding cells, the basal lamina influences cell polarity, metabolism,

organize the proteins in adjacent plasma membranes, promote cell proliferation, migration and differentiation. Basal lamina are specific to the specific types of cells that establish the basement membrane. The basal lamina in this valve and in many tissues is composed of laminin and collagen type IV.

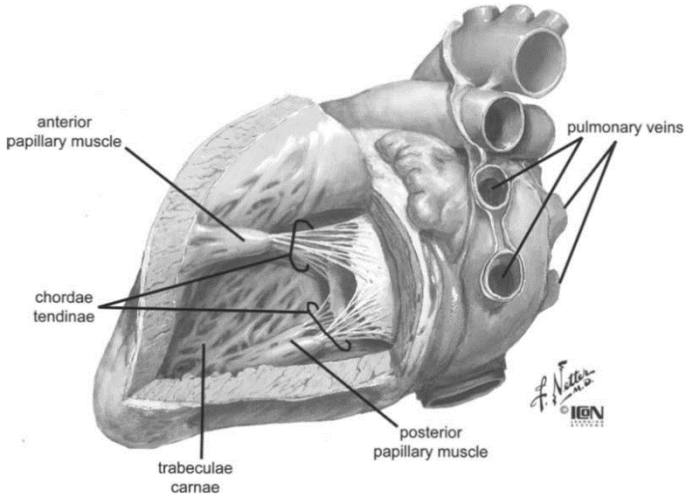

Figure 1.5: Papillary muscles and their corresponding attachments to chordae and left ventricle wall.[26]

There are two main classes of ECM macromolecules, fibrous proteins and polysaccharide chains of the type called glycosaminoglycans or GAGs. Fibrous proteins are largely glycoproteins, which have oligosaccharide side chains attached. These glycoproteins play an important role in cell-to-cell interactions. One of the most common examples of fibrous proteins are collagens and elastins. GAGs are usually found linked covalently to specific core proteins to form proteoglycans. These serve as the ground substance of many types of connective tissue. Because they are so heavily glycosylated, the balance has shifted close to carbohydrates in nomenclature. The carbohydrate chains attached to the core proteins are negatively charged due to their sulfate or carboxyl groups bound to their sugars.

1.1.7 Annulus:

As form follows function, the annulus acts as the transition zone from the aortic annulus on the anterior side and the myocardium on the posterior side of the valve. Anteriorly, collagenous fibers radiate into the annulus form the collagenous root to which it is attached. Collagen, a common fibrous protein is a triple stranded helical structure. This rope-like structure is perfect for resisting the tension felt on the valves. The annulus, as the transition region from the myocardium and aortic root is moving constantly in several directions while also allowing for contraction. Resistance to tension is essential for its function. To also assist with the tensile stresses, the annulus's ECM contains elastic fibers. The main component of the elastic fibers in the annulus is elastin, a highly hydrophobic protein, is elastic and supports tensile resistance while also allowing for stretching or contracting. The posterior annulus, which attaches to the myocardium, is muscular while also containing collagen and elastin within its matrix. From both annuli, radiates collagen and elastin into the leaflets which also have a unique matrix composition

1.1.8 Leaflets:

The mitral valve leaflets have a layered microstructure that readily supports the environment with which it functions. From top (atrial side) to bottom (ventricular side), the primary layers are the atrialis, spongiosa, and ventricularis[14,17]. The atrialis layer is largely built of elastin fibers providing elasticity to the leaflet. The ventricularis, also called the fibrosa layer, is a thick collagenous layer built to withstand the tension caused by the high pressures of the ventricle. In the mitral valve, the collagen show a circumferential alignment in the leaflets[14,17,18]. The inner layer contains proteoglycans and the GAG

hyaluronan. GAGs, one of the two main classes of macromolecules in the ECM, are unbranched polysaccharide chains composed of repeating disaccharide units. GAGs are naturally negatively charged because of the sulfate and carboxyl groups on most of these sugars. This high density of negative charge attracts cations like Na^+ that are osmotically active and therefore attract large amounts of water into the matrix. This causes a swelling pressure that enables this GAG layer to withstand the compressive forces experienced by the leaflets. It is important to note that these layers are not exclusive to one type of ECM. The atrialis and spongiosa both contain some collagen and the spongiosa contains a network of elastic fibers[14]. These layers are found in both leaflets. There are variations in the thickness of the layers. This is especially evident in the anterior leaflet, where the proximal third of the leaflet is marked by a very thick ventricularis, rich in highly aligned collagen and small leucine-rich PG, with only minor presence in the other layers.

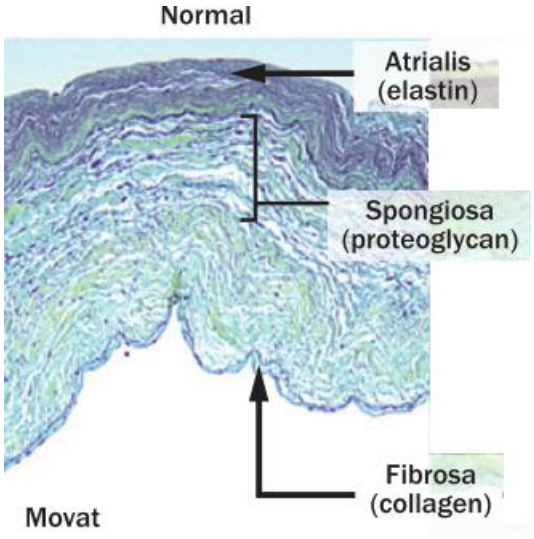

Figure 1.6: Three-layered extracellular matrix of the mitral valve leaflet. [27]

1.1.9 Chordae Tendinae:

The chordae attached to the ventricular side of the leaflets are largely composed of collagen with some elastin fibers as well. This combination allows of elastic and highly crimped collagen fibers allows for appropriate deformations needed to handle the tension brought on the chords from the papillary muscles and translate this to the leaflets to which they are also attached. As mentioned, the chordae vary in thickness and collagen density. The thinner chordae have a greater fiber density than the thicker chords and thus show an increased modulus.

1.1.10 Papillary Muscle:

The papillary muscles as expected are largely composed of myocardium due to their origins from the muscle in the left ventricle.

1.2 Valvular Interstitial Cells:

Valvular interstitial cells (VICs) are the prevailing cell type in the heart valves and are found within each fibrosa, spongiosa, and ventricularis layer of the valve[28–33]. They are a dynamic population of valvular-specific cells and are the living component of heart valves. VICs are responsible for synthesizing and preserving the composition of the valve matrix, which largely determines the valve's ability to function as well as its material behavior[28]. The central role of the VIC is to maintain the structural integrity of the valve and to act when the valve is in need of repair. These responsibilities are extremely important as heart valves are the most mechanically stressed tissue found in the body. VICs also function as key role players in the body's pathological response to heart valve disease as well as regulating processes following valve injury.

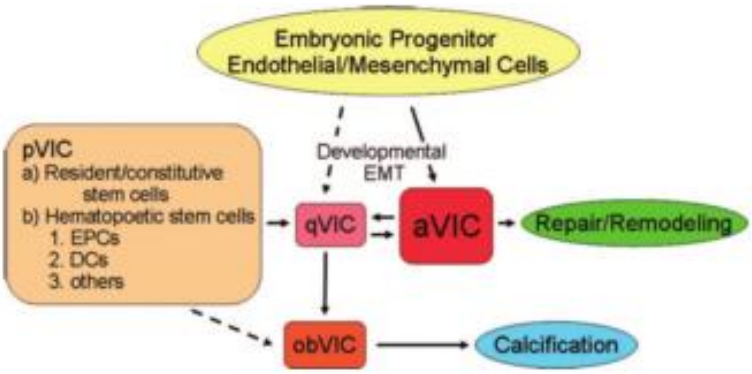

Figure 1.7: The five phenotypes of valvular interstitial cells[34].

Current literature supports five heterogeneous VIC phenotypes[14,28]. Each of these phenotypes exhibits specific sets of cellular functions necessary for proper valve function, injury repair, and pathological processes. The five phenotypes would be: embryonic progenitor endothelial/mesenchymal cells, qVICs (quiescent VICs), pVICs (progenitor VICs), aVICs (activated VICs) and obVICs (osteoblastic VICs). These phenotypes are shown in **Figure 1.7**. It is important to note the differentiating potential for each phenotype into another as well as the plasticity that exists between qVICs and aVICs. This relationship is crucial for proper valve repair and can result in pathological problems if proper balance between them is not achieved.

Embryonic progenitor endothelial/mesenchymal cells are included in the VIC family because the EMT (endothelial-mesenchymal transdifferentiation) paradigm, apparent in heart valve development, reappears in adult valves in response to injury[28]. The endothelial cells involved in EMT actually have properties similar to heart valve progenitor cells and may give rise to VICs. As the potential originator of VICs, as illustrated in **Figure 1.7**, many have investigated what factors contribute to the transformation of endothelial cells into these VICs. Transforming growth factor (TGF)-β and bone morphogenic

proteins, particularly BMP-2 have been noted to influence the pathway to VICs[28,35,36]. The Notch and vascular endothelial growth factor (VEGF) are also well known to have distinct regulatory effects on EMT. Armstrong and Bischoff, understanding that VEGF is highly suggestive and its expression tightly controlled during development, concluded that VEGF facilitates valve formation by establishing an equilibrium between proliferation and differentiation[37]. Others looking into developmental studies concluded that BMP-2 is essential for EMT it devotes progenitor cells into endothelial cells[38]. Also, the Notch signaling pathway, often interacting with the TGF-β superfamily, is implicated in development of endocardial cushions and normal development of the aortic and mitral valves[28].

1.2.1 VIC Phenotypes:

qVICs are the predominant VIC phenotype in healthy valves and are thought to maintain the valves overall structure and function[28,29,32,36,39,40]. In this resting state of VICs they act similar to fibroblasts[41,42]. It is from this phenotype that VIC plasticity stems. From here, as shown in **Figure 1.7**, multiple phenotypes can be achieved by providing certain mechanical or chemical factors. To communicate, qVICs show two types of intercellular junctional complexes, gap and adhesion junctions[28–30]. Gap junctions, commonly Connexin-26 and -45, are used to communicate with adjacent VICs. Adhesion junctions may be important in allowing gap junction function[28]. N-cadherin and desmoglein are found faintly in these junctions. While the physiological presence of these junctions is not completely understood, it has been theorized that they are used to transmit information from mechanical cues for example across the cellular structure network.

Progenitor VICs or pVICs, are essentially valvular stem cells and can be derived from various origins such as bone marrow stem cells. Unfortunately, these are the least understood VIC. Identification of this phenotype is difficult but some have differentiated hematopoietic stem cells into VIC like cells. Others have isolated progenitor cells from the pulmonary valves. There is some evidence that the microenvironment of the heart valve ECM influences bone-marrow stem derived pVICs once they are present in the valve, possibly arriving via microvessels at the base of the leaflets[28]. How these pVICs travel to injury locations however is less understood. Perhaps it is done through some soluble signal molecules arising from the tissue injury and/or pathological effects occurring in a diseased valve.

obVICs are VICs that undergo osteoblastic differentiation and promote calcification within the valve. This phenotype is not typical of normally cultured VICs. TGF-β and BMP-2, may regulate valve calcification based on the increased rate of nodule formation after their application. Cultured VICs do not normally promote calcification. When cultured with media supplemented with organic phosphate, VICs begin to express chondrogenic and osteogenic markers and form calcific nodules[28,43,44]. The calcification process relies on the upregulation of alkaline phosphatase activity because prevention of such inhibits in vitro calcification. To evaluate differentiation into obVICs, calcific nodule formation is often used as a barometer. TGF-β, as discussed before, promotes migration and activation of VICs but it can also promote the formation of these apoptotic alkaline phosphatase-enriched nodules. Literature shows us that TGF-β mediates the calcification of these VICs through mechanisms of apoptosis[28]. Valvular endothelial cells (VECs) may

also play a role in encouraging an obVIC phenotype; however, this role is most likely as an outside transducer rather than a direct promoter.

In response to injury or disease, qVICs become activated VICs (aVICs) and take on the features of myofibroblasts. This phenotype is characterized by increased α-smooth muscle actin (α-SMA) expression, contractility, stress fiber formation, secretion of matrix remodeling enzymes (MMP-1, MMP-2, MMP-9, MMP-13), cytokines (TGF-β), and cathepsins[28,40,45,46]. aVICs also exhibit heterogeneity in their morphologies. Round aVICs have more α-SMA stress fibers, while spindle-shaped aVICs show higher motility and are more proliferative[47]. Activation of qVICs is brought on by changes in the mechanical environment or from several cytokines, often TGF-β. These changes in the ECM microenvironment are often due to disease or damage to the valvular tissue. When activated these VICs increase their secretion of extracellular matrix while also degrading the existing matrix, expressing MMPs and TIMPs. Proliferation and migration of aVICs is also increased, which is important for wound repair. After completing the necessary remodeling, many aVICs are eliminated by apoptosis or return to qVICs[28]. It his however this regulation of aVICs that is crucial to valvular homeostasis. Many pathologies result in high cellularity and abnormal changes in ECM content; these are often caused by the dysregulation of aVICs. By persisting and not returning to the qVIC phenotype, pathological fibrosis, angiogenesis, chronic inflammation, and calcification can result from abnormal remodeling[28]. Therefore, aVICs are crucial to valve remodeling and repair but a balance and proper regulation must be achieved or these interstitial cells cause more harm than good.

1.2.2 Regulation of VIC Activation:

TGF-β, a superfamily of proteins, is a well-known group of peptide growth factors that regulate biological processes and cellular systems in the body. It also has well documented effects on VICs differentiation into the activated phenotype. TGF-β binds to the cell surface to the TGF-β receptors I and II leading to signaling through the Smad proteins. Smad proteins reside intracellularly and transduce extracellular signals from TGF-β ligands. This pathway may also influence others including MAPK. Overall, these pathways regulate the cell cycle, their migration, proliferation, ECM synthesis and degradation and cytokine secretion. When VICs are bound to TGF-β, α-SMA, smooth muscle myosin and calponin all increase in expression[28]. It is important to note that the expression of these proteins and the differentiation of the qVIC into the aVIC through interaction with TGF-β is unique. Cellular response to TGF-β is dependent on the cell types present and the environment with which the interactions are taking place. By becoming aVICs, contractility and fibronectin remodeling also increase. Fibronectin and other matrix components such as heparin, play important roles in regulating TGF-β's interaction with VICs. When heparin is present, the stability of TGF-β's binding to the pericellular microenvironment increases which causes an increase in α-SMA expression[48]. TGF-β binds directly to fibronectin and VICs express and actively remodel fibronectin, a major ECM component. Because fibronectin can bind directly to TGF-β, it allows it to activate VICs. It is important to remember that induction into aVICs corresponds to a significant increase in stress-fiber formation and enhanced contractility and increased mechanical

stress. These changes can link aVICS to pathological matrix remodeling[28,43]. This is one reason why bioavailability of TGF-β is tightly regulated by the body.

Wound repair is also an essential role of VICs, and is one inducer of the aVIC phenotype. TGF-β is well known to play a role in wound repair, but its effects on cell growth remain in question, this in part due to TGF-β's effects varying from cell to cell and between environments. VICs, as mentioned have specific reactions to TGF-β, encouraging the activated phenotype. Most fibroblast cells proliferate in the presence of TGF-β. However for VICs, and also for endothelial cells, TGF-β actually inhibits proliferation in aortic VICs.[35] This could be a function of VICs retaining characteristics of endothelial cells during EMT. The outcome of TGF-β depends on cell type and local environment. It is important to remember that VICs activate and proliferate during valve injury. TGF-β is often found at these wound sites. One would question as to how this proliferation of VICs could occur given the above comments. Proliferation during wound models may allude to the fact that wounds act as an external stimulus that alters this specific qVIC signaling profile. Mechanical factors must effect this activation and proliferation. These interstitial cells are context dependent. VICs essentially could modulate their Smad signaling due to differing external stimuli. This would then mean that VICs proliferate during wound (external) and are active, but not proliferating during normal physiological conditions (as during normal remodeling) so as not to disrupt the valvular environment[35]. If this signaling regulation were to malfunction, as it must do in some, pathological valve tissue results.

1.2.3 VICs in the ECM:

As mentioned, VICs are the key modulators of ECM quality and content. In this matrix that they remodel, there are variations of amounts of VICs in each layer due to ECM stratification and compartmentalization during development. VICs may play a role in this spatiotemporal coordination due to embryonic progenitor endothelial/mesenchymal cells' activation, proliferation, and expression of MMPs[28]. VICs interact with their matrix by focal and fibrillary adhesions. These two distinct adhesion complexes differ in morphology, protein composition, and location on the cell membrane. Focal adhesions are composed of FAK (focal adhesion kinase), as well as the cytoskeletal markers vinculin, talin, paxillin and α-actinin[33]. Fibrillar adhesions are small globular or elongated adhesion complexes. This complex lacks cytoplasmic proteins paxillin and vinculin. Both adhesion complexes utilize the $\alpha_5\beta_1$ integrin, while focal adhesions also use $\alpha_v\beta_3$[33]. These focal adhesions make contact with fibronectin, which provides a suitable matrix for cells to migrate. VICs secrete Fibronectin; the $\alpha_5\beta_1$ integrin in migrating cells interacts thereby linking the actin cytoskeleton to fibronectin via tensin and the $\alpha_5\beta_1$ integrin. Fibronectin acts as a means of motility and activation. VICs express it at the wound edge, thus facilitating VIC migration. aVICs, known to activate and quickly migrate to these wounded areas utilize the fibronectin they produce to move. Therefore, in qVICs, fibronectin expression is decreased. VICs also play a significant role in matrix degradation, expressing MMPs and TIMPs. MMPs and TIMPs vary among the different valve types, for example, MMP-2 is only expressed in the pulmonary and aortic valves.

VICs reside in one of the most mechanically stressed environments. Heart valves undergo hemodynamic shear, cyclic flexure and bending, and compressive stresses and strains. VICs respond to these mechanical cues and forces altering their cellular stiffness and utilizing their influence on the ECM. On the left side of the heart for example, VICS show increased α-SMA content and collagen synthesis due to the fact that the heart's left side faces larger transvalvular pressure which poses a larger tissue stress when compared to the right side of the heart[32]. The degree of collagen synthesis is dependent on the degree and duration of the forces encountered. The obVIC phenotype can also be encouraged by matrix stiffness[44].

Mechanical cues can also be transduced by valvular endothelial cells (VECs) to regulate VICs. These cells are directly influenced by shear and hemodynamic stresses of the heart. VECs provide a protective and selective boundary between blood and VICs. The mechanical influences from the stressed valve exterior make VECs a critical modulator of VICs and their phenotype. In fact, VICs that have been co-cultured with VECs show an increase in vimentin expression and a decrease in the aVIC marker α-SMA, a possible indication that VECs encourage qVECs over aVICs[49]. It is likely that VECs function to a similar importance that vascular endothelial cells have in regards to maintenance of vessel tone and inhibition of pathological differentiation of the interstitial smooth muscle cells. VECs can significantly reduce or reverse the activation of VICs[49].

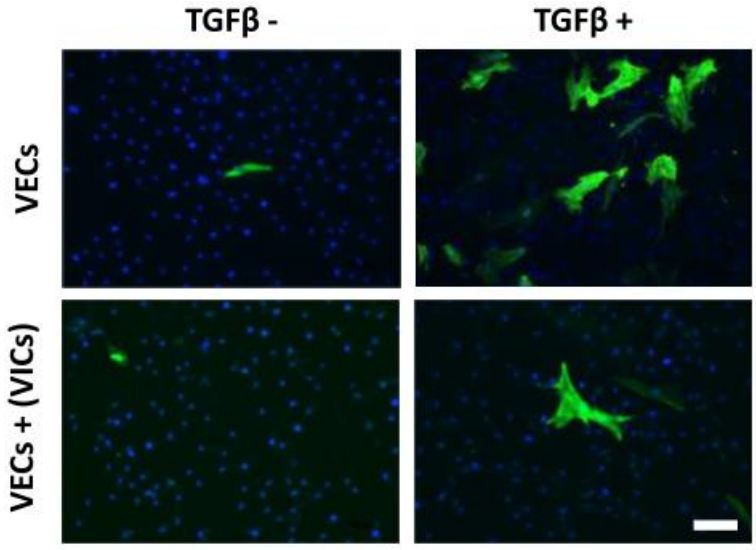

Figure 1.8: VICs suppress TGF-β1-induced VEC EndMT. Immunofluorescence staining of a-SMA (green), cell nuclei (DAPI/blue)[50].

Through paracrine signaling, VECs release factors to affect VIC function, one such factor is nitric oxide (NO). NO, a known vasodialator is a free radical with many biological uses. NO released by iNOS, (inducible nitric oxide synthase) has been shown to play a role in valve wound repair[49,51]. Possibly through proper regulation of VIC phenotype and its movement or proliferation. Under physiologically relevant stresses, NO has been shown to have beneficial effects on VICs. VIC contraction and activation have also been prevented through dosage of the VEC produced free radical[51]. NO may act through the cGMP pathways, which ultimately down regulates Rho kinase (ROCK), which regulates α-SMA in VICs. Therefore, NO may act through cGMP to regulate VIC activation[51]. It is also likely that other factors release by VECs, like c-type natriuretic peptide (CNP) and/or prostaglandins may play a role in regulating VIC phenotype[39]. VICs may also release their own paracrine signaling which could influence VEC protein expression. Even in the presence of TGF-β1, which induces EMT, VICs can inhibit the transformation of VECs in

EMT[50]. Otherwise, these transformed endothelial VICs (eVICs), can differentiating into obVICs, contributing to pathological remodeling and calcification. Therefore, communication between VICs and VECs remains crucial for the health and coaptation of the valve.

1.2.4 VICs in Aortic and Mitral Valves:

VICs are the most abundant cell type within each of the heart valves, however transcriptional profiles of VICs varies between mitral and aortic valves. Differences in blood flow dynamics between the valves may explain some of this variation. Among the differences was expression of transcription factors NKX2-5, an important regulator during embryonic development, and TBX-5, which is very important for cardiogenesis. TBX-5, expressed significantly higher in mitral VICs, is expressed in developing atrioventricular valves and likely accounts for the mitral valve's structural differences like the chordae tendinae[52]. Expression of matrix degrading protein, MMP1, was also highly expressed only in mitral VICs[52]. MMP1 mediates osteoblastic differentiation in osteogenic cells. When comparing migration and proliferation profiles between aortic and mitral VICs, both interstitial cells shows similar migration abilities, but mitral VICs showed greater proliferation than aortic VICs.

Regional interstitial cell variation also exists within sections of the mitral valve itself. Mitral valve tissue varies regionally when considering the different mechanical loads experience on each tissue type. As, previously mentioned, the matrix-VIC relationship is crucial in deciding VIC phenotype. Regionally the mitral valve does not possess homogeneity in the forces acting on the tissue. There are for example regions such as the

chordae tendinae and the anterior leaflet that are stiffer because they need to be stronger due to the forces acting upon them. These regions expressed higher amounts of α-SMA and vimentin. The α-SMA may be indicative of the contractile nature of these regions, which in turn could describe the type of loading experienced by these tissues[32]. The "clear zone" on the posterior leaflet is a region that does not possess chordal attachment. The VICs present within this region expressed vimentin but at a much lower intensity[32]. The cells in this region are also more like the VICs widely described by literature. GAG content also differs regionally, being secreted greatly by the more tensile-intensive regions.

1.3 Pathology of the Mitral Valve:

Pathologies of all heart valves affect an average of 2.5% of the population in the United States[53]. This number drastically increases with age, as many heart valve diseases are degenerative in nature. The majority of this 2.5% of the country are sufferers of mitral valve pathologies[53]. About 44,000 hospitalizations per year are due to mitral valve disease and this number represents about 44% of those who would benefit from some form of surgical correction[14]. As the health of the mitral valve goes, so too does the health of the heart. Mitral pathologies can lead to atrial fibrillation, arterial thromboembolism, pulmonary edema, pulmonary hypertension, cardiac hypertrophy and heart failure[54–57]. Of the many ailments that strike the mitral valve, most are degenerative in nature. This is a shift from the predominance of rheumatic diseases to degenerative etiologies. In developing countries, valvular diseases are still substantially caused by rheumatic heart disease. A consequence of acute rheumatic fever, rheumatic heart disease is still prevalent in developing nations. It is important to note that developing nations represent about 80%

of the world's population, so while most journals report the importance and the alarming rise of degenerative mitral valve disease, the majority of the world's patients suffering from valvular disease are caused by rheumatic heart disease[58].

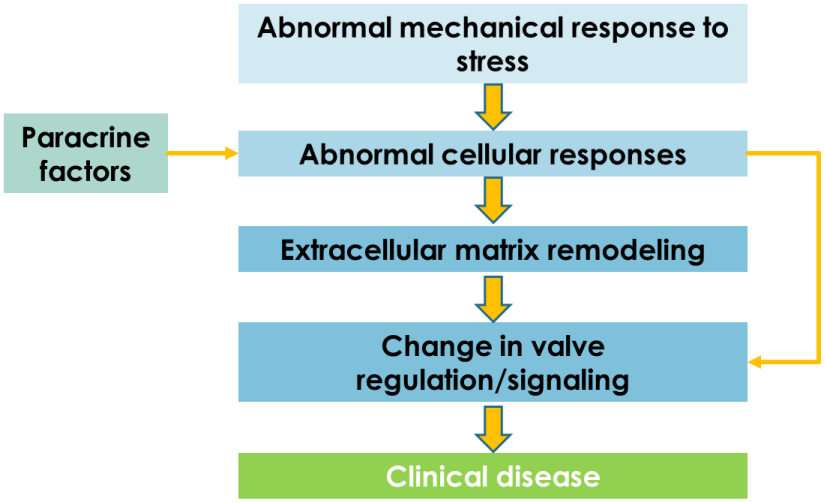

Figure 1.9: Conceptual model for mitral valve pathologies. Adapted from Levine et al., 2015[27].

Degenerative etiologies of the mitral valve are however becoming increasingly the dominant focus for treating these diseases. Of the heart valves, the mitral valve is the most degenerative in nature. Mitral regurgitation, which can be caused by several other contributing ailments, is the most common form of heart valve disease in industrialized countries. It is especially prevalent in older patients, affecting almost 15% of the population that is 75 or older[58]. This is largely due to an altered architectural organization of the ECM within the components of the valve. Each of these components of the valve are interdependent upon the other. This living apparatus, exhibits plasticity in that it can change cellular phenotype and behavior to adapt to its current ailment. Adaptive matching of valve mechanics to the needs for normal function illustrate the valve's adaptability. Many of these self-incurred adaptations for coaptation, however show themselves in pathological

valves. There is a crucial interplay between biomechanics and biology[27]. There are three major types of mitral valve diseases that can affect any part of the mitral apparatus. These include mitral stenosis, regurgitation, and prolapse. Each of these types of disease lead to failure of coaptation and could eventually lead to heart failure and death.

1.3.1 Mitral Stenosis:

Mitral valve stenosis is the least common valvular disease in industrialized nations, however it is the most common valvular disease in developing nations.[58]. This again represents roughly 80% of the world's population. Prevalence in these non-industrialized regions is largely due to poor socioeconomic conditions. Mitral stenosis is largely a result of repeated infection with Group A β-hemolytic *Streptococci*, which eventually leads to Rheumatic heart disease (RHD) from acute rheumatic fever (ARF). This disease primarily affects children and young adults, in fact acute rheumatic fever is the leading cause of heart disease in children worldwide[59]. Given its distribution amongst the population, rheumatic mitral stenosis accounts for a large portion of pregnancy-related complications in developing countries[58]. Based on conservative estimates by the WHO, at least 15.6 million people worldwide have RHD, and about 233,000 deaths annually are directly attributable to acute rheumatic fever or RHD[60]. ARF (and eventually RHD) are a consequence of repeated infection with Class I strains of group A streptococcus. The role this virus plays in ARF is complex and not fully understood, however it appears that repeated exposure is necessary to "prime" the immunological response both qualitatively and quantitatively, before ARF occurs[60]. It is believed that the autoimmune response caused by ARF could be triggered by molecular mimicry between the epitopes of specific human tissues and the

virus itself[60,61]. Structurally, streptococcal M protein (a major virulence factor) and myosin are very similar. Both are alpha-helical coiled-coil molecules[60,61]. This similarity seems to be essential in the autoimmune response. CD4+ T-cells proliferate in response to both the streptococcal M protein and cardiac myosin but not skeletal muscle myosin[60].

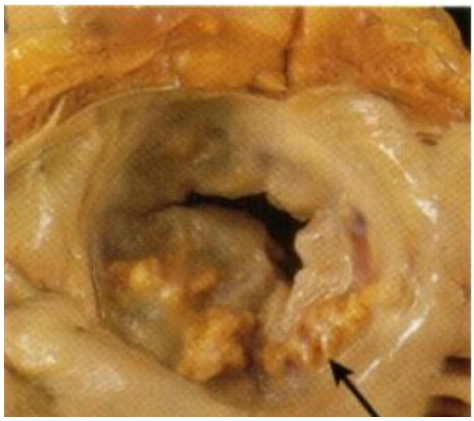

Figure 1.10: Example of stenosis in the mitral valve. Clear calcification of the leaflets is visible[54].

It is important to note however, that only a small portion of the mitral valve is composed of myosin, and diseases of the valve rather than acute myocarditis are responsible for most cardiac morbidity and mortality of ARF and mitral stenosis. How then can an immune response against myosin induce ARF and eventually mitral stenosis? It appears that several common valvular proteins including laminin and vimentin have several autoantigens that are recognized by T cells. Laminin is also structurally similar to the streptococcal M protein[60]. Initial streptococcal infection with activation of B and T lymphocytes by streptococcal antigens would lead to antibody and cytokine production. The presence and increased production of these antibodies and cytokines leads to an autoimmune response to the valvular proteins through binding to the valvular endothelium leading to inflammation, cellular infiltration and valve scarring[61]. The valve endothelium

is the prominent site of lymphocytic infiltration in RHD. The lymphocytes that adhered to the valve surface expressed VCAM-1, a protein responsible for adhering lymphocytes to vascular endothelium[59]. Endothelial transmigration of these lymphocytes at the valve endothelium is an important step in ARF and mitral stenosis. The presence of activated macrophages in rheumatic lesions is characteristic of granuloma formation. These lesions are characteristic of mitral stenosis and the presence of CD4+ T-cell proliferation has been noted here indicating their role in the pathogenesis of RHD in mitral stenosis. With the upregulation of VCAM-1 on the endothelium and the binding of auto-antigenic antibodies, the valve becomes a localized microenvironment for continuous cytokine production and infiltration from lymphocytes[59]. Repeated infection would result in larger and more frequent lesions, exposing more autoantigens on valvular proteins. Thus explaining why several infections are necessary to prime the immunological response before ARF occurs. Scaring is also an important event in the progression of this disease because this leads to neovascularization. The mitral valve is largely avascular, therefore, once scaring and neovascularization occurs, the transendothelial migration of lymphocytes is allowed[59]. The activated endothelium and the valvular proteins play a large role in the development of ARF and mitral stenosis. It is important to note that the valvular endothelium is important in the regulation of phenotype in interstitial cells. It is likely that endothelial cells on valves function similarly to that of vascular endothelial cells in regards to maintenance of vessel tone and inhibition of pathological differentiation. Therefore, these lesions created on the valve endothelium most likely contribute to activation of VICs and aggressive remodeling of the valve's interior.

The main pathologic features of mitral stenosis are leaflet thickening, nodularity, and commissural fusion[54]. All of these features contribute to a narrowing of the valve and are a result of the repeated inflammatory response brought on by RHD. The normal mitral valve area ranges from 4—6 cm^2 and symptoms from the narrowing show roughly, when the area has decreased by about 1.5 cm^2. Chordal fusion and shortening are also caused by mitral stenosis and add further resistance to blood flow. Calcification of the annulus and leaflets can also occur, but rarely contributes to severe mitral stenosis. Calcification due to stenosis is seen in patients 65 years or older[58]. Atrial fibrillation is often associated with mitral stenosis as is pulmonary hypertension. Mitral stenosis is also one of the common lesions found during pregnancy and is associated with high morbidity[54].

1.3.2 Mitral Regurgitation:

Mitral regurgitation is a large-encompassing and prevalent disorder of the mitral valve. It affects about 2% of the US population which equates to around 4 million patients[53]. About 250,000 new patients are diagnosed yearly[57]. These sizable statistics highlight the many mitral regurgitation (MR) can effect. MR is also however a broad term as it includes any mitral valve pathologies that allow regurgitant blood back into the atrium during ventricular systole. Regurgitation could be the result of mitral stenosis, annular calcification, degeneration, prolapse of the leaflets and other valvular diseases. The wide net that this pathology casts can and has caused serious illness and death. When the atrium is forced to handle additional regurgitant blood, it becomes dilated overtime and this leads to pulmonary edema, heart failure, and death. Degeneration of the valve is a certain factor as almost 10% of patients 75 and older are affected by MR[53]. A particularity of MR is that

it can be the consequence of two primary abnormalities. Functional MR is caused by left ventricular remodeling, which results in incomplete closure of the valve through anatomical misalignment of the valvular components. The second type of MR, organic MR, is a consequence of primary anatomical abnormalities caused by valvular degeneration of the mitral apparatus. These two types are totally different diseases in both their pathophysiology and in how they are treated[58]. Carpentier introduced a functional classification of MR based on leaflet movement. Type I with normal leaflet movement (e.g., MR caused by annular dilatation or leaflet perforation); Type II with exaggerated leaflet movement (e.g., mitral valve prolapse); and Type IIIa and IIIb with restricted leaflet movement in diastole and systole, respectively[57]. There are varying degrees of regurgitation. Those with acute severe regurgitation, the pulmonary venous and atrial pressures increase quickly, leading to pulmonary congestion and edema[56]. Edema is an abnormal accumulation of fluid in the cavities in the body, in this case with obstructions in the pulmonary veins, fluid builds in the lungs. Chronic regurgitation leads to a gradual increase in atrial size. The atrium compensates and as a result, the left atrium and pulmonary venous pressures do not increase until late in the course of the disease. Due to this compensation from the body, many patients with chronic or severe mitral regurgitation will be asymptomatic for years because the regurgitant volume load is tolerated. In addition, as mentioned, the ventricle experiences a significant overload. The ventricle, like the atrium will attempt to compensate, becomes hyperdynamic and dilates. Pathological hypertrophy also leads to an increase in muscle mass, but the muscle does not increase its pumping ability, and instead accumulates myocardial scarring.

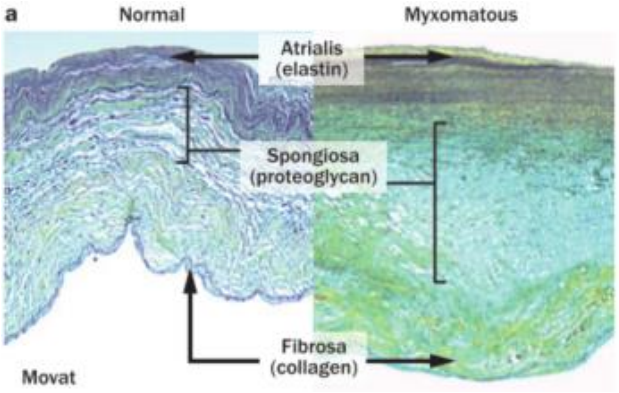

Figure 1.11: Histological example of degeneration in the mitral valve ECM with an enlarged spongiosa[56].

Functional MR is a consequence of abnormalities of the segmental left ventricle wall motion, dilation of the left ventricle, or papillary muscle displacement[57,58]. Many times in functional MR, the structure of the mitral valve is normal, however due to its attachment to a diseased left ventricle, this can cause an incompetent valve. There are two categories for functional MR, ischemic and non-ischemic. Ischemic MR is associated with coronary artery disease most often associated with myocardial infarction and non-ischemic is associated with idiopathic dilated cardiomyopathies[57]. Due to left ventricle dysfunction or remodeling, papillary muscles can be displaced laterally, apically and posteriorly. Because the chordae tendinae are not extensible enough to compensate for this displacement, the leaflets of the valve are affected causing tethering, apical leaflet displacement and dysfunction of the valve. This is a vicious cycle because the higher the degree of functional MR, the larger the left ventricle; the larger this left ventricle, the larger the displacement of the papillary muscles and thus the higher the degree of functional MR. It is also possible that the annulus experiences an increase in size due to its attachment to other areas of a diseased heart. The posterior leaflet's insertion to the myocardium of the left ventricle is the cause for this. In functional MR, the annulus is dilated along the septo-

lateral from about 28.2 to 35.1mm[62]. This makes the annulus more circular in shape with a larger annular orifice area as well which decreases its ability to contract. The leaflets have also been known to increase in size by roughly 35% to cover the increased orifice area due to the left ventricle dilation[62]. This adaptive mechanism is still insufficient to allow proper function of the mitral valve in patients with functional MR. The prevalence of functional MR is underestimated because heart failure in patients is often owed to left ventricular systolic dysfunction rather than a valvular disease.

Organic MR is a degeneration of the valvular apparatus. Degeneration in this case does not always mean loss or degradation of tissue but rather a disruption from the homeostasis of the mitral valve's ECM. Organic MR includes mitral valve prolapse, the most prevalent form of mitral valve diseases[55,57,58,63]. Prolapse of the mitral valve means that the leaflets are allowed to billow into the atrium. This incompetence leads to regurgitation. However, this will be discussed in the next section. Other forms of organic MR include annular calcification, however this rarely becomes clinically important despite its high prevalence[58]. Most literature however is focused on myxomatous mitral valve disease (MMVD), or degenerative mitral valve disease. Age is considered an important contributor to these forms of organic MR.

MMVD is typified by enlarged leaflets and annular dilation[64]. Mechanically the diseased leaflets are one third less stiff and considerably more extensible compared to healthy leaflets[65]. It also commonly features thickened chordae, which over time become elongated. The chordae are about 75% less strong than normal chordae, thus promoting rupture[65]. Microscopically MMVD is characterized by expansion of GAG and

proteoglycan content in the spongiosa, expanding this region of the ECM. Elastic fibers are often appear as granulated and fragmented clusters instead of stretching across the valve. It is important to note that there are varying degrees of MMVD causing organic MR. Barlow's disease and fibroelastic deficiency (FED) present very different examples of degeneration. VICs dictate many of these changes in the ECM. As the resident response team for remodeling and preserving the matrix, VICs are responsible for the quality of the valve's ECM. In MMVD, VICs are found in their activated state meaning they are behaving in a myofibroblastic manner and producing large amounts of ECM, particularly GAGs and proteoglycans. It has been mentioned in literature that the key to the VIC's safe remodeling of the valve was the cell's ability to deactivate into a quiescent state. If however, these cells remain in the activated state, they can overproduce ECM and MMVD can result. In progressively myxomatous valves, VICs can even shift further to a myofibroblastic phenotype[64]. Activated VICs (aVICs) also secrete matrix remodeling enzymes (MMP-1, MMP-2, MMP-9, MMP-13) while collagen synthesis remain unchanged[28]. This is important to note because it suggests that abnormalities in the valve's leaflet structure and mechanical integrity are not a product of decreased collagen production, but rather an increase in collagenolytic activity[46,65]. Cathepsins S and K are also released by aVICs and are heavily involved in elastin remodeling, especially Cathespin K[46].

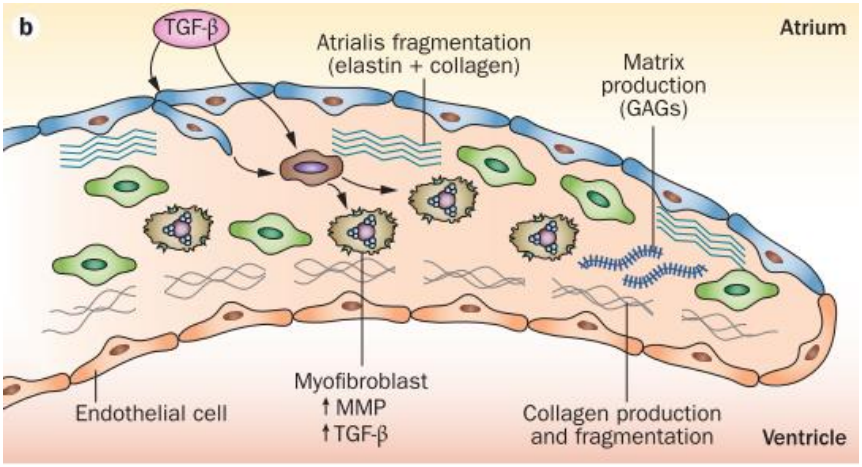

Figure 1.12: A schematic showing the mechanisms of myxomatous degeneration, with activated VICs becoming myofibroblast-like which in turn increases matrix production and turnover. This increases MMP production and TGF-β production, which cyclically promotes further cell proliferation and activation of VICs.

Endothelial cells will also show atypical phenotypes in advanced stages of mitral valve disease. The constantly changing leaflet environment and altered ECM environment lead to altered endothelial function[64]. As described earlier, aVICs produce significant amounts of GAGs that accumulate within the tissue leading to its altered structure. Literature shows increases in proteoglycan and elastin content being 59% and 62% respectively[64]. MR is perpetuated by this accumulation of proteoglycan content interstitially due the increasing stiffness of the leaflets. Accumulation of GAGs in the fibrosa are a common indicator of degeneration and a sign of the interplay between biomechanical forces outside the valve and the biological adjustments made interstitially. VICs in MMVD, largely aVICs, act as myofibroblasts which increase matrix production and turnover through the release of MMPs. MMPs drive the fragmentation of collagen and elastin, which releases peptides and additional TGF-β1 that further encourages

proliferation of cells and myofibroblast differentiation[27]. TGF-β1 on a stressed valve's exterior will also encourage VECs to undergo EMT, in which VECs retreat interstitially and become VICs, thereby increasing the number of matrix-producing cells.

Also contributing to these aVICs and the dysregulation of ECM homeostasis are several signaling pathways implicated in MMVD. It is important to note that inflammatory cells are not found in degenerating valves and thus inflammation is not likely a player in the pathogenesis of MMVD[66]. Much focus in literature has recently centered on the pathways that affect MMVD and have identified several signaling mechanisms that control the expression of key effector proteins. Meaning that MMVD while clearly associated with aging, is not solely a consequence of time. Progressive weakening of the ECM associated with aging does provide mechanical stimuli for VIC activation and proteoglycan accumulation mentioned above. Many chemical stimuli are being investigated in literature. Circulating serotonin has received attention lately not because serotoninergic valvulopathy and MMVD are identical, but because they share several features including increased GAG/proteoglycan deposition. Serotonin synthesis is governed by tryptophan hydroxylase (TPH). TPH1, the peripheral isoform, mediates the release of serotonin[66]. Studies have shown significant increases in TPH1 expression in MMVD, and inhibition of this factor diminishes expression of myxomatous effector proteins in mitral valves[66]. It has also been shown that serotonin (5-HT) induces an upregulation of TGF-β1 in VICs[67]. The TGF-β superfamily of growth factors play a role in ECM production. Their overexpression is often linked to several valvular diseases including degenerative mitral valves[66,67]. BMPs are also members of the TGF-β family and are a factor in their expression through Smad

phosphorylation[66]. It is not only their association with TGF-β and its link to MMVD, but BMP2 induces the activation of Sox 9 which mediates expression of cartilage-specific structural genes[66,67]. The similarities between chondrogenesis and MMVD implies BMP-Sox 9 signaling as contributing pathways for MMVD. The role of nitric oxide (NO) is unclear as it relates to MMVD, however there is evidence of increased endothelial nitric oxide synthases (eNOS) activity and NO release in MMVD[66,67]. However, this increased expression may merely be a response to the disturbed flow associated with MMVD.

Despite increases in ECM content, there is no increase in mature collagen or elastic fibers[64]. In fact, the compositionally collagen types change within myxomatous valves. The collagen content of a healthy mitral valve consists 74% Type I, 24% Type III, and 2% Type V. In myxomatous valves, the collagen type I decreases slightly and type III significantly increases by 53%[68]. This change in collagen content has been debated in literature depending on which methods were used. It has been shown however that with higher collagen type III content stiffening can occur and a correlation seems to exist with other cardiovascular diseases[69]. Also collagen type III has been shown to be more associated with GAGs and has more distensible properties than type I[70]. Despite continued production of collagen, in myxomatous valves much of what is produced is immature collagen. Collagen is synthesized as the precursor procollagen containing non-triple-helical extensions[71]. Formation of collagen fibrils requires an initial linear and lateral aggregation that is promoted by these extensions[71]. As fibrils mature, they transition from a highly soluble material to an insoluble structure. Strong inter- and intramolecular forces cross-links are the reason for this transition to maturity[71]. These cross-links are vital to the

tensile strength and integrity to collagen matrices. Cross-links contribute to collagen's mechanical strength. By lacking these cross-links or having abnormal cross-linkages, there is a marked decrease in mature collagen output, failure to form collagen fibrils and overall loss of mechanical integrity[69,71]. The absence of these cross-links results in very weak and extensible fibers. In myxomatous valves, immature procollagen expression is upregulated by a factor of two[72]. Collagen fibers in MMVD are also sparsely and irregularly arranged, characterized by fragmentation of the collagenous bundles[73]. Often in these myxomatous tissues, fibrils had a spiraling substructure. These fibrils are larger in diameter and can have a "flower-like" appearance[68]. Spiraling collagen is thought to develop due to dissociation or fraying of existing fibrils or defective aggregation of collagen filaments[68]. Orientation of collagen fibrils is also irregular in MMVD. Fiber direction and organization is the most effective way to optimize strength without increasing weight and this direction reflects the existing forces acting upon the tissue[74]. One possible explanation for this haphazard and disorganized fiber orientation could be the accumulation of GAGs. GAGs play a role in maintaining spatial order in the ECM as they act as space fillers. The significant increase in GAG composition in the ECM would certainly disturb this spatial order[74]. Also overtime, alignment of the fibrils declines in MMVD. Age of the patient, as mentioned several times previously, is in clear association with the prevalence of MMVD. Collagen is the only protein in humans that shows definite age changes[70]. Aging collagen and its effects in MMVD are not fully defined in literature; however, a clear correlation exists between them. It should be noted that despite this significant correlation, that MMVD is not simply an aging process. As mentioned, in MMVD collagen fibrils become

disorganized thus endangering the mechanical integrity of the valve. In elderly healthy patients however, collagen tends to have the best defined patterns and degree of regularity[74]. Also depending on the form of MMVD, Barlow's disease for example, the patients most affected by the disease may in fact be younger in age when compared to other forms such as fibroelastic deficiency[73].

1.3.3 Mitral Prolapse:

Mitral valve prolapse is the most prevalent form of mitral valve disease and is largely degenerative in nature. It affects more than 144 million people worldwide and about 3% of the adult population in the US[75]. It is the most frequent cause of chronic, pure and isolated mitral regurgitation[75]. More specifically, mitral valve prolapse (MVP) is a form of organic mitral regurgitation. It is simply characterized by incorrect closure of the leaflets resulting in their billowing into the atrium. This inadequacy in function allows regurgitant blood to flow back up into the atrium and contribute to the well-known and deadly downstream effects. As a form of organic MR, this specific pathology is predominantly a result of the degenerative etiologies present in MMVD, described above.

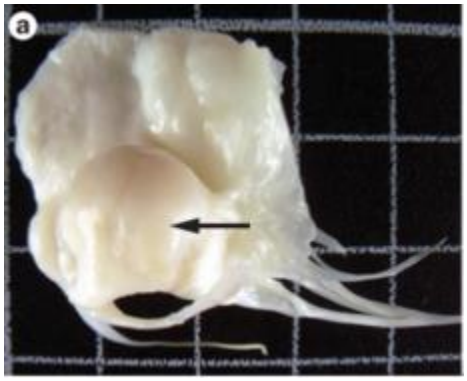

Figure 1.13: A resected mitral valve with prominent leaflet thickening and opacity and a prolapsing and domed posterior leaflet (arrow)[27].

As a form of MMVD, there are various causes of mitral valve prolapse, all of which are some disruption of ECM homeostasis resulting in incompetent valvular components. For example, degeneration in a myxomatous valve can result in changes to the annular complex. Changes to this or other structures can cause regurgitation from prolapse[76]. Degeneration of the chordae tendinae can result in chordal rupture, which is in fact the most common finding with sufferers of mitral prolapse[63]. There are many affected by abnormal leaflet structures are well. In fact, there is a spectrum of prolapse diseases that result from abnormal leaflet sizes. Common examples include Barlow's disease and fibroelastic deficiency (FED), which range from excessive to insufficient ECM content respectively. In fact, MMVD is more currently called Barlow's disease and is characterized by large valvular size with excessive leaflet tissue, dilated annulus, as well as thickened and elongated chordae. FED, a less common etiology, is more prevalent in older patients. This condition is associated with a fibrillin deficiency that often lead to a rupture of one or more thinned and elongated chordae, usually involving the middle scallop of the posterior leaflet. The chordae are thin and friable. This can all contribute to regurgitation and lessened coaptation[63]. Marfan's syndrome is a common condition of degenerative valves. It is a genetic disorder of the connective tissue[63]. Similar to Barlow's disease, a patient with Marfan's will also experience a dilated annulus; however, unlike Barlow's this syndrome involves the aortic root and aorta. It can be a systemic disease than Barlow's often affecting the other connective tissues.

Another etiology of mitral valve prolapse is bacterial endocarditis. Endocarditis occurs when bacteria enter the bloodstream (bacteremia) and attach to a damaged portion

of the inner lining of the heart or abnormal heart valves. Only those bacteria that are able to stick to the surface lining of the heart and to abnormal valves tend to cause endocarditis. The ability of these bacteria to stick to the surface lining is aided by a preexisting microscopic clot that often forms at these abnormal sites. This often results in ruptured chordae[77]. Bacterial endocarditis is associated with necrotizing lesions in the leaflets, and annular abscess[55].

Papillary muscle rupture is also a common cause of mitral valve prolapse. This can occur through myocardial infarctions. After infarction, the papillary muscles are displaced laterally, apically and posteriorly, pulling the leaflet into the left ventricle. Distortion is prominent in the basal anterior leaflet, creating a bend[57]. Papillary muscle dysfunction plays only a minor role compared with apical and inferior papillary muscle displacement caused by ischemic LV remodeling and dilatation. As described above, due to the mechanical limitations of the chordae, the displacement of the papillary muscles is distributed to the leaflets, causing apical leaflet displacement, and impaired coaptation. Together with annular flattening, enlargement, and reduced contraction, mitral valve tenting affects leaflet coaptation and causes functional mitral regurgitation[57].

1.4 Current Solutions for Mitral Valve Insufficiency:

Dysfunction of the mitral valve (MV) apparatus is a common ailment of the global population. It is especially common with advanced age, affecting almost 10% of individuals 75 years of age[78]. The sheer number of sufferers of mitral valve pathologies warrant a myriad of solutions aiming for the reestablishment of proper function for the valvular apparatus. Pathological prevalence has driven demand from both the clinical and

engineering spheres to develop a solution for dysfunctional mitral valves. Over the course of several decades, beginning in the 1960's, advancements in engineering and material sciences led to advances in treating these diseases. Annually there are more than 300,000 people worldwide, 44,000 from the United States alone, that undergo open heart surgery to treat mitral valve diseases[79]. Many of these operations utilize replacement prostheses or advanced repair techniques. Replacement of the mitral valve has been available to patients for the greater part of 4 decades. Mitral valve replacement is still the gold standard in developing countries[55,80–82]. During these decades of prosthetic mitral valves, advances in surgical techniques and improvements in imaging and material development have paved the way for the successful restoration of mitral valve function using surgical repair. While there are various methods for repair, generally all repair methods aim to achieve the best leaflet coaptation area during systole and reduction of any regurgitant flow[83]. Recent advances in repair have focused on restoring and/or reducing the annular area, preserving the 3D annular geometry. Due to the success of surgical repair of the mitral apparatus, rates for repair have gone significantly up in recent years. Currently MV repair represents over 60% of surgical cases compared to valve replacement[84]. In developing countries, however this number is reversed largely due to the lack of education, experience and therefore skill to repair the MV. Of the 44,000 MV surgeries in the US, this represents less than half of the patients with severe MV regurgitation and could benefit from some form of intervention[14,78,85]. This is a similar statistic in most of the world due the pathology's asymptomatic presentation.

Predictable and reproducible results are considerable motivators when choosing repair vs replacement. Thanks to the work of Carpentier, Duran, and others, MV repair is generally the accepted alternative to valvular prostheses with most surgeons recognizing its superiority in both early and late results. However as there are many pathologies of the MV, there are several general considerations that must be made to determine the best course of action. Surgeons must bear in mind the continued degeneration of the valve. How will functional vs organic regurgitation affect the choosing of the repair or replacement? Will this surgical correction need to grow with the pediatric patient? The left ventricle is remodeling, will a repair now serve the patient years from now? Surgeons must tailor their solutions to the patients they have. Trends in MV dysfunction however due point to a heavy increase in reparative methods as compared to replacement, at least in the western world.

1.4.1 Mitral Valve Replacement:

Heart valve prosthetics were born from concomitant developments in engineering and material science that solved a basic engineering question, how to fix a leaking valve. The first valve replacement, the ball and cage model, was used in 1960 and improvements upon the design and the materials used were completed over the next decade[81]. Alongside the advancements of mechanical prosthetics, so too did the advancement of fixative techniques on tissue. Glutaraldehyde was initially used to fix porcine tissue, thus creating bioprosthetic mitral valve replacements with much improved hemodynamics[86]. These two avenues for MV replacement, mechanical and bioprosthetic, are still the current treatment options several decades later. During their tenure, minor yet important improvements on their designs were achieved with advancements in polymer science and tissue fixation.

Mitral valve replacement surgery is most commonly performed using a vertical sternotomy[86].

As mentioned, mechanical prosthetics evolved originally from the ball and cage model, current models consist of pyrolytic carbon, a material similar to graphite. This material helps limit blood clots from forming on the material. Most models for MV replacement utilize a bileaflet design, with two semicircular disks surrounded by a suturing ring[83]. There are several large companies that offer their own take on this general bileaflet, pyrolytic carbon design. Each of these companies which include Medtronic, St. Jude, On-X, Sorin Group, etc. claim to have advantages over the other, many of which are minute changes in the hinges or use of an open pivot design which is intended to minimize the recesses or cavities present for example. Due to its design and material properties, mechanical replacements, as compared to bioprosthetics, tend to be more durable as a replacement[83]. Three important factors that define mechanical valves' durability are closing load, material fatigue and cavitation[81]. Transvalvular pressures are the major load placed on mechanical valves, which is generated at and after closure. This can lead to impact wear and friction wear in the prosthetic. This load is felt the most at the hinges and joints associated with the bileaflet design. Use of pyrolytic carbon largely alleviated the material fatigue that metals and alloys experience as the initial mechanical valves. The third mode of failure, cavitation, is due to the formation of microbubbles due to pressure reduction.

Figure 1.14: Examples of variability in mechanical heart valves. Ball and cage, tilting disk and bileaflet valves are and have been used[81].

Bioprosthetic valves were developed to answer the thromboembolic complications found with mechanical valves. Animal tissues had to be chosen due their availability and the quantity needed for commercial use, therefore antigen-masking techniques were developed. Glutaraldehyde was chosen as the cross-linking chemical to treat either porcine valve leaflets or bovine pericardium. By extracting any un-bound glutaraldehyde from the treated tissues, improvements were seen in allowing endothelial growth and calcification was markedly decreased in patients[81]. While not as durable as a mechanical valve, bioprosthetics generally last between 15 to 20 years[87].

Due to their differing material compositions and benefits each affords, choice of the surgeon to choose a mechanical or bioprosthetic valve is largely patient specific.

Figure 1.15: Bioprosthetic heart valves from four of the major manufacturers[83].

There are many criteria that must go into this selection including symptomatic status, occurrence of thromboembolic episodes, and myocardial function[86]. Evaluating the patient's age, whether they have co-morbidities, and the risks associated with reoperation are all criteria that need to be determined before a surgeon decides on the proper valve prosthetic to use. Age is one of the most important criteria when determining valvular prostheses. For example, elderly patients (65 years or greater), are often given bioprosthetic valves due to lack of anticoagulant therapy needed for this valve. Younger patients often receive mechanical valves instead. Surgeons will also need to look into the lifestyle of the patients, their body size and thus their left ventricle function[88].

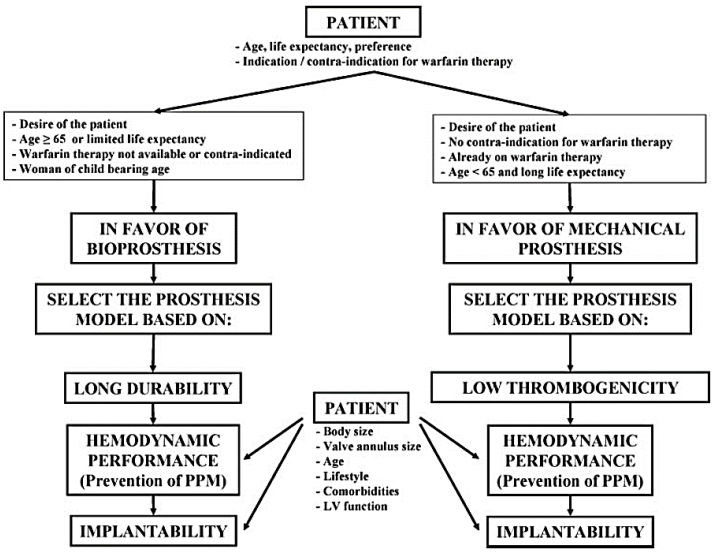

Figure 1.16: Decision tree for valvular prosthetic options[88].

Mechanical valves are preferred when the patient has no contradiction to anticoagulant therapies or is already on one, the patient is at risk of accelerated bioprosthesis structural deterioration due to their age (young patients) and the patient is younger than 65 years and has a long life expectancy. The bioprosthetic valve is preferred

on the other hand if an anticoagulant regimen is unavailable for them due to compliance problems or lifestyle, and the patient is at or greater than 65 years of age and has a limited life expectancy. Also worth noting is that bioprosthetics are preferred for woman of childbearing age. This is due to the fact that these women, who are or may become pregnant, cannot undergo anticoagulant regimens. It is also important to note however, that bioprosthesis degenerate more rapidly during pregnancy and in younger patients[88].

Despite some success from mitral valve replacements, improvement in their design and functionality stalled several decades ago and remain an unsatisfying option for valvular replacement. Given the fact that these prosthetics are foreign objects in a high stress environment consisting of living cells and rapid fluid flow, evidence has shown that these replacements cannot avoid cascades of biological events. For example, shearing and fluid flow across the mitral valve leads to platelet activation, which launches the coagulation cascade. Despite small advances in material science, the body still chronically reacts to these nonnative devices. This has been confirmed in mechanical valves' continued vulnerability to thrombus formation due to high shear stress (activating platelets), flow separation, and blood damage. The most commonly used mechanical valve, the bileaflet valve, encourages thrombus formation at its hinges due to high stress, leakage regurgitation and stagnant flow in this area[81]. Due to this risk of thrombus formation, anticoagulation is still required for patients. The rate of embolic events ranges from 0.6 to 6.5% with bileaflet prosthesis[89]. Due to the need of long-term anticoagulation, there are inherent risks for hemorrhagic complications[81,90]. Total rates of major bleeding were between 3.2 and 12.9%[91]. Thromboembolic events showed up in about 4.4% of pregnant women[92].

The anticoagulants used ranging from Coumadin, heparin and warfarin, were also associated with fetal malformation[92].

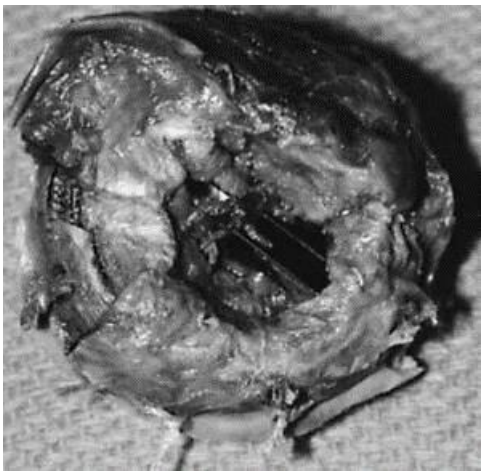

Figure 1.17: Example of thrombus formation on a bileaflet mechanical valve replacement[93].

Another risk associated with mechanical heart valves is pannus overgrowth. Excessive tissue growth can occur at the sewing ring and can lead to insufficiency of the prosthetic. Pannus overgrowth is associated with obstructive valve failure in 53% of cases[94]. Mitral valves show pannus formation on both the atrial and ventricular sides. This pannus formation is largely caused by macrophages and foreign giant body cells reacting to the sewing ring material.

Pediatric patients are also sufferers of the consequences of mechanical MV prostheses. When replacement is elected as the best option for pediatric patients, mortality rates range between 10 and 20%[95]. This is due to the complexity of the surgery and coexisting cardiac abnormalities. It also goes without saying that long-term results for these children are difficult to obtain due to somatic growth of the patient. There is not a solution that exists for replacement options that can withstand normal growth of the patient. Tissue-derived bioprosthetics were supposed to solve the issue of thrombogenicity presented from

the mechanical valves by using tissue that was much more hemodynamically efficient. This risk undoubtedly went down, although the rate of thrombus formation during the initial three months post bioprosthetic insertion occurred at a rate of 55% often incurring an initial anticoagulant regimen[96]. This rate steadily declines at rate of about 10% and falls to 2.4% thereafter[96]. Despite this apparent alleviation of the mechanical valve's Achilles heel, bioprosthetic valves face other inherent complications. Due to the absence of living tissue and the attempt to mask xenogeneic antigens, faults in this valve's design are numerous. Similar to the triggers mechanical valves put forth to initiate tissue overgrowth on the sewing ring, this process is also experienced by tissue valves due to insufficient masking of antigens and the onset of inflammation. This is not a new problem however as low-grade glutaraldehyde used in commercial fixation has long known to reduce immunogenicity but not abolish it[97]. In addition to the immune response elicited by the patient, degradation of the prosthesis is common through inflammation. In the majority of explanted bioprosthetic valves, inflammatory cells are found rampant within and covering the surface of the tissue[98]. Macrophage-mediated degradation is then shown to break down these tissue valves over time. Mechanically speaking, bioprosthetics are also not very stable. The VICs inside the tissue are devitalized due to crosslinking and therefore cannot repair or remodel the tissue due to the harsh mechanical stresses these valves endure. As many as 75% of failed porcine prostheses in the mitral position show a rupture on one of the free edges[81]. Structural degradation is also due to calcification of the valve. For one, glutaraldehyde is a known promoter of calcification. More importantly though is that this chemical treatment destroys the viability of the resident cells in the tissues. These nonviable cells are incapable

of remodeling collagen and therefore ongoing repair of bioprosthetic valves is impossible. Also, devitalized VIC fragments serve as nuclei for calcification[90]. Calcification is initiated predominantly at the devitalized VICs membranes and at areas where mechanical stress is concentrated. Normal VIC function involves maintaining a proper calcium gradient in the cytoplasm, and this cannot happen in nonviable cells[99]. Initial calcium deposits will eventually enlarge and coalesce grossly affecting the bioprosthetic valve. The biochemical differences in younger patients disallows long implant survival due to advanced calcification in the prostheses. It has also been shown that denuding of VECs during the handling process increased availability for infiltration by host cells.

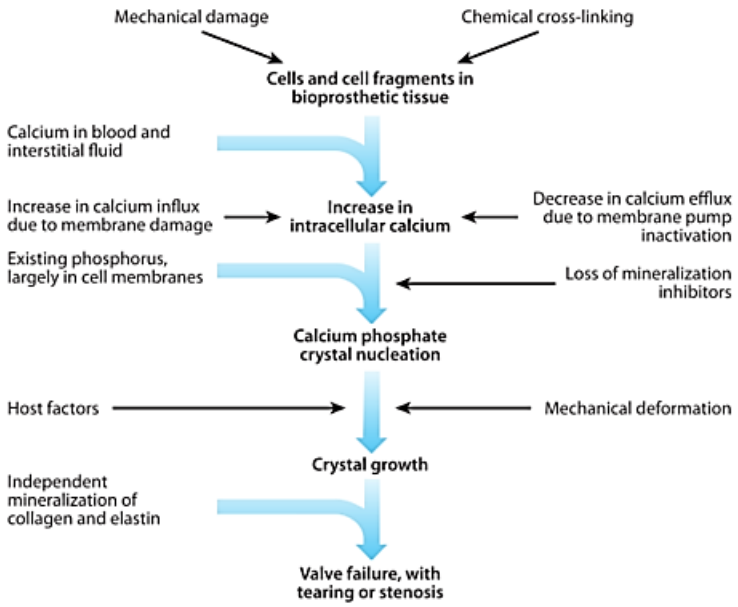

Figure 1.18: Mechanisms of calcification in bioprosthetic heart valves[90].

Overall, heart valve replacements have aided many patients. However, these prostheses have many drawbacks and are not permanent solutions. In fact the ten year survival rate following mitral valve replacement is about 50%[86]. While structural degradation is not relevant in mechanical heart valves, thrombus formation and chronic

reaction from the host limit its lifespan within the patient. Structural degeneration is quite relevant with bioprosthetic valves as it typically affects 20-40% of recipients after 10 years and over 60% after 15 years[86]. Due to their unreliability patients often must undergo repeated surgeries to replace these failing prosthetics, and with each successive surgery patient mortality can increase up to 20% each time[100]. Therefore, pediatric patients face a dire future with heart valve replacements. Lack of progress in this field of cardiovascular engineering has especially hurt developing nations, who represent about 80% of the world's population and cardiovascular disease sufferers. Many of these countries do not have the socioeconomic capabilities to support heart valve surgeries for its citizens and once they do reach this point, heart valve replacements will dominate their options as complicated reparative techniques are out of the question. Therefore lack of innovation and improvements for these designs have really hurt the developing world.

1.4.2 Mitral Valve Repair:

To combat the well-known and chronicled failures of replacements, surgical correction of the mitral valve apparatus through repair has risen in support. While the complicated anatomy of this "valvular machine" presents an intricate case for any surgeon, success rates and usage rates of these techniques have risen as replacement technologies decrease in use.

Table 1 Functional classification of mitral valve regurgitation

- Type I : normal leaflet motion
- Type II : excessive leaflet motion (one or both leaflets prolapse)
- Type III : restricted leaflet motion
  - IIIa: opening is restricted
  - IIIb: closure is restricted

Figure 1.19: Carpentier's classification of mitral valve regurgitation[101].

The overarching goal of surgical repair of the MV is to restore the gross natural geometry of the mitral valve to allow for coaptation. Some of the advantages of mitral valve repair include low rates of thromboembolism, reduced need for anticoagulation, good long term prognosis and a decreased risk of endocarditis[102]. As mentioned, Carpentier, Duran and others developed several surgical techniques and classifications for mitral valvuloplasty. Many of the advantages with surgical repair parallel the disadvantages of valvular replacement. Long term results for repair also appear to show good results with valvuloplasty having lower operative mortality, better preservation of left ventricular function and superior survival rates[103]. Many of these corrections pioneered by Carpentier were based on a classification system. Because of the apparent advantages, the threshold for patients has been lowered to allow those patients with asymptomatic or early symptoms. Trends in mitral valve surgeries have shown a significant increase in the use of repair over recent years. This however represents less than half of those that would benefit from some form of surgical intervention[14]. This, as mentioned, is often due to mitral pathology's tendency to be asymptomatic and show itself in the later decades of life. It is important to note however, that valvuloplasty is far from being the norm in the developing world. Due to socioeconomic difficulties, lack of experience and education in these regions, surgical

repair of the mitral valve is unpopular. It could be argued that first world countries are at fault for this in that they had not developed innovative solutions for decades regarding mitral valve pathologies. Whatever the case, replacement surgeries still dominate the regions of the world that have the most patients that need such interventions.

According to the classifications defined by Carpentier, general considerations must be taken when evaluating which type of repairs would best benefit the patient. This is dependent on the pathology afflicting the patient and the severity. Type I is present when there is dilation of the annulus due to endocarditis or some cardiomyopathy. Type II pertains to rupture or elongation of chordae tendinae, often due to degeneration or papillary misalignment. Type III has two sub-types, type IIIa occurs with commissural fusion, leaflet, and chordae thickening as in myxomatous valves or rheumatic disease. The second subtype, type IIIb, is often due to chordal retraction (rheumatic) or papillary retraction (ischemic) or displacement due to functional or ischemic cardiomyopathy[(101)]. For a repair to be successful, proper preoperative or intraoperative work, such as a transesophageal examination, are imperative for full evaluation of dysfunction. Overall, the goal of any mitral repair is to first address the dysfunctioning motion of the valve, and secondly to correct and stabilize the shape of the annulus by an annuloplasty ring. Therefore providing a valve that no longer leaks while achieving anatomical restoration.

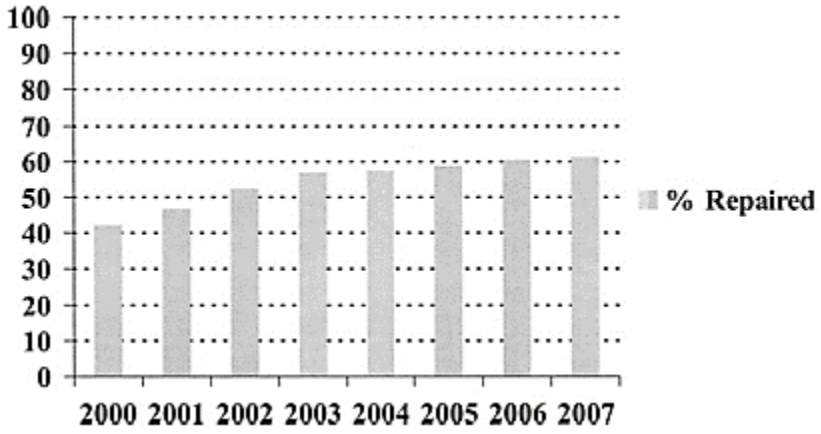

Figure 1.20: Trends in mitral valve surgeries favor reparative techniques in recent years[84].

One of the drawbacks of mitral valve repair that will be discussed later is that there are many different ways to repair a mitral valve. This can differ between each of the classifications mentioned above and even within each classification. Therefore, to avoid creeping of the scope in this review, concentration will be placed on several general areas and common reparative techniques. The first of which is the use of the annuloplasty ring. It is important to remember that the hyperbolic paraboloid shape of the mitral annulus is crucial for optimal force distribution throughout each of the valve's components. Therefore, reestablishment of this shape is paramount in mitral repair. This is the goal of the annuloplasty ring, to restore mitral valve competence by reestablishing anatomical equilibrium in the valvular apparatus. Originally the annuloplasty ring used by Carpentier was rigid and flat, this was called the "French Correction"[104]. However, it was apparent that the annulus moves dynamically during normal function, therefore the Physio ring was developed and more surgical techniques surrounding these annuloplasty ring like the "American Correction" were designed[83,104]. Today, all manner of annuloplasty rings exist, including rigid, flexible, semi-rigid, incomplete or complete, planar or saddle-shaped,

adjustable and non-adjustable[83]. In general, flexible incomplete bands are designed to preserve the contour of a healthy annulus, semi-rigid rings are to maintain coaptation and integrity of the valve especially during systole, and finally rigid valves are used to provide solid support to reshape very dilated annuli when the patient has significant ventricular dilation[79]. Overall, the mitral annuloplasty has become the gold standard for treatment of most mitral etiologies.

Prolapse of the leaflets can often be a result of degenerating or ruptured chordae tendinae[105]. Originally reparative techniques centered on chordal transfer where one chordae would be removed and then re-sutured where the surgeon saw fit[101]. However, results from this procedure were not optimal and therefore other sources of chordae had to be used. Expanded polytetrafluoroethylene or ePTFE, was then discovered to provide adequate mechanical strength and host incorporation. ePTFE is a thermoplastic polymer used first in several other applications. It has great physical, chemical, thermal and of course mechanical properties. It is highly flexible with a high tensile strength and is also resistant to fatigue[105]. ePTFE is a nonabsorbable monofilament that along with its micropores allows for great mechanical and biological properties. The pores allow for the covering of these neochordae in fibrous endothelial tissues and it provides attachment for fibroblasts[105]. Chordal length for surgical repair is often decided using transesophogeal echocardiography. While mid-term results seem promising for this avenue of repair however long term results are very limited[105].

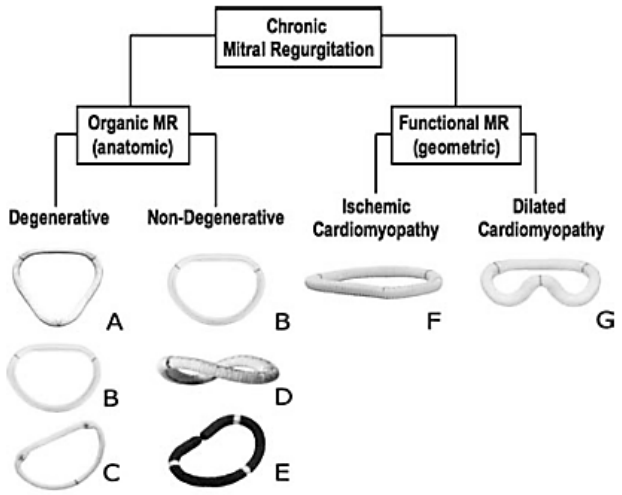

Figure 1.21: Variability in annuloplasty ring design for various pathological classifications[85].

As mentioned, mitral repair methods were used to parallel the disadvantages of replacement. One example of this is the utilization of catheter-based interventions as opposed to vertical sternotomy used in replacement surgery. There are two areas of the mitral valve where catheter interventions are used, the leaflet and the annulus. The Mitra-Clip™ from Abbott Laboratories is the only FDA approved that is alternate to mitral regurgitation surgery[83]. This device used a small clip to grasp the two leaflets of the mitral valve thus emulating the edge-to-edge repair instigated by Dr. Alfieri. Edge-to-edge repair essentially creates a tissue bridge between the two leaflets alleviating some regurgitation in patients with decent efficiency[57,85]. Intervention of the annulus via catheter is for reduction of annular dilation, attempting to restore the optimal valvular shape. Percutaneous valve replacement and treatment are also growing minimally invasive surgeries. Percutaneous mitral balloon valvutomy has emerged as a choice for patients with severe mitral stenosis brought on by rheumatic fever[106]. Complete valve replacement through transcatheter mitral valve replacement has also been attempted. Several products

including the Tiara™ from Neovasc, The Mitralign™ from Mitralign, and FORTIS from Edwards Lifesciences to name a few[83]. Other minimally invasive surgeries include the use of robotics to repair an insufficient mitral valve[107].

In this review of literature regarding mitral valve repair, many of the articles report large success with the majority of corrections quite durable while still avoiding the apparent disadvantages of valvular replacement. However, a very recent review by the New England Journal of Medicine on the two year outcomes of patients with mitral repairs paints a different picture[108]. Overall, patients who received repairs had significantly more reoccurrence of moderate or severe regurgitation two years after surgery. In fact the rate of reoccurrence for replacement patients was 3.8%, while the rate for the repair group was 58.8%[108]. Part of these discrepancies may lie in the controversy surrounding the most effective surgical strategies. Many clinicians prefer differing strategies for mitral valve repair. Not only that, but many articles in current literature note that repairs should only be conducted by experienced centers and surgeons as mitral valve repair surgeries are inherently complicated[107]. Therefore severely bottlenecking opportunities for patients to receive treatment. A recent review also noted severe practice gaps in clinicians pertaining to mitral valve repair, proper identification of pathological classifications, and preferred choice of treatment for their patients[109]. Annuloplasty treatment, the current gold standard for repair, can result in function mitral stenosis and is associated with a high rate of recurrent regurgitation[108]. The much maligned mitral valve replacement on the other hand has shown less reoccurrence of mitral regurgitation with favorable ventricular remodeling. Compared to replacement, reparative techniques had significantly higher incidence of heart

failure, reoccurrence of moderate or severe mitral regurgitation[108]. Reoccurrence of regurgitation is of course directly related to a predisposition to heart failure, atrial fibrillations and repeated visitations to the hospital for treatment. Replacement chordae have also show to rupture over time[105]. In addition, it goes without saying that reparative techniques are difficult to perform on pediatric patients due to their smaller valve anatomy. Also, any repairs such as an annuloplasty ring or artificial chordae cannot grow with the patient overtime, still opening these patients up for reoperation in their near future. Overall, from this two-year study, replacement techniques are largely more reliable long term compared to reparative techniques and shows significantly less reoccurrence for mitral regurgitation.

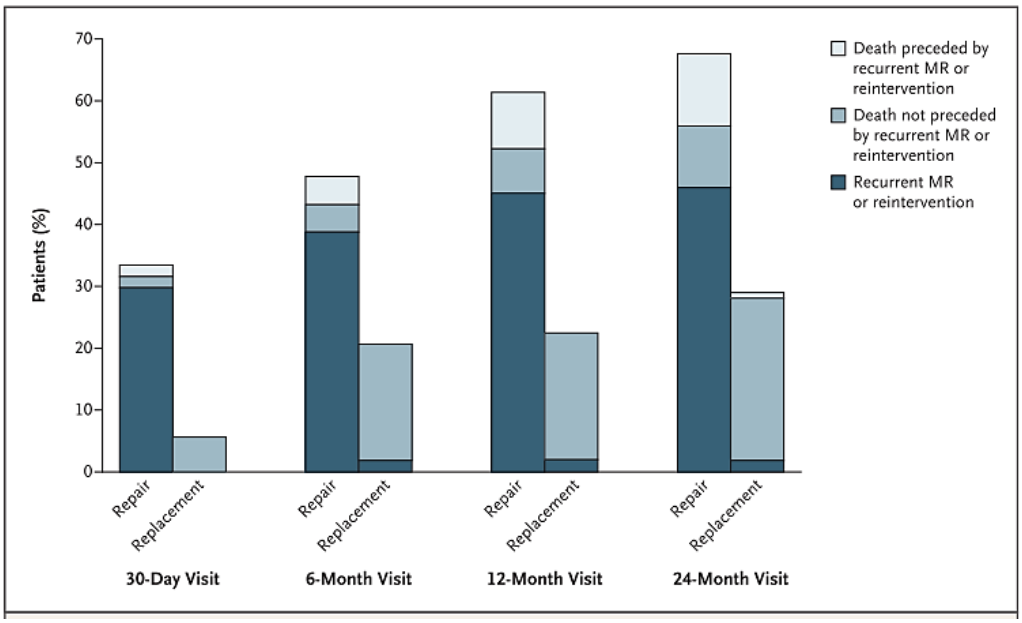

Figure 1.22: Cumulative failure of mitral valve repair or replacement[108].

This revelation regarding mitral valve repair leaves one surely disconcerted. On the one hand, mitral valve replacements have a long history of complications including thrombogencity, anticoagulant therapy, degradation, calcification and many more. On top

of this replacement techniques and devices have largely remained unchanged for 4 decades. To combat this reparative techniques were developed and while these do report in some cases improved success in treating mitral insufficiency, it appears that these positive results were short lived as reviews show that patients who undergo surgical repair are significantly more likely to have recurrent regurgitation resulting in reoperations, higher chances for related heart failure, ventricular remodeling and more. Neither option offers optimal results for pediatric patients who are in need of a more permanent solution for their growing bodies. This is nothing to say that developing countries are also far worse than first world nations that at least have opportunities for repairs. These countries' patients, who are the bulk of valvular disease sufferers, often have no access to heart surgery. Cardiac surgery is only available to about 11% of Chinese citizens and 6.9% of the Indian population[81]. There is serious deficiency is satisfactory and long lasting solutions for patients with mitral valve pathologies. Considerable progress must be achieved for all patients due to the lack of ideal solutions and the rising prevalence of mitral valve diseases.

1.5 Heart Valve Tissue Engineering:

Current treatment options for mitral valve insufficiency are limited in their duration, functionality, and true benefit to patients around the world and in any age range. This is true despite the enormous demand for permanent solutions to mitral valve diseases. Mitral valve replacements are thrombogenic, elicit pannus overgrowth, and calcification. Similarly as noted, reparative techniques offer significantly worse results regarding reoperation which leads to a steep slope of dangers for the patient. Also, it is important to remember that there are no true options for pediatric patients. No current option in mitral

valve repair or replacement can survive growth of the patient. Therefore, researchers have turned to tissue engineering to deliver an ideal solution to combat mitral valve pathologies.

1.5.1 Introduction to Tissue Engineering Paradigm:

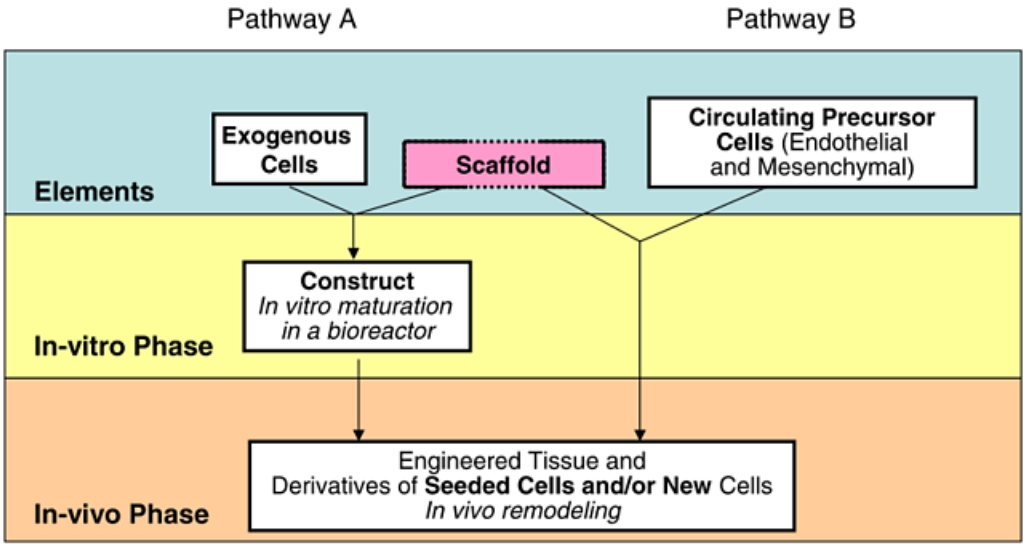

Figure 1.23: The general tissue engineering paradigms. (Pathway A) This is the conventional incorporation of seeding cells into a scaffold, an in-vitro phase for preconditioning and an in-vivo phase of tissue growth and remodeling. (Pathway B) This modified paradigm does not utilize the in-vitro phase but instead depends on resident, circulating cells of the patient in-vivo to repopulate the scaffold and spur tissue growth and remodeling[110].

Tissue engineering is a cross-disciplinary science between engineering principles and biology to overcome the limitations of artificial heart valves. The aim of tissue engineering is to utilize a 3D scaffold as a specific tissue template to develop new, healthy tissues from their specific cellular components[111]. The scaffold, which provides the crucial microenvironment, allows for cell attachment and tissue growth. Specific cells are incorporated in these matrices to develop or regenerate new tissue to replace diseased or damaged tissues. The ultimate goal of tissue engineering is to fabricate a patient-tailored

neotissue from the combination of matrix and specific cells. Thus utilizing the characteristics of the original tissue, such as adequate mechanical properties, optimum hemodynamics, non-inflammation, non-immunogenic, and durability due to the capacity to remodel and heal. Tissue engineered constructs for mitral valve tissue engineering (MVTE) should be non-thrombogenic, non-obstructive, non-immunogenic, self-repairing, it should allow growth with the patient, allowing for a pediatric solution, and these constructs should be a permanent, integrated tissue replacement[110,112–115]. As discussed, the general tissue engineering paradigm follows the incorporation of 3D scaffolds, with a cell-source specific to or with the potential to, differentiate to the neotissue, in-vitro preconditioning of the constructs to encourage cell attachment and development, finally followed by implantation into the patient and in vivo remodeling. As defined by Mendelson's review, the more traditional, paradigm of scaffold, cells and maturation before implantation into the patient is widely accepted as framework from which most tissue engineering ventures follow.

In above the classical paradigm, there are specific design criteria that must be met for a tissue engineered mitral valve. Considerations for these must include their overall function as a valve, the extreme stresses and strains experienced repeatedly by this tissue, cellular function, surgical considerations, and risks during implantation like infection and thrombogenesis. Many of these design criteria are a function of the environment with which these tissues would experience. Rapid and repetitious opening and closing corresponding to the pressure and shear forces acting on the valve define the needs for durability and resistance to degradation. Also, to be successful as a tissue engineered

construct, the living cells within the scaffold should inhibit thrombosis, resist degradation, resist calcification, have remodeling potential, and function as healthy quiescent VICs and VECs.

Table 1: Design criteria for tissue engineered mitral valve[112].

Design Parameter	Tissue Engineered Mitral Valve
Closure of leaflets	Rapid and complete
Fluidic function	Identical to the native valve
Risk of thrombosis	Inhibition by functioning VECs
Surgical insertion and considerations	Easy and permanent insertion using current surgical methods
Risk of structural degradation	Resistant to degradation and calcification
Risk of infection	Resistant
Cellular function	Quiescent VIC and VEC function
Tissue function	Durable and stable
In-vivo monitoring requirements	Cellular physiological and phenotype Changes in mass and/or tissue components Structure and mechanical properties

Specific to the mitral valve, each of these design criteria must apply to the four tissue types working cohesively in the valvular apparatus. While unique in their role for mitral coaptation, the annulus, leaflet, chordae tendinae, and papillary muscles making up the mitral valve scaffold must be able to function under each of those design criteria. It could also be added that in addition to functioning under these criteria, it is imperative that they all function together as unit. Difficulties in developing a mitral valve scaffold may in fact lie in the complexity of its anatomy. Literary searches for mitral valve tissue engineering to date yields 145 search results in PubMed, many of which are found in review articles. This is compared to the 518 for aortic valve tissue engineering and 1223 for heart

valve tissue engineering in general. This discrepancy isn't for lack of need as mitral valves are the most diseased and degenerative in the world[53]. The rise of successful surgical repairs in treating mitral valve insufficiency has probably driven this shortage. However, recent literature as mentioned, draws the durability of these repairs deeply into question[108]. The potential for a tissue engineered mitral valve is great.

1.5.2 Scaffolds in Heart Valve Tissue Engineering:

To achieve each of the above design criteria and produce a functional, durable valve tissue, choice of scaffold is critical. Scaffolds provide cells a microstructure that guide their growth, differentiation and synthesis of extracellular matrix[116]. Therefore, knowledge of how the native valvular environment controls cell fate and function should serve as a guide. It is also important to note that these environments also play a large role in progression of mitral valve pathologies and therefore knowledge of the role this microstructure plays in mitral valve disease can be useful. The mechanical and biochemical makeup of the VIC extracellular matrix are developed and defined by the specific cells that populate it. VICs are very sensitive to this environment. Regulation of these cells is often determined by the mechanical properties or ECM elasticity which can regulate the pathological differentiation of these cells[117]. For example, depending on the elasticity of the ECM, VICs can remain fibroblast-like on soft substrates or differentiate to osteoblasts or myofibroblasts on intermediate to stiff substrates[44,116,118]. Aside from mechanotransductive cues provided by the microenvironment, scaffold choice is also influenced by protein interactions providing biochemical information and direction for the incorporated cells. Myofibroblast differentiation is generally promoted by adhesive proteins like fibronectin, fibrin, elastin

and adhesion peptides RGDS[119–121]. Incorporation of growth factors like TGF-β1 can also be utilized within scaffolds to encourage the desired activation or differentiation of the VICs. Interest in the customization of scaffold properties has led to the development of synthetic scaffolds for heart valve tissue engineering.

The popularity of synthetic scaffolds lies in their advantage of control over their material properties. These properties should encourage cell attachment, migration, proliferation, differentiation, and eventually matrix formation. Bioresorbable scaffolds serve as a temporary scaffold which cells can remodel and develop their own ECM. The chemical and physical properties determining how long this scaffold lasts are tailored to the cell types and applications of the finished tissue. Structurally, these scaffolds should have an extensive network of pores and channels not only for cellular attachment, but also for the delivery and diffusion of nutrients and oxygen. As mentioned these materials should all be biodegradable and biocompatible. Mechanically speaking, the properties of a synthetic scaffold should be prepared to handle the large and repeated loads experienced billions of times in one's life. Synthetic materials are easily reproducible and well conceived which allows for a more customizable and easily translatable scaffold material. There are several common polymeric materials used to develop synthetic scaffolds for tissue engineered heart valves. These include polylactic acid (PLA), polyglycolic acid (PGA), polycaprolactone (PCL), Polyfumarates (PF), and polyglycerol sebacate (PGS). Each of these has been reported for use in cardiovascular uses and are all approved by the FDA as biocompatible polymeric materials[111]. PLA and PGA are probably the most commonly used for tissue engineering purposes. PCL and PF are largely used for drug

delivery purposes and have a long degradation rate of about 3 years, while PLA has a degradation rate of 2 years. This is in comparison to the 2-3 months it takes for PGA scaffolds to degrade[111]. Unfortunately, studies have shown that these common copolymers were thicker and less flexible than natural valves[122]. This rigidity would not allow for proper coaptation. To solve this, application of P4HB (poly-4-hydroxybutyrate) was used to enhance the flexibility and plasticity of these polymers[123]. This combination allows for much greater flexibility of these polymeric heart valves. Use of these synthetic materials for a tissue engineered valve however introduces several challenges. PGA and PLA for example are considered poor substrates for cell growth in-vitro[110]. In addition, ECM proteins are not usually constituents in a synthetic environment. To combat these disadvantages, bioactive synthetic materials are being developed to mimic the natural ECM and its function[124]. Recent advances show the incorporation of synthetic polymers that carry spatial and biochemical information affecting cellular function and remodeling[125]. These scaffolds can also be used as a vehicle for drug delivery. Growth factors, known to influence cell growth, proliferation, and migration, can be incorporated into these synthetic scaffolds[114]. Mostly synthetic hydrogels can also be used as an injectable scaffold. Despite some of their advances, there are some drawbacks to using these synthetic scaffolds. These scaffolds still have difficulty controlling cell adhesion and tissue reorganization, this is shown partly in the limited diffusion of cells into the scaffolds. If the polymers do not completely degrade, there is a risk of inflammation. After and during degradation, any space that was formerly occupied by the synthetic material is often replaced with scar tissue[110].

There are four common methods for fabricating synthetic scaffolds. One of the more common methods is solvent casting. In this method the polymer solution is cast with water soluble particulates into a mold[111]. The evaporation of the solvent makes the pores. Extensive use of this solvent may affect cell attachment and proliferation. Electrospinning is also used as a versatile yet straightforward technique. With this approach, a high electric field is used for the ejection of the conductive polymer jet from a needle which is connected to the solution containing the polymer[111]. Using this technique, electrospun scaffolds are highly porous with a high density. Diameter of the electrospun fibers can be tailored to the scaffolds requirements. Process factors include polymer and solvent, voltage, flow rate from the needle, and the distance from the needle and collector. Electrospinning is probably the preferred scaffold generating technique due to its customizability and porosity for VICs. The fourth most common approach for synthetic scaffold fabrication is solid free form. This translates computer data from drawings or MRI data for example and is 3D printed. 3D bioprinting has begun to rise in popularity due to the flexibility and tailoring it allows using the CAD programs on the computer.

Issues surround biocompatibility; a low degradation rate and inflammation are major drawbacks of synthetic scaffolds. Therefore, utilization of natural materials present within the mitral valve ECM have been used for scaffold fabrication. These biologically derived materials are inherently recognizable by cells which are susceptible to the receptor binding ligands and cell-triggered proteolytic enzymes presented by biological scaffolds[124]. Constructs composed of collagen for example have been used to generate tubular blood vessels, chordae tendinae, and of course heart valve leaflets[126]. Scaffolds

made from natural materials give cells, in both their material properties and application type, a familiar environment. Valvular interstitial cells are very conscious to the chemical and mechanical environment surrounding them. Natural scaffolds utilize ECM components familiar to VICs to encourage a controlled, healthy proliferation, migration, and differentiation.

One of the most commonly used natural scaffold materials collagen, comprises the largest percentage of material in the valvular ECM. It is therefore one of the most commonly used platforms for developing living tissue engineered constructs. Due to collagen's less than ideal mechanical characteristics as well as antigenicity concerns, other materials are often used in conjunction. Elastin for example, one of the other major players in ECM makeup. Collagen and elastin scaffolds have elicited much improved mechanical properties[111]. Fibrin gels are another commonly seen natural scaffold. Easily prepared from the patient's blood, despite its poor mechanical properties, fibrin utilizes its bioactive nature to enhance cell growth and attachment[111,127]. Fibrin and its common partner fibrinogen, play large roles in blood clotting, cellular matrix interactions, and wound healing[128]. It is also useful as a sealant in a variety of clinical applications[127]. Glycosaminoglycans (GAGs), a common element in the heart valve ECM, can also be used as a scaffold for tissue engineering. Hyaluronic acid, like other natural scaffolds, relies on its bioactivity and the familiarity seeded cells have with it as an ECM component. Hyaluronic acid (HA) is largely presented as a hydrogel and can bind to proteins and cells through cell receptors. It is a key component in the wound healing process, and can maintained in hydrated environments conducive to cell infiltration[129]. As briefly

mentioned, hydrogels have often been used as a natural and as a synthetic 3D matrix in tissue engineering. Natural hydrogels like those composed of hyaluronic acid and fibrin, are inherently bioactive but also biocompatible[130]. Due their cell-friendly characteristics, production of ECM and an increase in cell proliferation are seen when using natural hydrogels for scaffolds or used to fill the interstitial space of other scaffolds[111]. VIC have also been incorporated in natural and cross-linked hydrogels facilitating good viability and providing a physiological representative environment to study VIC behavior[40]. Fibrin hydrogels are also common scaffolds for heart valve tissue engineering. They are constructed from purified fibrinogen and thrombin. It is common to include other plasma proteins such as fibronectin and other growth factors in fibrin gels to assist cellular function and proliferation[127]. One of the pitfalls of hydrogels however is their lack of mechanical stability[115]. This is especially critical for heart valves due to their incessant opening and closing. They also lack the anisotropic mechanical properties and topographical cues that provide mechanotransductive direction to seeded cells.

Another commonly utilized technique for scaffold fabrication is the decellularization of xenogeneic or allogenic heart valves. The goal of a decellularized scaffold is to take advantage of the ECM environment it can provide to seeded cells while also providing a collagen and elastin based scaffold that cells are inherently familiar with. The benefits of using the niche ECM for tissue engineering are great as this matrix provides the mechanical framework for the heart valve. The ECM acts as an inductive scaffold both mechanically and chemically. Mechanically speaking, this tissue was developed, repaired, and remodeled by the specific cells that inhabited it. Therefore structurally, it provides the

correct rigidity, porosity, insolubility and topography that heart valve tissues should possess[131]. The ECM also contains many functional components within it including collagens, glycoproteins, proteoglycans, elastic fibers and growth factors[131]. The specificity of this local microenvironment can also influence the maintenance of stem cell phenotype and differentiation. This ability allows decellularized matrices to be open for regenerative medicine applications. The process of decellularization is a technique that varies widely across the tissue engineering field. The overall goal of this technique is to eliminate the cellular content of a tissue while retaining the ECM structure and its proteins. To achieve this end, various methods of decellularization are used including physical, chemical and biological agents. Many researchers use a combination of detergents and biological agents including SDS, trypsin, EDTA, Triton X-100, sodium deoxycholate, sodium hydroxide, DNase/RNase[132,133]. Criteria for a successful decellularization have been established by several researchers for tissues to contain: less than 50ng dsDNA/mg ECM, less than 200 bp DNA fragment lengths, and no nuclear material in histological samples[132,133]. Any lack of confidence surrounding decellularized scaffolds centers on the danger of a residual cellular presence and lack of control over remaining ECM quality and defined components. However it is important to point out that there are at least 30 products currently on the market, including small intestinal submucosa (SIS), placed in thousands of patients that have gone successfully[134]. Potential for recellularization for seeded cells is also a recent design criteria, especially for decellularized scaffolds[135]. Overall, decellularized scaffolds have yielded the fasted method clinically through animal and

human studies and thus promises the most clinically translatable scaffold for tissue engineering[135–137].

Scaffold durability is of prime importance when considering scaffold potential. The mitral valve opens and closes an estimated 3 billion times during the average lifetime. Constant and repeated loads from transvalvular pressures also act on the valve. As mentioned, the mitral valve is hit with 120mmhg during ventricular systole and 10mmhg during diastole requiring an unparalleled resistance to cyclic failure[115]. Cardiac valves are also subject to large blood shear forces. The average peak systolic blood velocity usually averages about 1m/s through heart valves. These pressure and shear forces experience by the tissue engineered constructs must be a serious consideration.

1.5.3 Choice of Cells in Heart Valve Tissue Engineering:

In the traditional paradigm for tissue engineering, the incorporation of cells into scaffolds is critical for creating a vital construct. For a tissue, engineered mitral valve the obvious choice of cell type would be the VIC. This is the chief resident cell within the valvular matrix and therefore would be primed for utilization in a valvular scaffold. A similar sentiment would be made for VECs. However in no way could these cell types be used in a successful or clinically translatable fashion. To obtain these cells would require risky invasive surgery, and would damage the already diseased valve structure. Therefore, other sources of cells must be considered. Some researchers argue that there may not be a need to seed cells into or onto scaffolds prior to in-vivo transplantation. Long-term animal experiments have to clarify the need for pre-vitalization of the scaffolds is necessary to demonstrate growth and remodeling[135]. Difficulties lie still however with the efficiency

of cell seeding. There have been many attempts at recellularization of heart valve leaflets, but due to inadequate penetration of the cells or the length of time this scaffold-infiltration took, researchers are still looking for a more optimized approach[138]. Nevertheless, scaffolds recellularized with various cell types, to then be preconditioned in bioreactor systems is the current paradigm most researchers are following.

Choice of cell type is relegated to the specific applications researchers choose. There are however, several commonly utilized cell types used often. Stem cells offer a unique avenue for scaffold revitalization due to their capabilities of self-renewal and ability to differentiate into a variety of cell types. Ideally, for a clinically translatable option, autologous stem cells are used to eliminate the risk of immunorejection. Several common stem cell types are used in heart valve tissue engineering. Because stem cell differentiation can be directed by mechanical and biochemical stimulation, there are few constraints as to which type of stem cell should be used. The more important question becomes which microenvironmental cues will be used to induce the desired cellular behavior. One is the mesenchymal stem cell, which has the ability to differentiate into chondrogenic, adipogenic, myogenic and osteogenic lineages[139]. This lineage of cells has been used successfully in other cardiac tissue engineering applications[110]. They have also shown to be able to differentiate into endothelial and cardiac myocytes. Mesenchymal stem cells have also been used for their VIC-like phenotype and their ability to overcome immunogenicity barriers associated with donor cells[115]. Despite their ethical concerns, embryonic stem cells could allow for production of specific tissues in scaffolds[114]. They have a well-known pluripotency and can be maintained for long periods of time and in

large quantities. Their differentiation methods are similar to those like bone-marrow derived stem cells. Bone-marrow derived stem cells (BMSCs) can be isolated from bone marrow and has been shown to have good differentiation potential. BMSCs have been shown to engraft into heart valves and synthesize collagen as part of normal valve homeostasis[140]. Induced pluripotent stem cells (iPSCs) represent another cell source for tissue engineered mitral valves. It is important to note that while their ability to differentiate to the same lineage of as the somatic cells that they derive, more research needs to be conducted to evaluate whether these are trusted cell source. Human adipose derived stem cells (hADSCs) have also shown great promise and feasibility for mitral valve tissue engineering. These cells are easily and minimally-invasively obtained, can be cryogenically stored, and possess multipotent mesodermal, ectodermal and endodermal potentials[141–145]. Such tri-germ layer potential makes this cell-type an excellent choice for translational applications. hADSC's yield significantly large and clinically relevant cell numbers when isolated from adipose tissue. In fact, as a source for regenerative stem cells, adipose tissue may have no equal[146–149]. A recent study found in fact that hADSC's yielded tenfold more CFU-F units compared to bone-marrow derived stem cells, a characteristically similar stem cell[146]. Current literature also supports hADSC use in organized ECM remodeling. Colazzo et al. stated that hADSCs have the ability to synthesize and process ECM components suitable for tissue engineering a heart valve[143]. This was largely based on their ability to differentiate hADSCs into VIC-like cells, thus allowing for remodeling of heart valve ECM[150,151]. Adipose-stem cells also possess a

unique secretome containing angiogenic cytokines such as VEGF, FGF-2, and HGF, which allow it to more fully integrate in vivo[141,152–154].

One of the major drawbacks of both types of scaffolds are their inclusion of cells. Synthetic scaffolds have a greater chance of recellularization due to the ability to control their pore size. However even with this level of customization, efforts are still difficult. Natural scaffolds, despite their success and obvious biological advantage, lack the ability to alter their physical properties to the extent synthetic scaffolds can. Therefore, a myriad of different recellularization techniques exist in an effort to bring cells into the matrix either forcibly or through biochemical coaxing. There are various researchers attempting to coax migration of seeded cells using growth factors and other proteins like fibronectin[155–159]. Vacuum seeding has also been utilized in vascular grafts successfully[160]. Hydrogels are also used both as a chemical attractant and as a physical means to get cells into the matrix utilizing the gel's space-filling capabilities[130,158,159,161,162]. Despite various methods and attempts for recellularization of scaffolds, there does not exist a gold standard for seeding cells in valvular scaffolds. This is especially true for the mitral valve and its four components. Most research literature is solely focused on revitalization of the leaflets. Regardless, there are various ways to attempt cell seeding depending on the application of the construct.

1.5.4 Bioreactor Conditioning in Heart Valve Tissue Engineering:

Historically, mechanical conditioning of heart valve constructs has been considered an essential step for the maturation of the cells within the scaffold, thus promoting a structurally and mechanically competent construct. Maturation of the scaffolds can be

achieved in-vitro using a bioreactor which provides the necessary mechanical and biochemical cues these constructs would experience in the human body but in a controlled, sterile environment. Forces such as cyclic stretch and flexure, oscillating fluid shear stress, pressures and flexural deformations[115]. Such indications for maturation directs cell proliferation, differentiation, attachment and alignment[115]. By pointing these cells in the proper direction, researchers can develop constructs that eventually will mimic the mature ECM and overall properties of the tissue they are attempting to replace or regenerate. This in-vitro preparation allows for immediate implantation of a functional construct in the native hemodynamic environment. Through this in-vitro adaptation in a bioreactor system, scaffold material turnover will occur, thus circumventing this response and other adverse host-tissue reaction that would have occurred post-implantation.

The primary goals of a bioreactor system are: offering uniform cell distribution, keeping concentrations of gas and cell-culture nutrients available to the construct, offering mass transport to and from the construct, and of course, being able to provide adequate and accurate mechanical cues to induce the seeded cells to differentiate and remodel the scaffold thus producing an adequate ECM[163]. Dynamic seeding through use of a bioreactor has shown to greatly improve cell attachment to the scaffold[163]. Depending on the purpose for the construct, different pressures and shear stresses may be applied. This of course would affect the needs and design of the bioreactor system.

Figure 1.24: Mitral valve bioreactor used in our laboratory.

There are three main categories for bioreactor design, each depending on the amount and types of mechanical stimulation being applied. These include: flow-based whole valve conditioning bioreactors, strain-based whole valve conditioning bioreactors, and isolated cusp stimulation bioreactors[164]. Flow-based whole valve conditioning bioreactors aim to mimic both diastolic and systolic phases in the bioreactor. This type of bioreactor, originally conceived by Hoerstrup et al., utilizes a pulsatile flow that exposes the developing construct to all of the mechanical cues that would be experience in the body[165]. Sierad et al. have greatly improved upon this design and have achieved anatomical pressures in the aortic position[166]. In-vitro findings for this type of bioreactor have shown cell migration into the scaffold, an increase in ECM deposition, and increase in construct stiffness, and lamellar tissue organization[115,164]. The second type, the strain-based whole valve bioreactor, mimics only one component experienced by native heart

valves, strain. This is done by periodically pressurizing the media around the valve constructs in line with transvalvular pressures a native valve would face. In-vitro findings are similar for this bioreactor. Cell migration was not increased, however ECM deposition and stiffness were increased. Lamellar tissue organized and the construct showed mechanical anisotropy[115,164]. Bioreactors have also been made to isolate one cusp and stimulate this part of the construct; the third type is the isolated cusp stimulator. Bioreactors in this category expose their constructs to cyclic stretch flexure and oscillating shear stress[115]. Within these three major categories are several popular designs utilized in the valvular tissue engineering space. These include spinner flasks, rocker platforms, rotating walls, compression, and perfusion systems.

While there are many different designs for heart valve bioreactors, most are designed specifically for aortic valves. Very few flow-based bioreactors accommodate for each component of the mitral valve. However, for proper in-vitro preconditioning, the entire apparatus must be considered. One bioreactor from Barzilla's group utilizes a "splashing bioreactor"[167]. This is placed on a rotating wheel and uses gravity to open and close the leaflets. While this bioreactor did encourage improved cell density of the mitral valve leaflet, proper mechanical cues must be applied for an environment mimicking the native mitral valve. First, transvalvular pressures have to be achieved using a system that incorporates the entire valve, exposing it to these pressures along with shear forces. In addition, annular shape should be considered as a foundation for mounting the valve. This unique shape provides optimal force distribution throughout the valve. Lastly, tension must be applied to the chordae tendinae. These tensile forces are critical in developing mature

chordae tissue, as well as functional leaflet tissue. Overall, bioreactor development in this tissue engineering paradigm can resolve many of the issues and limitations of currently available options. Complexity in design, assurance of sterility and providing monitoring capabilities hinder the application of tissue-engineered heart valves. There is also a balance that must be achieved when using heart valve bioreactors that the in-vitro conditions used do not overstimulate the living constructs to then stimulate pathological over production of ECM and over-activation of seeded cells.

1.6 References:

1. Of, M. & Regurgitation, C. M. Evaluation and management of chronic mitral regurgitation. *N. Engl. J. Med.* **345,** 740–746 (2001).
2. Silbiger, J. J. & Bazaz, R. Contemporary insights into the functional anatomy of the mitral valve. *Am. Heart J.* **158,** 887–95 (2009).
3. Ho, S. Y. Anatomy of the mitral valve. *Heart* **88,** 5iv–10 (2002).
4. Silbiger, J. J. Anatomy, mechanics, and pathophysiology of the mitral annulus. *Am. Heart J.* **164,** 163–76 (2012).
5. Lawrie, G. M. Structure, function, and dynamics of the mitral annulus: importance in mitral valve repair for myxamatous mitral valve disease. *Methodist Debakey Cardiovasc. J.* **6,** 8–14 (2010).
6. Timek, T. a *et al.* Annular height-to-commissural width ratio of annulolasty rings in vivo. *Circulation* **112,** I423-8 (2005).
7. Jensen, M. O. *et al.* Saddle-shaped mitral valve annuloplasty rings experience lower forces compared with flat rings. *Circulation* **118,** S250-5 (2008).
8. Jimenez, J. H., Soerensen, D. D., He, Z., He, S. & Yoganathan, A. P. Effects of a saddle shaped annulus on mitral valve function and chordal force distribution: An in vitro study. *Ann. Biomed. Eng.* **31,** 1171–1181 (2003).
9. Levine, R. a *et al.* Three-dimensional echocardiographic reconstruction of the mitral valve, with implications for the diagnosis of mitral valve prolapse. *Circulation* **80,** 589–598 (1989).
10. Mahmood, F. *et al.* Three-dimensional echocardiographic assessment of changes in mitral valve geometry after valve repair. *Ann. Thorac. Surg.* **88,** 1838–44 (2009).
11. Mahmood, F. *et al.* Intraoperative application of geometric three-dimensional mitral valve assessment package: a feasibility study. *J. Cardiothorac. Vasc. Anesth.* **22,** 292–8 (2008).

12. Salgo, I. S. *et al.* Effect of Annular Shape on Leaflet Curvature in Reducing Mitral Leaflet Stress. *Circulation* **106,** 711–717 (2002).
13. Mahmood, F. *et al.* Mitral annulus: an intraoperative echocardiographic perspective. *J. Cardiothorac. Vasc. Anesth.* **27,** 1355–63 (2013).
14. Grande-Allen, K. J. & Liao, J. The heterogeneous biomechanics and mechanobiology of the mitral valve: implications for tissue engineering. *Curr. Cardiol. Rep.* **13,** 113–20 (2011).
15. Borin, C., Vanhercke, D. & Weyns, A. Innervation of the Atrioventricular and Semi-Lunar Heart Valves. *Acta Cardiol.* **61,** 463–470 (2006).
16. Victor, S. & Nayak, V. M. Definition and function of commissures, slits and scallops of the mitral valve: Analysis in 100 hearts. *Asia Pacific J. Thorac. Cardiovasc. Surg.* **3,** 10–16 (1994).
17. Misfeld, M. & Sievers, H.-H. Heart valve macro- and microstructure. *Philos. Trans. R. Soc. Lond. B. Biol. Sci.* **362,** 1421–36 (2007).
18. Krishnamurthy, G., Itoh, A., Swanson, J. C., Miller, D. C. & Ingels, N. B. Active Stiffening of Mitral Valve Leaflets in the Beating Heart. *Am. J. Physiol. Heart Circ. Physiol.* **296,** H1766–H1773 (2009).
19. Sacks, M. S., David Merryman, W. & Schmidt, D. E. On the biomechanics of heart valve function. *J. Biomech.* **42,** 1804–1824 (2009).
20. May-Newman, K. & Yin, F. C. Biaxial mechanical behavior of excised porcine mitral valve leaflets. *Am. J. Physiol.* **269,** H1319–H1327 (1995).
21. Sacks, M. S. & Yoganathan, A. P. Heart valve function: a biomechanical perspective. *Philos. Trans. R. Soc. Lond. B. Biol. Sci.* **362,** 1369–1391 (2007).
22. Hartiala, J. J. *et al.* Velocity-encoded tine MRI in the evaluation of left ventricular diastolic function : Measurement of mitral valve and pulmonary vein flow velocities and flow volume across the mitral valve. *Am. Heart J.* **125,** 1054–1066 (1993).
23. Ritchie, J., Warnock, J. N. & Yoganathan, A. P. Structural characterization of the chordae tendineae in native porcine mitral valves. *Ann. Thorac. Surg.* **80,** 189–197 (2005).
24. Jimenez, J. H., Soerensen, D. D., He, Z., Ritchie, J. & Ajit, P. Effects of Papillary Muscle Position on Chordal Force Distribution : An In-vitro Study. (2005).
25. Liao, J. & Vesely, I. A structural basis for the size-related mechanical properties of mitral valve chordae tendineae. *J. Biomech.* **36,** 1125–1133 (2003).
26. Iaizzo, P. *Handbook of cardiac anatomy, physiology, and devices*. *Vasa* (Humana Press, 2005).
27. Levine, R. A. *et al.* Mitral Valve Disease - Morphology and Mechanisms. *Nat. Publ. Gr.* **12,** 689–710 (2015).
28. Liu, A. C., Joag, V. R. & Gotlieb, A. I. The emerging role of valve interstitial cell phenotypes in regulating heart valve pathobiology. *Am. J. Pathol.* **171,** 1407–18 (2007).

29. Chester, A. H. & Taylor, P. M. Molecular and functional characteristics of heart-valve interstitial cells. *Philos. Trans. R. Soc. Lond. B. Biol. Sci.* **362,** 1437–43 (2007).
30. Taylor, P. M., Batten, P., Brand, N. J., Thomas, P. S. & Yacoub, M. H. The cardiac valve interstitial cell. *Int. J. Biochem. Cell Biol.* **35,** 113–8 (2003).
31. Brand, N. J., Roy, A., Hoare, G., Chester, A. & Yacoub, M. H. Cultured interstitial cells from human heart valves express both specific skeletal muscle and non-muscle markers. *Int. J. Biochem. Cell Biol.* **38,** 30–42 (2006).
32. Blevins, T., Peterson, S. & Lee, E. Mitral valvular interstitial cells demonstrate regional, adhesional, and synthetic heterogeneity. *Cells Tissues …* **187,** 113–122 (2008).
33. Fayet, C., Bendeck, M. & Gotlieb, A. Cardiac valve interstitial cells secrete fibronectin and form fibrillar adhesions in response to injury. *Cardiovasc. Pathol.* **16,** 203–211 (2007).
34. Liu, A. C., Joag, V. R. & Gotlieb, A. I. The emerging role of valve interstitial cell phenotypes in regulating heart valve pathobiology. *Am. J. Pathol.* **171,** 1407–18 (2007).
35. Li, C. & Gotlieb, A. I. Transforming growth factor-β regulates the growth of valve interstitial cells in vitro. *Am. J. Pathol.* **179,** 1746–55 (2011).
36. Han, L. & Gotlieb, A. I. Fibroblast growth factor-2 promotes in vitro mitral valve interstitial cell repair through transforming growth factor-β/Smad signaling. *Am. J. Pathol.* **178,** 119–27 (2011).
37. Armstrong, E. J. & Bischoff, J. Heart Valve Development: Endothelial Cell Signaling and Differentiation. *Circ. Res.* **95,** 459–470 (2010).
38. Rivera-Feliciano, J. & Tabin, C. J. Bmp2 instructs cardiac progenitors to form the heart-valve-inducing field. *Dev. Biol.* **295,** 580–588 (2006).
39. Gould, S. T., Matherly, E. E., Smith, J. N., Heistad, D. D. & Anseth, K. S. The role of valvular endothelial cell paracrine signaling and matrix elasticity on valvular interstitial cell activation. *Biomaterials* **35,** 3596–606 (2014).
40. Hjortnaes, J. *et al.* Directing Valvular Interstitial Cell Myofibroblast-Like Differentiation in a Hybrid Hydrogel Platform. *Adv. Healthc. Mater.* 1–10 (2014). doi:10.1002/adhm.201400029
41. Duan, B., Hockaday, L. A., Kapetanovic, E., Kang, K. H. & Butcher, J. T. Stiffness and adhesivity control aortic valve interstitial cell behavior within hyaluronic acid based hydrogels. *Acta Biomater.* **9,** 7640–7650 (2013).
42. Stephens, E. H., Durst, C. a, West, J. L. & Grande-Allen, K. J. Mitral valvular interstitial cell responses to substrate stiffness depend on age and anatomic region. *Acta Biomater.* **7,** 75–82 (2011).
43. Gu, X. & Masters, K. S. Role of the Rho pathway in regulating valvular interstitial cell phenotype and nodule formation. *Am. J. Physiol. Heart Circ. Physiol.* **300,** H448-58 (2011).
44. Yip, C. Y. Y., Chen, J.-H., Zhao, R. & Simmons, C. a. Calcification by valve interstitial

cells is regulated by the stiffness of the extracellular matrix. *Arterioscler. Thromb. Vasc. Biol.* **29,** 936–42 (2009).
45. Rabkin-Aikawa, E., Farber, M., Aikawa, M. & Schoen, F. J. Dynamic and reversible changes of interstitial cell phenotype during remodeling of cardiac valves. *J. Heart Valve Dis.* **13,** 841–7 (2004).
46. Rabkin, E. *et al.* Activated Interstitial Myofibroblasts Express Catabolic Enzymes and Mediate Matrix Remodeling in Myxomatous Heart Valves. *Circulation* **104,** 2525–2532 (2001).
47. Liu, a C. & Gotlieb, a I. Characterization of cell motility in single heart valve interstitial cells in vitro. *Histol. Histopathol.* **22,** 873–82 (2007).
48. Cushing, M. C., Liao, J. T. & Anseth, K. S. Activation of valvular interstitial cells is mediated by transforming growth factor-??1 interactions with matrix molecules. *Matrix Biol.* **24,** 428–437 (2005).
49. Butcher, J. T. & Nerem, R. M. Valvular endothelial cells regulate the phenotype of interstitial cells in co-culture: effects of steady shear stress. *Tissue Eng.* **12,** 905–915 (2006).
50. Hjortnaes, J. *et al.* Valvular interstitial cells suppress calcification of valvular endothelial cells. *Atherosclerosis* **242,** 251–260 (2015).
51. Durbin, A., Nadir, N. A., Rosenthal, A. & Gotlieb, A. I. Nitric oxide promotes in vitro interstitial cell heart valve repair. *Cardiovasc. Pathol.* **14,** 12–18 (2005).
52. Sun, W. *et al.* Comparative study of human aortic and mitral valve interstitial cell gene expression and cellular function. *Genomics* **101,** 326–35 (2013).
53. Mozaffarian, D. *et al. Heart Disease and Stroke Statistics--2015 Update: A Report From the American Heart Association*. *Circulation* **131,** (2014).
54. Chandrashekhar, Y., Westaby, S. & Narula, J. Mitral stenosis. *Lancet* **374,** 1271–83 (2009).
55. Shah, P. M. Current concepts in mitral valve prolapse--diagnosis and management. *J. Cardiol.* **56,** 125–33 (2010).
56. Curtin, R. J. & Griffin, B. P. Mitral Valve Disease: Stenosis and Regurgitation. *Clevel. Clin. Cent. Contin. Educ.* 1–15 (2010).
57. Pedrazzini, G. B., Faletra, F., Vassalli, G., Demertzis, S. & Moccetti, T. Mitral regurgitation. *Swiss Med. Wkly.* **140,** 36–43 (2010).
58. Iung, B. & Vahanian, A. Epidemiology of valvular heart disease in the adult. *Nat. Rev. Cardiol.* **8,** 162–72 (2011).
59. Roberts, S. *et al.* Pathogenic mechanisms in rheumatic carditis: focus on valvular endothelium. *J. Infect. Dis.* **183,** 507–511 (2001).
60. Carapetis, J. R., McDonald, M. & Wilson, N. J. Acute rheumatic fever. *Lancet* **366,** 155–168 (2005).
61. Guilherme, L. & Kalil, J. Rheumatic fever: From sore throat to autoimmune heart lesions. *Int. Arch. Allergy Immunol.* **134,** 56–64 (2004).
62. Di Mauro, M. *et al.* Functional mitral regurgitation: From normal to pathological

anatomy of mitral valve. *Int. J. Cardiol.* **163,** 242–248 (2013).
63. Adams, D. H., Rosenhek, R. & Falk, V. Degenerative mitral valve regurgitation: best practice revolution. *Eur. Heart J.* **31,** 1958–66 (2010).
64. Richards, J. M., Farrar, E. J., Kornreich, B. G., Mose, N. S. & Butcher, J. T. The mechanobiology of mitral valve function, degeneration, and repair. *J. Vet. Cardiol.* **14,** 47–58 (2012).
65. Aikawa, E. & Grande-allen, K. J. in *Cardiac Valvular Medicine* (ed. Rajamannan, N. M.) 173–185 (Springer London, 2013). doi:10.1007/978-1-4471-4132-7
66. Orton, E. C., Lacerda, C. M. R. & MacLea, H. B. Signaling pathways in mitral valve degeneration. *J. Vet. Cardiol.* **14,** 7–17 (2012).
67. Hulin, A. *et al.* Emerging pathogenic mechanisms in human myxomatous mitral valve: lessons from past and novel data. *Cardiovasc. Pathol.* **22,** 245–50 (2013).
68. Tamura, K. *et al.* Abnormalities in elastic fibers and other connective-tissue components of floppy mitral valve. *Am. Heart J.* **129,** 1149–1158 (1995).
69. Lis, Y. *et al.* Biochemical characterization of individual normal, floppy and rheumatic human mitral valves. *Biochem. J.* **244,** 597–603 (1987).
70. Gazoti Debessa, C. R., Mesiano Maifrino, L. B. & Rodrigues de Souza, R. Age related changes of the collagen network of the human heart. *Mech. Ageing Dev.* **122,** 1049–1058 (2001).
71. Hadian, M., Corcoran, B. M. & Bradshaw, J. P. Molecular changes in fibrillar collagen in myxomatous mitral valve disease. *Cardiovasc. Pathol.* **19,** 6–8 (2010).
72. Kunzelman, K. S., Quick, D. W. & Cochran, R. P. Altered collagen concentration in mitral valve leaflets: Biochemical and finite element analysis. *Ann. Thorac. Surg.* **66,** (1998).
73. Fornes, P. *et al.* Correlation Between Clinical and Histologic Patterns of Degenerative Mitral Valve Insufficiency. *Cardiovasc. Pathol.* **8,** 81–92 (1999).
74. Hadian, M., Corcoran, B. M., Han, R. I., Grossmann, J. G. & Bradshaw, J. P. Collagen organization in canine myxomatous mitral valve disease: an x-ray diffraction study. *Biophys. J.* **93,** 2472–2476 (2007).
75. Prunotto, M., Caimmi, P. P. & Bongiovanni, M. Cellular pathology of mitral valve prolapse. *Cardiovasc. Pathol.* **19,** e113–e117 (2010).
76. Grewal, J. *et al.* Mitral annular dynamics in myxomatous valve disease: new insights with real-time 3-dimensional echocardiography. *Circulation* **121,** 1423–31 (2010).
77. Cabell, C. H., Abrutyn, E. & Karchmer, A. W. Cardiology patient page. Bacterial endocarditis: the disease, treatment, and prevention. *Circulation* **107,** e185-7 (2003).
78. Maisano, F. *et al.* The future of transcatheter mitral valve interventions: Competitive or complementary role of repair vs. Replacement? *Eur. Heart J.* **36,** 1651–1659 (2015).
79. Rausch, M. K. *et al.* Mitral Valve Annuloplasty: A quantitative clinical and

mechanical comparison of different annuloplasty devices. *Ann. Biomed. Eng.* **40,** 750–761 (2013).
80. Gersh, B. J., Sliwa, K., Mayosi, B. M. & Yusuf, S. Novel therapeutic concepts: the epidemic of cardiovascular disease in the developing world: global implications. *Eur. Heart J.* **31,** 642–8 (2010).
81. Zilla, P., Brink, J., Human, P. & Bezuidenhout, D. Prosthetic heart valves: catering for the few. *Biomaterials* **29,** 385–406 (2008).
82. Nkomo, V. T. *et al.* Burden of valvular heart diseases: a population-based study. *Lancet* **368,** 1005–11 (2006).
83. Kheradvar, A. *et al.* Emerging Trends in Heart Valve Engineering: Part III. Novel Technologies for Mitral Valve Repair and Replacement. *Ann. Biomed. Eng.* **43,** 858–870 (2015).
84. Gammie, J. S. *et al.* Trends in mitral valve surgery in the United States: results from the Society of Thoracic Surgeons Adult Cardiac Surgery Database. *Ann. Thorac. Surg.* **87,** 1431-7-9 (2009).
85. Fedak, P. W. M., McCarthy, P. M. & Bonow, R. O. Evolving concepts and technologies in mitral valve repair. *Circulation* **117,** 963–74 (2008).
86. Wheatley, D. & Will, M. Mitral valve replacement with mechanical or bioprosthetic valve. *Multimed. Man. Cardio-Thoracic Surg.* **2005,** (2005).
87. Vesely, I. Heart valve tissue engineering. *Circ. Res.* **97,** 743–55 (2005).
88. Pibarot, P. & Dumesnil, J. G. Prosthetic heart valves: Selection of the optimal prosthesis and long-term management. *Circulation* **119,** 1034–1048 (2009).
89. Benussi, S., Verzini, A. & Alfieri, O. Mitral valve replacement and thromboembolic risk. *J. Heart Valve Dis.* **13 Suppl 1,** S81-3 (2004).
90. Schoen, F. J. Mechanisms of function and disease of natural and replacement heart valves. *Annu. Rev. Pathol.* **7,** 161–83 (2012).
91. Levine, M. N., Raskob, G., Landefeld, S. & Kearon, C. Hemorrhagic complications of anticoagulant treatment. *Chest* **119,** 108S–121S (2001).
92. Ayhan, a, Yucel, a, Bildirici, I. & Dogan, R. Feto-maternal morbidity and mortality after cardiac valve replacement. *Acta Obstet. Gynecol. Scand.* **80,** 713–8 (2001).
93. Tang, G. H. L., Rao, V., Siu, S. & Butany, J. Thrombosis of mechanical mitral valve prosthesis. *J. Card. Surg.* **20,** 481–6 (2005).
94. Girard, S. E. *et al.* Reoperation for prosthetic aortic valve obstruction in the era of echocardiography: Trends in diagnostic testing and comparison with surgical findings. *J. Am. Coll. Cardiol.* **37,** 579–584 (2001).
95. Sim, H.-T. *et al.* Mitral valve replacement using mechanical prostheses in children: early and long-term outcomes. *Pediatr. Cardiol.* **33,** 639–45 (2012).
96. Heras, M. *et al.* High risk of thromboemboli early after bioprosthetic cardiac valve replacement. *J. Am. Coll. Cardiol.* **25,** 1111–1119 (1995).
97. Human, P. & Zilla, P. Characterization of the immune response to valve bioprostheses and its role in primary tissue failure. *Ann. Thorac. Surg.* **71,** 20–23

(2001).
98. Ferrans, V. J., Spray, T. L., Billingham, M. E. & Roberts, W. C. Structural changes in glutaraldehyde-treated porcine heterografts used as substitute cardiac valves. Transmission and scanning electron microscopic observations in 12 patients. *Am. J. Cardiol.* **41,** 1159–1184 (1978).
99. Schoen, F. J. & Levy, R. J. Calcification of tissue heart valve substitutes: progress toward understanding and prevention. *Ann. Thorac. Surg.* **79,** 1072–80 (2005).
100. Jones, J. M. *et al.* Repeat heart valve surgery: risk factors for operative mortality. *J. Thorac. Cardiovasc. Surg.* **122,** 913–8 (2001).
101. Oliveira, J. M. F. De & Antunes, M. J. Mitral valve repair: better than replacement. *Heart* **92,** 275–81 (2006).
102. Savage, E. B., Ferguson, T. B. & DiSesa, V. J. Use of Mitral Valve Repair : Analysis of Contemporary United States Experience Reported to Database. *Ann. Thorac. Surg.* **75,** 820–825 (2003).
103. Braunberger, E. *et al.* Very long-term results (more than 20 years) of valve repair with Carpentier's tehcniques in nonrheumatic mitral valve insufficiency. *Circulation* **104,** I8–I11 (2001).
104. Lawrie, G. M. Mitral valve: toward complete repairability. *Surgical technology international* **15,** 189–97 (2006).
105. Bortolotti, U., Milano, A. D. & Frater, R. W. M. Mitral valve repair with artificial chordae: a review of its history, technical details, long-term results, and pathology. *Ann. Thorac. Surg.* **93,** 684–91 (2012).
106. Fawzy, M. E. Percutaneous mitral balloon valvotomy. *Catheter. Cardiovasc. Interv.* **69,** 313–21 (2007).
107. Algarni, K. D., Suri, R. M. & Schaff, H. Minimally invasive mitral valve surgery: Does it make a difference? *Trends Cardiovasc. Med.* **25,** 456–465 (2015).
108. Goldstein, D. *et al.* Two-Year Outcomes of Surgical Treatment of Severe Ischemic Mitral Regurgitation. *N. Engl. J. Med.* 1–10 (2015). doi:10.1056/NEJMoa1512913
109. Wang, A. *et al.* Practice gaps in the care of mitral valve regurgitation: Insights from the American College of Cardiology mitral regurgitation gap analysis and advisory panel. *Am. Heart J.* **172,** 70–79 (2016).
110. Mendelson, K. & Schoen, F. J. Heart valve tissue engineering: concepts, approaches, progress, and challenges. *Ann. Biomed. Eng.* **34,** 1799–819 (2006).
111. Fallahiarezoudar, E., Ahmadipourroudposht, M., Idris, A. & Mohd Yusof, N. A review of: Application of synthetic scaffold in tissue engineering heart valves. *Mater. Sci. Eng. C* **48,** 556–565 (2015).
112. Sacks, M. S., Schoen, F. J. & Mayer, J. E. Bioengineering challenges for heart valve tissue engineering. *Annu. Rev. Biomed. Eng.* **11,** 289–313 (2009).
113. L, F. & B, S. Adipose Derived Tissue Engineered Heart Valve. *J. Tissue Sci. Eng.* **6,** (2015).
114. Howard, D., Buttery, L. D., Shakesheff, K. M. & Roberts, S. J. Tissue engineering:

strategies, stem cells and scaffolds. *J. Anat.* **213,** 66–72 (2008).
115. Parvin, S., Blaser, M. C., Santerre, J. P., Caldarone, C. A. & Simmons, C. A. Biomechanical conditioning of tissue engineered heart valves : Too much of a good thing ? ☆. *Adv. Drug Deliv. Rev.* **96,** 161–175 (2016).
116. Kheradvar, A. *et al.* Emerging Trends in Heart Valve Engineering: Part I. Solutions for Future. *Ann. Biomed. Eng.* **43,** 833–843 (2015).
117. Trappmann, B. *et al.* Extracellular-matrix tethering regulates stem-cell fate. *Nat. Mater.* **11,** 742–742 (2012).
118. Kloxin, A. M., Benton, J. A. & Anseth, K. S. In situ elasticity modulation with dynamic substrates to direct cell phenotype. *Biomaterials* **31,** 1–8 (2010).
119. Cushing, M. C., Liao, J. T., Jaeggli, M. P. & Anseth, K. S. Material-based regulation of the myofibroblast phenotype. *Biomaterials* **28,** 3378–3387 (2007).
120. Gu, X. & Masters, K. S. Regulation of valvular interstitial cell calcification by adhesive peptide sequences. *J. Biomed. Mater. Res. - Part A* **93,** 1620–1630 (2010).
121. Rodriguez, K. J. & Masters, K. S. Regulation of valvular interstitial cell calcification by components of the extracellular matrix. *J. Biomed. Mater. Res. - Part A* **90,** 1043–1053 (2009).
122. Sodian, R. *et al.* Early In Vivo Experience With Tissue-Engineered Trileaflet Heart Valves. *Circulation* 22–29 (2000).
123. Neuenschwander, S. & Hoerstrup, S. P. Heart valve tissue engineering. *Transpl. Immunol.* **12,** 359–365 (2004).
124. Lutolf, M. P. & Hubbell, J. a. Synthetic biomaterials as instructive extracellular microenvironments for morphogenesis in tissue engineering. *Nat. Biotechnol.* **23,** 47–55 (2005).
125. Pratt, A. B., Weber, F. E., Schmoekel, H. G., M??ller, R. & Hubbell, J. A. Synthetic Extracellular Matrices for in Situ Tissue Engineering. *Biotechnol. Bioeng.* **86,** 27–36 (2004).
126. Shi, Y. & Vesely, I. Fabrication of mitral valve chordae by directed collagen gel shrinkage. *Tissue Eng.* **9,** 1233–1242 (2003).
127. Ahmed, T. a E., Dare, E. V & Hincke, M. Fibrin: a versatile scaffold for tissue engineering applications. *Tissue Eng. Part B. Rev.* **14,** 199–215 (2008).
128. Mosesson, M. W., Siebenlist, K. R. & Meh, D. A. The structure and biological features of fibrinogen and fibrin. *Ann. N. Y. Acad. Sci.* **936,** 11–30 (2001).
129. Collins, M. N. & Birkinshaw, C. Hyaluronic acid based scaffolds for tissue engineering - A review. *Carbohydr. Polym.* **92,** 1262–1279 (2013).
130. Tibbitt, M. W. & Anseth, K. S. Hydrogels as Extracellular Matrix Mimics for 3D Cell Culture. *Biotechnol. Bioeng.* **103,** 655–663 (2010).
131. Brown, B. N. & Badylak, S. F. Extracellular Matrix as an Inductive Scaffold for Functional Tissue Reconstruction. *Transl. Res.* (2013). doi:10.1016/j.trsl.2013.11.003

132. Gurung, P., Lukens, J. R. & Kanneganti, T. Current Progress in Tissue Engineering of Heart Valves: Multiscale Problems, Multiscale Solutions. *Expert Opin. Biol. Ther.* **21,** 193–201 (2016).
133. Crapo, P. M., Gilbert, T. W. & Badylak, S. F. An overview of tissue and whole organ decellularization processes. *Biomaterials* **32,** 3233–43 (2011).
134. Badylak, S. F. Decellularized Allogeneic and Xenogeneic Tissue as a Bioscaffold for Regenerative Medicine: Factors that Influence the Host Response. *Ann. Biomed. Eng.* (2014). doi:10.1007/s10439-013-0963-7
135. Dijkman, P. E., Driessen-Mol, A., Frese, L., Hoerstrup, S. P. & Baaijens, F. P. T. Decellularized homologous tissue-engineered heart valves as off-the-shelf alternatives to xeno- and homografts. *Biomaterials* **33,** 4545–4554 (2012).
136. Driessen-Mol, A. *et al.* Transcatheter implantation of homologous 'off-the-shelf' tissue-engineered heart valves with self-repair capacity: Long-term functionality and rapid in vivo remodeling in sheep. *J. Am. Coll. Cardiol.* **63,** 1320–1329 (2014).
137. Weber, B. *et al.* Off-the-shelf human decellularized tissue-engineered heart valves in a non-human primate model. *Biomaterials* **34,** 7269–7280 (2013).
138. Syedain, Z. H., Bradee, A. R., Kren, S., Taylor, D. A. & Tranquillo, R. T. Decellularized Tissue-Engineered Heart Valve Leaflets with Recellularization Potential. *Tissue Eng. Part A* **19,** (2013).
139. Pittenger, M. F. & Martin, B. J. Mesenchymal stem cells and their potential as cardiac therapeutics. *Circ. Res.* **95,** 9–20 (2004).
140. Hajdu, Z. *et al.* Recruitment of bone marrow-derived valve interstitial cells is a normal homeostatic process. *J. Mol. Cell. Cardiol.* **51,** 955–965 (2011).
141. Zuk, P. Review Article Adipose-Derived Stem Cells in Tissue Regeneration : A Review. *ISRN Stem Cells* **2013,** 1–36 (2013).
142. Helder, M. N., Knippenberg, M., Klein-Nulend, J. & Wuisman, P. I. J. M. Stem cells from adipose tissue allow challenging new concepts for regenerative medicine. *Tissue Eng.* **13,** 1799–808 (2007).
143. Colazzo, F. *et al.* Extracellular matrix production by adipose-derived stem cells: implications for heart valve tissue engineering. *Biomaterials* **32,** 119–27 (2011).
144. Williams, K. J., Godke, R. A. & Bondioli, K. R. Adipose-Derived Stem Cells. **702,** 77–86 (2011).
145. Gimble, J. & Guilak, F. Adipose-derived adult stem cells: isolation, characterization, and differentiation potential. *Cytotherapy* **5,** 362–9 (2003).
146. Zhu, X., Shi, W., Tai, W. & Liu, F. The comparition of biological characteristics and multilineage differentiation of bone marrow and adipose derived Mesenchymal stem cells. *Cell Tissue Res.* **350,** 277–87 (2012).
147. Aust, L. *et al.* Yield of human adipose-derived adult stem cells from liposuction aspirates. *Cytotherapy* **6,** 7–14 (2004).
148. Zhu, Y., Liu, T., Song, K. & Fan, X. Adipose-derived stem cell: a better stem cell than BMSC. *Cell Biochem. …* 664–675 (2008). doi:10.1002/cbf

149. Oedayrajsingh-Varma, M. J. *et al.* Adipose tissue-derived mesenchymal stem cell yield and growth characteristics are affected by the tissue-harvesting procedure. *Cytotherapy* **8,** 166–77 (2006).
150. Tedder, M. & Simionescu, A. Assembly and testing of stem cell-seeded layered collagen constructs for heart valve tissue engineering. *… Eng. Part …* **17,** (2010).
151. Huang, W. *et al.* Fn14 promotes differentiation of human mesenchymal stem cells into heart valvular interstitial cells by phenotypic characterization. *J. Cell. Physiol.* 1–20 (2013). doi:10.1002/jcp.24480
152. Elman, J. S., Li, M., Wang, F., Gimble, J. M. & Parekkadan, B. A comparison of adipose and bone marrow-derived mesenchymal stromal cell secreted factors in the treatment of systemic inflammation. *J. Inflamm. (Lond).* **11,** 1 (2014).
153. Carvalho, P. P., Gomes, M. E., Reis, R. L. & Gimble, J. M. in *Mesenchymal Stromal Cells* (eds. Hematti, P. & Keating, A.) 663–681 (Springer New York, 2013). doi:10.1007/978-1-4614-5711-4
154. Gimble, J. M., Katz, A. J. & Bunnell, B. a. Adipose-derived stem cells for regenerative medicine. *Circ. Res.* **100,** 1249–60 (2007).
155. Greiling, D. & Clark, R. A. F. Fibronectin provides a conduit for fibroblast transmigration from collagenous stroma into fibrin clot provisional matrix. **870,** 861–870 (1997).
156. Thievessen, I. *et al.* Vinculin is required for cell polarization , migration , and extracellular matrix remodeling in 3D collagen. *Fed. Am. Soc. Exp. Biol. J.* **29,** 4555–4567 (2015).
157. Rhee, S., Ho, C. & Grinnell, F. Promigratory and procontractile growth factor environments differentially regulate cell morphogenesis. *Exp. Cell Res.* **316,** 232–244 (2009).
158. Martino, M. M., Briquez, P. S., Ranga, A., Lutolf, M. P. & Hubbell, J. a. Heparin-binding domain of fibrin(ogen) binds growth factors and promotes tissue repair when incorporated within a synthetic matrix. *Proc. Natl. Acad. Sci. U. S. A.* **110,** 4563–8 (2013).
159. Lee, K., Silva, E. a & Mooney, D. J. Growth factor delivery-based tissue engineering: general approaches and a review of recent developments. *J. R. Soc. Interface* **8,** 153–170 (2011).
160. Soletti, L. *et al.* A seeding device for tissue engineered tubular structures. *Biomaterials* **27,** 4863–4870 (2006).
161. Tayalia, P. & Mooney, D. J. Controlled growth factor delivery for tissue engineering. *Adv. Mater.* **21,** 3269–85 (2009).
162. Momtahan, N., Sukavaneshvar, S. S. T. C., Roeder, B. L. & Cook, A. D. Strategies and processes to decellularize and recellularize hearts to generate functional organs and reduce the risk of thrombosis. *Tissue Eng. Part B. Rev.* 1–58 (2014). doi:10.1089/ten.TEB.2014.0192
163. Amrollahi, P. & Tayebi, L. Bioreactors for Heart Valve Tissue Engineering: A

Review. *J. Chem. Technol. Biotechnol.* **49,** n/a-n/a (2015).
164. Spoon, D. B., Tefft, B. J., Lerman, A. & Simari, R. D. Challenges of biological valve development. *Interv. Cardiol.* **5,** 319–334 (2013).
165. Hoerstrup, S. P., Sodian, R., Sperling, J. S., Vacanti, J. P. & Mayer, J. E. New Pulsatile Bioreactor for In Vitro Formation of Tissue Engineered Heart Valves. *Tissue Eng.* **6,** 75–79 (2000).
166. Sierad, L. N. *et al.* Design and Testing of a Pulsatile Conditioning System for Dynamic Endothelialization of Polyphenol-Stabilized Tissue Engineered Heart Valves. *Cardiovasc. Eng. Technol.* **1,** 138–153 (2010).
167. Barzilla, J. E., McKenney, A. S., Cowan, A. E., Durst, C. a & Grande-Allen, K. J. Design and validation of a novel splashing bioreactor system for use in mitral valve organ culture. *Ann. Biomed. Eng.* **38,** 3280–94 (2010).

CHAPTER 2 – PROJECT MOTIVATION, SPECIFIC AIMS, SIGNIFICANCE

2.1 Introduction and Clinical Relevance:

In the United States alone, 2.5% of the population suffers from some form of valvular disease[1]. Degenerative etiologies are largely responsible for these statistics[2]. The most degenerative of the four heart valves is the mitral valve making it the most frequently diseased valve in the heart [2, 3]. Approximately 41,000 hospitalizations per year are due to surgical corrections of mitral valve regurgitation (MR) in the United States, yet this number represents only 44% of persons with severe MR who would benefit from surgical correction[3]. The prevalence of mitral valve disease increases substantially with age, from less than 2% before the age of 65 to 8.5% in those aged 65-75, and 13.2% after the age of 75[3]. The lethality of mitral valve diseases stems from the three primary pathologies that affect the valve, i.e. stenosis, regurgitation, and prolapse. These three pathologies can result in atrial fibrillation, arterial thromboembolism, pulmonary edema, pulmonary hypertension, cardiac hypertrophy and heart failure[4–7]. **Prevalence of mitral valve insufficiencies is clear and thus verifies its significance as a crucial area for further research and development for translational solutions.**

2.2 Current Standards of Care and Limitations:

Current clinical solutions available to patients with mitral valve pathologies are surgical repair or total valve replacement. Replacement strategies include mechanical valves and chemically-fixed xenogeneic valves. Each of these prosthetic devices however has often resulted in thromboembolic complications, calcification, and most require additional reoperations due to their limited functioning lifespans. Because the body

chronically reacts to the artificial valves, the lifespan of bioprosthetic and mechanical valves ranges from 15 to 20 years. This poses a difficult decision for surgeons if their patients are younger. Each additional replacement surgery causes an enormous increase (almost 20% in some cases) in mortality risk[8–12]. Determination of reparative or replacement therapy is often based on the age of the patient and other health related factors. Women who are or are planning to become pregnant must weigh their safety and the child's safety because they cannot undergo anticoagulation therapy during this time[13]. Also, children with congenital heart defects have limited options for mitral valve replacement. Small diameter mechanical valve replacements are rare due to high mortality and morbidity rates. Mitral valve repair is the preferred solution due to its less invasive nature and higher success rates when compared to replacement[14,15]. Anatomical complexity however is a limiting factor when repairing the mitral valve. There are four tissue types present in the valve's entirety: the annulus, the leaflets, the chordae tendinae, and the papillary muscles. Reparative technologies center on band annuloplasty and artificial chordae made of PTFE. Both are used to reconstitute the correct physical anatomy of the valve, thus optimizing force distributions and overall coaptation[16,17]. Despite the successes of mitral valve repair, recent studies have shown that the rate of reoccurrence in patients following repair (58.8%) was significantly larger than patients who underwent valve replacement (3.8%) after two years[18]. Overall, mitral regurgitation recurred more frequently in patients receiving repair treatments, resulting in more heart failure-related events and cardiovascular admissions[18]. A tissue engineered mitral valve could provide patients with a permanent regenerative solution. These could provide a living valve replacement using already existing surgical

techniques. With the advancement of stem cell capabilities, one can employ them along with growth factors and engineered matrices to eventually create an autologous implant that can not only grow with the patient but also create a superior alternative to repair and replacement therapies. There has been considerable research into heart valve tissue engineering, but limited clinical testing, especially with the mitral valve. This may be a result of the mitral valve's complicated anatomy or the prevalence of other diseased valves like the aortic valve. A mitral valve tissue engineered solution is an exciting concept, yet very early in practice.

The **overall goal** of this project is to develop a biocompatible and clinically translatable tissue engineered mitral valve. To realize this goal, the engineered construct must be mechanically robust, biologically compatible with future hosts, and should allow sufficient bioactivity for cellular seeding and signaling. The valve should allow for rapid opening and closure, no need for rigid support, and maintain correct physiological structure from annulus to papillary muscle. Because ECM and biochemical composition are crucial, our construct will be an acellular, non-immunogenic collagen and elastin-based scaffold. To impede degradation of the tissue, the decellularized xenogeneic scaffolds, will be treated with **penta-galloyl glucose** (PGG), an antioxidant polyphenol and matrix stabilizing agent, with high affinity for collagen and elastin, to slow down matrix degradation [(19)].

We **hypothesize**, that this tissue engineered mitral valve consisting of a decellularized porcine mitral valve scaffold, treated with PGG, recellularized with relevant VIC-like cells, and finally pre-conditioned in a mitral valve bioreactor will immediately

provide a working and living valve construct. Pre-conditioning of the revitalized construct will allow for maturation of the seeded cells and allow for initial and essential remodeling of the mitral construct. In addition, due to PGG's ability to stabilize collagen and elastin, and its antioxidant, anti-inflammatory, and anti-calcification activities, the polyphenol will protect the scaffold from degradation and prevent degradation of the valves structures. Translationally, this approach is patient specific and should immediately integrate and grow with the host.

2.3 Specific Aims

Three overlying and interrelated aims were established toward achieving the overall goal of this research, and they are directed at understanding: 1) How to develop a stable, acellular, cytocompatible scaffold capable of supporting cellular infiltration, limiting protease degradation, and maintaining adequate mechanical properties; 2) Achieving an effective and optimized recellularization approach, while determining PGG's beneficial effects on limiting scaffold degradation and reducing over-activation of the seeded cells; 3) Development and utilization of a mitral valve bioreactor that takes into account the mitral valve's unique anatomy while providing physical cues and proper force distribution from the annulus, closure of the two leaflets, and adequate tension provided to the chordae tendinae.

Aim 1 *(Chapter 3)***: Develop an acellular scaffold with ECM and mechanical properties similar to the human mitral valve.**

Hypothesis*: A detergent based decellularization method will remove all cellular materials from a porcine mitral valve while retaining sufficient extracellular matrix*

content, including basal lamina proteins. Chemical treatment with PGG will stabilize the matrix scaffold and yield physiologically similar mechanical strength.

Approach: Scaffolds will be generated using a decellularization protocol that employs Triton X-100, SDS, EDTA, Deoxycholic Acid, NaOH and a treatment of RNase/DNase. In doing so, the scaffolds should: 1) have all xenogeneic cellular and nuclear components removed; 2) retain ECM architecture and composition while also preserving all ECM proteins (e.g. collagen type I and IV, elastin, laminin, and fibronectin); and 3) Maintain necessary mechanical properties for leaflets and chordae tendinae while incorporating PGG.

Innovation: We will develop a decellularized, non-immunogenic collagen and elastin scaffold for mitral valve tissue engineering. Through decellularization of porcine tissue, we will able to conserve the niche valvular microstructure of the ECM.

Aim 2 *(Chapter 4)***: To characterize host response and determine resistance to degradation of the scaffold treated with PGG.**

Hypothesis*: The stabilizing, anti-inflammatory, anti-calcification function of PGG will limit scaffold degradation and mitigate immune rejection.*

Approach: As shown in previous studies and in current literature, treatment with PGG, a well-characterized matrix binding polyphenol, will protect scaffolds from calcification, discourage degeneration from proteases, and mitigate immune rejection. Decellularized scaffolds will be treated with PGG and degradation by collagenase and elastase will be evaluated and compared to fresh and untreated decellularized scaffolds. Also, PGG-treated scaffolds will be implanted subdermally in rats. At 4 and 8 weeks,

scaffolds will be explanted and immune response to these treated scaffolds characterized using immunohistochemistry. Host response as well as degradation will be evaluated and compared to non-treated scaffolds.

Innovation: Utilization of scaffolds in tissue engineering, while a part of the classical paradigm, still are hindered by questions concerning their fate once implanted in patients. How long these scaffolds will last within the patient, should the scaffolds be remodeled, and will the patients' body accept them are all common inquiries. Our approach aims to be some of the first to investigate the stabilizing and degeneration-inhibiting affects PGG has on a decellularized mitral valve scaffold. Our novel approach, incorporating PGG, aims to solve these questions, determining the degradation of the scaffold and evaluating the nature of the host response as being inflammatory or remodeling.

Aim 3 *(Chapter 5)***: Develop a mitral valve bioreactor able to provide physiological loading and biochemical environment characteristic to mitral valves.**

Hypothesis: *Optimally seeded constructs will flourish under physiologic conditions provided by a bioreactor that provides correct anatomical positioning and force distribution from annulus to papillary muscles.*

Approach: Pre-differentiated fibroblasts will be manually injected utilizing a fibrin gel as the carrier of these cells. Valves will be first inflated with sterile air, then the fibrin and cell mixture injected into multiple areas of the tissue. Pre-differentiated endothelial cells will then be drop-seeded onto the scaffolds. Recellularized constructs will then be placed in the mitral valve bioreactor with flow, pressure and viscosity conditions gradually increased to allow maturation of cells until reaching physiological levels.

Innovation: Recellularization of any scaffolds into a living construct has been a crux in the paradigm of tissue engineering, especially in ECM-derived scaffolds. Our approach aims to achieve an acceptable level of cellular infiltration and migration initially, which then allows for full recellularization after pre-conditioning in a custom made mitral valve bioreactor. This novel bioreactor will recreate an appropriate force distribution throughout the entire construct.

2.4 Project Significance:

A central motivation for tissue engineering is the regeneration of diseased tissues. With the advancement of stem cell capabilities, one can employ them along with growth factors and engineered matrices to eventually create an autologous implant that can not only grow with the patient but also create a superior alternative to repair and replacement therapies. There has been considerable research into heart valve tissue engineering, but limited clinical testing, especially with the mitral valve. This may be a result of the mitral valve's complicated anatomy or the prevalence of other diseased valves like the aortic valve. A mitral valve tissue engineered solution is an exciting concept, yet early in practice. However, we expect the results of this translational research to have a positive impact on patients suffering from the many forms of mitral valve insufficiency. Success in this project would also lead to a much deeper understanding in the realm of stem cell and ECM interactions, especially in valvular tissues. Overall, this research will greatly contribute to the field of cardiovascular tissue engineering and enable clinicians to provide permanent, living solutions for their patients.

2.5 References:

1. Mozaffarian, D. *et al. Heart Disease and Stroke Statistics--2015 Update: A Report From the American Heart Association*. *Circulation* **131,** (2014).
2. Iung, B. & Vahanian, A. Epidemiology of valvular heart disease in the adult. *Nat. Rev. Cardiol.* **8,** 162–72 (2011).
3. Grande-Allen, K. J. & Liao, J. The heterogeneous biomechanics and mechanobiology of the mitral valve: implications for tissue engineering. *Curr. Cardiol. Rep.* **13,** 113–20 (2011).
4. Curtin, R. J. & Griffin, B. P. Mitral Valve Disease: Stenosis and Regurgitation. *Clevel. Clin. Cent. Contin. Educ.* 1–15 (2010). at <http://www.clevelandclinicmeded.com/medicalpubs/diseasemanagement/cardiology/mitral-valve-disease/>
5. Chandrashekhar, Y., Westaby, S. & Narula, J. Mitral stenosis. *Lancet* **374,** 1271–83 (2009).
6. Pedrazzini, G. B., Faletra, F., Vassalli, G., Demertzis, S. & Moccetti, T. Mitral regurgitation. *Swiss Med. Wkly.* **140,** 36–43 (2010).
7. Shah, P. M. Current concepts in mitral valve prolapse--diagnosis and management. *J. Cardiol.* **56,** 125–33 (2010).
8. Schoen, F. J. & Levy, R. J. Calcification of tissue heart valve substitutes: progress toward understanding and prevention. *Ann. Thorac. Surg.* **79,** 1072–80 (2005).
9. Levine, M. N., Raskob, G., Landefeld, S. & Kearon, C. Hemorrhagic complications of anticoagulant treatment. *Chest* **119,** 108S–121S (2001).
10. Schoen, F. J. Mechanisms of function and disease of natural and replacement heart valves. *Annu. Rev. Pathol.* **7,** 161–83 (2012).
11. Benussi, S., Verzini, A. & Alfieri, O. Mitral valve replacement and thromboembolic risk. *J. Heart Valve Dis.* **13 Suppl 1,** S81–3 (2004).
12. Tang, G. H. L., Rao, V., Siu, S. & Butany, J. Thrombosis of mechanical mitral valve prosthesis. *J. Card. Surg.* **20,** 481–6 (2005).
13. Ayhan, a, Yucel, a, Bildirici, I. & Dogan, R. Feto-maternal morbidity and mortality after cardiac valve replacement. *Acta Obstet. Gynecol. Scand.* **80,** 713–8 (2001).
14. Gammie, J. S. *et al.* Trends in mitral valve surgery in the United States: results from the Society of Thoracic Surgeons Adult Cardiac Surgery Database. *Ann. Thorac. Surg.* **87,** 1431–7; discussion 1437–9 (2009).
15. Oliveira, J. M. F. De & Antunes, M. J. Mitral valve repair: better than replacement. *Heart* **92,** 275–81 (2006).
16. Rausch, M. K. *et al.* Mitral Valve Annuloplasty: A quantitative clinical and mechanical comparison of different annuloplasty devices. *Ann. Biomed. Eng.* **40,** 750–761 (2013).
17. Zussa, C., Frater, R. W. M., Polesel, E., Galloni, M. & Valfré, C. Artificial mitral valve chorde: Experimental and clinical experience. *Ann. Thorac. Surg.* **50,** 367–373

(1990).
18. Goldstein, D. *et al.* Two-Year Outcomes of Surgical Treatment of Severe Ischemic Mitral Regurgitation. *N. Engl. J. Med.* 1–10 (2015). doi:10.1056/NEJMoa1512913
19. Zhang, Li Li, Sung-Hoon Kim, Ann E. Hagerman, J. L. Anti-Cancer, anti-diabetic and other pharmacologic and biological activities of penta-galloyl-glucose. *Pharm. Res.* **26,** 1–27 (2010).

CHAPTER 3: DEVELOPMENT AND CHARACTERIZATION OF A DECELLULARIZED MITRAL VALVE SCAFFOLD

3.1 Introduction:

At its core, the prevailing paradigm in heart valve tissue engineering has been the integration of scaffolds and specific cells to develop mature constructs with regenerative potential. As the foundation for these living constructs, scaffolds provide the framework for housing cells whether they are seeded onto the scaffolds or are repopulated in vivo. These cellular infrastructures can range in their originating materials, mechanical properties, and fabrication. While synthetic scaffolds provide easier customizability, support has risen for the use of naturally derived scaffolds using materials like fibrin and other degradable materials. Acellular tissue matrices derived from the heart valve extracellular matrix (ECM) are rising in popularity due to many of its advantages. Various tissues have been rendered acellular through the process of decellularization which employs chemical, physical, and enzymatic agents to remove any and all xenogeneic cellular and nuclear material from the tissue[1]. In a successful decellularization, the ECM components are largely preserved including structural proteins like collagen type I and elastin, as well as basal lamina proteins collagen type IV and laminin. These are largely conserved across species and thus permits their compatibility as biological scaffolds derived from xenogeneic sources[2,3]. After removal of these components, the remaining structure is a tailor-made structure specific to that tissue and the specific cells that built it. The ECM is a complex of both structural and functional biomolecules that are produced by the resident cells. As a custom built microstructure, the ECM can provide an enormous

amount of information in molecular and mechanical signals to their cellular inhabitants[3]. Therefore, creating a "niche" microenvironment and an inductive scaffold for the repopulating cells, providing the architecture, mechanical properties and binding sites needed.

Detractors of decellularization are the risk of an incomplete removal of cellular and nuclear material from the scaffolds. History has shown that the immunogenic response can be deadly for patients receiving improperly decellularized scaffolds[4]. The host response of an incomplete decellularization will lead to a pro-inflammatory response, invasion of type M1 macrophages and eventual dense scar formation[5]. These responses will disallow constructive remodeling of the scaffold and proper degradation of the scaffold and eventual replacement of anatomically appropriate and functional tissue will not occur. However, decellularized ECM scaffolds have been used in thousands of patients successfully without rejection from their hosts. Current literature has established criteria for a successful decellularization of tissue: 1) no visible nuclei per histological staining, 2) less than 50ng of DNA per mg of dry weight ECM, 3) any remaining DNA content should not exceed 200 base pair in length[3].

Of all the successfully decellularized scaffolds used today including lungs, skeletal muscle trachea and small intestinal submucosa (SIS), the heart valve proves to be uniquely challenging. This largely due to the complex anatomical requirements and the extreme environment for which it resides. The mitral valve resides in one of the most mechanically stressful environments in the body. Therefore, the mitral valve must endure the harsh and repetitive openings and closings during systole and diastole and the valvular ECM must

also withstand these extreme stresses for the lifetime of the patient. As a result, the average decellularization, constructive remodeling and eventual recellularization must be critically evaluated and optimized because this tissue will immediately be put to the test upon implantation. Currently, tissue engineering of the mitral valve utilizing a decellularized scaffold has just begun to scratch the surface with only a handful of groups reporting methods of decellularization[6,7]. This gap is worrying despite the apparent prevalence of mitral valve diseases.

An optimal decellularization for the mitral valve should fulfill the following criteria: 1) current literature standards for removal of xenogeneic cellular and nuclear material should be met as mentioned above, 2) mechanical testing should show preservation of mechanical characteristics, 3) Safeguarding of the ECM should be a top priority. Structurally, the collagen and elastin integrity within the scaffold should remain intact. Basal membrane proteins, which facilitates cellular attachment and migration, should also be present post-decellularization, 4) Degradation of the scaffold should be limited through treatment with PGG.

To achieve this, we decellularized porcine mitral valves using an optimized approach. A hypotonic shock followed by treatment with NaOH assures basic hydrolytic degradation of biomolecules[1]. Extraction of remaining cellular components, including the Gal-α(1,3) Gal epitope, are done with a 5-day immersion in a detergent-based decellularization solution. Additional enzymatic treatment with an RNase/DNase solution is used to remove all the remnant nuclear components. Histological analysis as well as gel electrophoresis and nanodrop techniques were used to evaluate complete removal of

cellular and nuclear material from the scaffolds. Biaxial mechanical testing was performed to evaluate the mechanical integrity of the scaffold. ECM preservation was evaluated using several histological techniques. Overall, we sought complete characterization of the decellularized mitral valve scaffold.

3.2 Methods and Materials:

3.2.1 Mitral Valve Decellularization:

Porcine mitral valves were collected from a local abattoir and transported to the laboratory on ice. After cleaning and trimming extraneous heart muscle, the valves were immersed in ddH_2O overnight at 4°C to induce hypotonic shock and cell lysis. The next day, the valves were treated with NaOH 0.05M for 2 hours, then incubated for 5 days under agitation, in a solution containing 0.2% SDS, 1% Triton X100, 1% deoxycholic acid, 0.4% EDTA, prepared in 20mM TRIS pH 7.4. To remove the detergents, the valves were rinsed 10 times for 15 minutes with ddH_2O, then treated with 70% ethanol for 20 minutes to reduce the bio-burden, and rinsed again 4 times for 15 minutes with ddH_2O. Nucleic acid removal was completed by incubation in a 720 mU/mL deoxyribonuclease, 720 mU/mL ribonuclease mixture in PBS for 2 days at 37°C. Finally, scaffolds were rinsed in ddH_2O (3 times for 15 minutes), and incubated in 70% ethanol overnight at room temperature. The mitral valve scaffolds were stored in sterile PBS with 1% protease inhibitors and 1% antibiotic/antimycotic (Pen-Strep) at 4°C.

3.2.2 DNA Extraction:

DNA was isolated from tissues following the instructions provided in the DNeasy® Blood & Tissue Kit from Qiagen (Germantown, MD). Concentration was measured using

a Nano Drop 2000, Spectrophotometer, UV-Vis; (Thermo Scientific) and by ethidium bromide agarose gel electrophoresis, using the Sub-Cell® GT electrophoresis instruments and instructions (170-4402) provided by BioRad.

3.2.3 Histology and Immunohistochemistry:

Rehydrated paraffin sections (5µm) were stained with Hematoxylin and Eosin (H&E), Movat's Pentachrome, and Verhoeff-Van Gieson (VVG), according to the instructions in the kits purchased from Poly Scientific R&D Corp. (Bayshore, NY). 4',6-diamidino-2-phenylindole (DAPI) was purchased from Sigma-Aldrich Corporation (Lakewood, NJ).

Immunohistochemistry (IHC) was performed on formalin-fixed and paraffin-embedded sections using heat-mediated antigen retrieval (10mM citric acid at pH of 6, for 10 min at 90°C), followed by exposure to 0.025% Triton X-100 for 5 minutes. After incubation in normal blocking serum for 45 minutes, the primary antibodies diluted to 2µg/mL were applied overnight at 4°C in a humidified chamber. The following antibodies were used: rabbit anti-Collagen IV (Abcam, Ab6586), rabbit anti-Laminin (Abcam, Ab11575), rabbit anti-Vimentin (Abcam, Ab92547). Negative controls were obtained by omitting the primary antibodies. The Vectastain Elite kit and the ABC diaminobenzidine tetrahydrochloride peroxidase substrate kit were purchased from Vector Laboratories (Burlingame, CA). Sections were counterstained with a diluted hematoxylin prior to mounting. Images were obtained at various magnifications on a Zeiss Axiovert 40CFL microscope using AxioVision Release 4.6.3 digital imaging software (Carl Zeiss MicroImaging, Inc. Thornwood, NY).

3.2.4 Penta-Galloyl Glucose (PGG) Treatment:

High-purity 1,2,3,4,6-Penta-O-galloyl-beta-D-glucose (PGG) was a generous gift from N.V. Ajinomoto OmniChem S.A., Wetteren, Belgium (www.omnichem.be). The acellular scaffolds were treated with sterile 0.3% PGG in 50mM Na_2HPO_4, 0.9% NaCl, pH 5.5 containing 20% isopropanol overnight at room temperature under agitation and protected from light. Scaffolds were then rinsed with sterile PBS 3 times, and then stored in sterile PBS with 1% protease inhibitors and 1% antibiotic/antimycotic (Pen-Strep).

3.2.5 Mechanical Testing:

The evaluation of biaxial mechanical properties of valve tissues was described previously[8]. Briefly, square tissue samples (~ 12 mm × 12 mm) were trimmed from the anterior leaflet with one edge of the sample aligned along leaflet circumferential direction and the other edge aligned along leaflet radial direction. Thickness of each sample was measured three times using a digital caliper. Four markers were placed in the center of the sample and were tracked with a CCD camera to obtain biaxial tissue deformation. Samples were attached to eight loops of 000 polyester suture of equal length via stainless steel hooks (two loops each edge) and mounted on the biaxial testing system. Membrane tension (force/unit length) was applied along each orthogonal axis (aligned with circumferential direction or radial direction of tissue sample), and was ramped slowly from a 0.5 N/m pre-load to a peak tension of 60 N/m. For testing, tissue sample was preconditioned for ten continuous cycles and followed by a 60 N/m equibiaxial tension protocol. Maximum stretch ratios along the circumferential direction (λ_{circ}) and radial direction (λ_{rad}) were used to assess the tissue extensibility. The biaxial testing was performed with samples immersed

in a PBS bath (pH 7.4). For tensile testing, 50 mm-long samples were cut and thickness was measured using digital calipers. Samples were analyzed at a constant uniaxial velocity of 0.1 mm/s until failure using a 10 Newton load cell on a Synergie 100 testing apparatus (MTS System Corporation, Eden Prairie, MN).

3.2.6 Differential Scanning Calorimetry:

Thermal denaturation temperature (T_d), was determined by differential scanning calorimetry (DSC, model 131 Setaram Instrumentation, Caluire, France) at a heating rate of 10°C/min from 20°C to 110°C in a N_2 gas environment. T_d was defined as the temperature at the endothermic peak[9].

3.2.7 Cell Seeding and Cytocompatibility:

PGG-treated scaffolds were equilibrated overnight in DMEM with 50% FBS, 1% antibiotics and seeded with human adipose tissue-derived stem cells (ASCs) internally and externally. For internal seeding, the base and free edges of the leaflets were inflated with sterile compressed air using a 33GA x 1½-inch needle, and then injected with 0.5 mL of a 1x106 cells/mL cell suspension. For external seeding, a 0.5 mL of 1x106 cells/mL cell suspension was added dropwise to scaffolds and cells allowed to adhere for one hour; then each scaffold was submerged in media (DMEM with 50% FBS, 1% antibiotics, sterile filtered) and statically incubated for days. The viability of the cells after incubation was tested using the Live/Dead Viability/Cytotoxicity Assay Kit (Invitrogen) was used.

3.2.8 Resistance to Collagenase and Elastase:

Tissue degradation by collagenase and elastase was described previously36. Briefly, approximately 15 mg scaffold fragments were lyophilized and the dried samples

weighed. The samples were then incubated with 1 ml of 6.25U/mL type 1 collagenase in 100mM Tris, 1mM CaCl2, 0.02% NaN3, pH 7.8 at 37°C, for 24 and 48 hours with agitation (n=6 per group). Similarly, 10U/mL elastase was used to test elastin stabilization. After removing the enzymes by centrifugation and rinsing in ddH2O, the samples were lyophilized and weighed. Resistance to enzymes was calculated as percent weight loss.

3.2.9 Statistical Analysis:

Results are expressed as means ± standard deviation (SD). Statistical analysis was performed using one-way analysis of variance (ANOVA). Differences between means were determined using the least significant difference (LSD) with an alpha value of 0.05.

3.3 Results:

3.3.1 Scaffold Preparation:

Scaffold color and appearance were indicative of an effective removal of cellular material from the dissected mitral valves. Initially, these valves showed a red and brown color in each of the four tissue types, but after the decellularization procedure they became progressively paler, eventually becoming white and translucent (**Figure 3.1A, B**). Porcine mitral valves were treated with alkali, detergents, and nucleases in order to remove the cells, but maintain the fibrous matrix composition of leaflets and chordae; the resulting scaffold preserved all the valve components.

Histological analysis of the decellularized scaffolds (**Figure 3.2C**) illustrated the removal of cells from the valve. To visualize the elimination of cells, sections of scaffolds and fresh mitral valves (leaflets and chordae) were stained with H&E and DAPI, which confirmed the complete removal of cellular components. In addition to these nuclear stains,

an immunohistochemistry (IHC) for actin, a common cellular protein, was performed for both the acellular scaffolds and fresh tissue. Decellularized scaffolds did not show positive for this protein, while fresh tissue did display the positive brown stain. To further validate the completeness of the decellularization, DNA was extracted from scaffold tissues and compared to the DNA content of fresh mitral valve tissues by electrophoresis, followed by densitometry. This analysis showed more than 96% DNA elimination from leaflets and chordae (**Figure 3.1D**). Quantification of DNA in the decellularized scaffolds with additional solutions, including DNase/RNase as described, resulted in further reduction of DNA content. Nanodrop analysis showed a significantly higher DNA content in the fresh mitral leaflets and chordae, about 500ng/mg fresh leaflet and chordae, and less than 50ng/mg of ECM for both decellularized the leaflet and chordae.

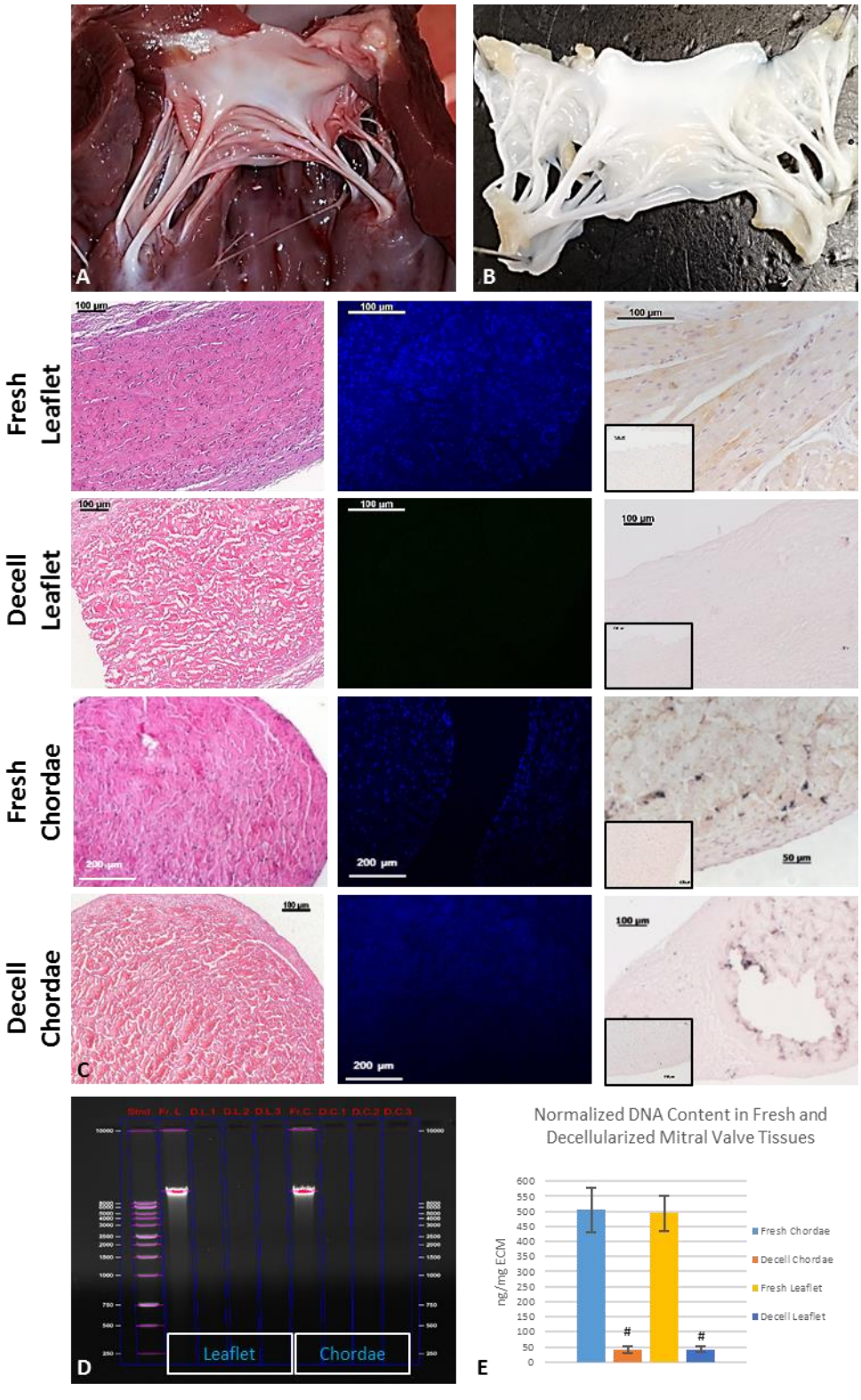
A
B
Fresh Leaflet
Decell Leaflet
Fresh Chordae
Decell Chordae
100 µm
200 µm
50 µm
C
D
Leaflet
Chordae
Normalized DNA Content in Fresh and Decellularized Mitral Valve Tissues
ng/mg ECM
600
550
500
450
400
350
300
250
200
150
100
50
0
#
Fresh Chordae
Decell Chordae
Fresh Leaflet
Decell Leaflet
E

Figure 3.1: Mitral valve decellularization. A) An aspect image of a fresh mitral valve still embedded in the left atrium of a porcine heart. B) A macroscopic aspect of a decellularized porcine mitral valve. Lack of coloring in the valve is indicative of removal of cellular material. C) Histological images indicating removal of all cellular components in the mitral valve leaflets and chordae tendinae. Fresh (native) and decellularized cross-sections of each tissue type are shown for comparison. These sections were stained with hematoxylin and eosin (H&E), which shows cell nuclei and background. Nuclei are shown in dark purple while background is shown in pink. Next sections were stained with DAPI, which also reveals nuclei in fluorescent blue dots. Last, and IHC for actin, a common cellular protein, was performed. Brown is an indicator for a positive stain, nuclei are stained purple. D) Ethidium Bromide agarose gel electrophoresis analysis was used from DNA extracted from fresh and decellularized leaflets and chordae. A standard was also included. Fresh samples are indicated with a "FL" for fresh leaflet, and "FC" for fresh chordae. Decellularized samples are indicated with a "DL" for decellularized leaflet and "DC" for decellularized chordae. No bands were detected for decellularized tissue verifying removal of all nuclear material from scaffolds. E) To quantify DNA content in each tissue type and for fresh and decellularized samples, a Nanodrop was used. Quantities of DNA for decellularized samples were significantly lower than fresh samples. In addition, each decellularized tissue was below 50ng of DNA.

3.3.2 Evaluation of Scaffold Structure and Matrix Integrity:

For a scaffold primarily comprised of collagen and elastin, preservation of these ECM components is critical for success of the scaffold. Collagen and elastin fibers, both crucial for maintaining valve shape and function, maintained their integrity in both leaflets and chordae after decellularization, as observed in sections stained with Movat's Pentachrome (**Figure 3.2A, F**). VVG, a specific stain for elastin, showed intact elastin fibers in the atrial and ventricular side, as well as in the structure of chordae (**Figure 3.2B, E**). Glycosaminoglycans were removed together with the cells, forming typical "pores" in the tissue, necessary for cell repopulation; this is illustrated in the Movat's Pentachrome

images for each tissue type. Basal lamina components, collagen IV and laminin, essential for cell adhesion, were detected using specific antibodies (**Figure 3.2C, D**).

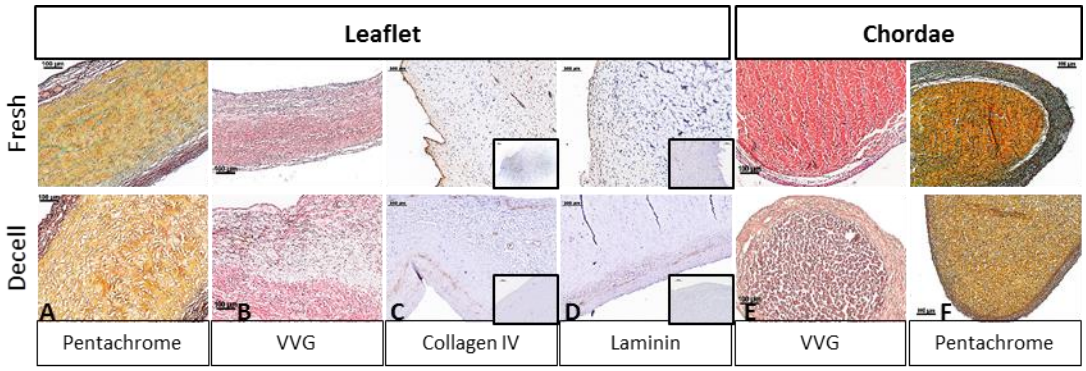

Figure 3.2: Histology of Mitral Valve Scaffold. To illustrate preservation of the extracellular matrix in the decellularized scaffolds, histology of fresh and decellularized leaflets and chordae were stained with Movat's pentachrome, which shows nuclei (dark red), collagen (yellow), elastin fibers (maroon), and cytoplasmic proteins (red). To further illustrate the conservation of elastin fibers, these sections were stained with Verhoeff-Van Gieson's (VVG) stain for visualization of nuclei (grey/black), elastin fibers (black), and collagen (pink). Loss of nuclei is illustrated as shown before, but these cross-sections show conservation of elastin and collagen in the decellularized scaffolds. An immunohistochemistry (IHC) for basal membrane proteins collagen IV and laminin were also performed with a positive stain showing in brown and nuclei showing in purple. Decellularized scaffolds stained positive for both basal membrane proteins.

3.3.3 Scaffold Stabilization and Crosslinking Evaluation:

The acellular scaffolds were treated with 0.3% PGG in order to stabilize the tissues and increase their strengths and resistance to degradation. Biaxial testing showed that decellularization significantly decreased the tissue stiffness in both the radial and circumferential directions, compared to fresh tissues (**Figure 3.3A, B**). Treatment with PGG, a polyphenolic compound that binds to proline-rich regions and induces the formation of crosslinks within the collagen and elastin molecules, contributed to the

increase of tissue stiffness, showing a doubling in elastic modulus for the chordae tendinae (from 23.4+/-4 MPa to 49.7+/-7 MPa) (**Figure 3.3C**). Differential scanning calorimetry (DSC) showed a slightly lower but statistically significant denaturation temperature (Td) for decellularized scaffolds when compared to the fresh tissue (66.4+/-6ºC vs. 70.7+/-8ºC) due to tissue destabilization after removal of cells). PGG-treated scaffolds exhibited significantly higher Td (84.5+/-9ºC) possibly due to the increase in number of crosslinks (**Figure 3.3D**).

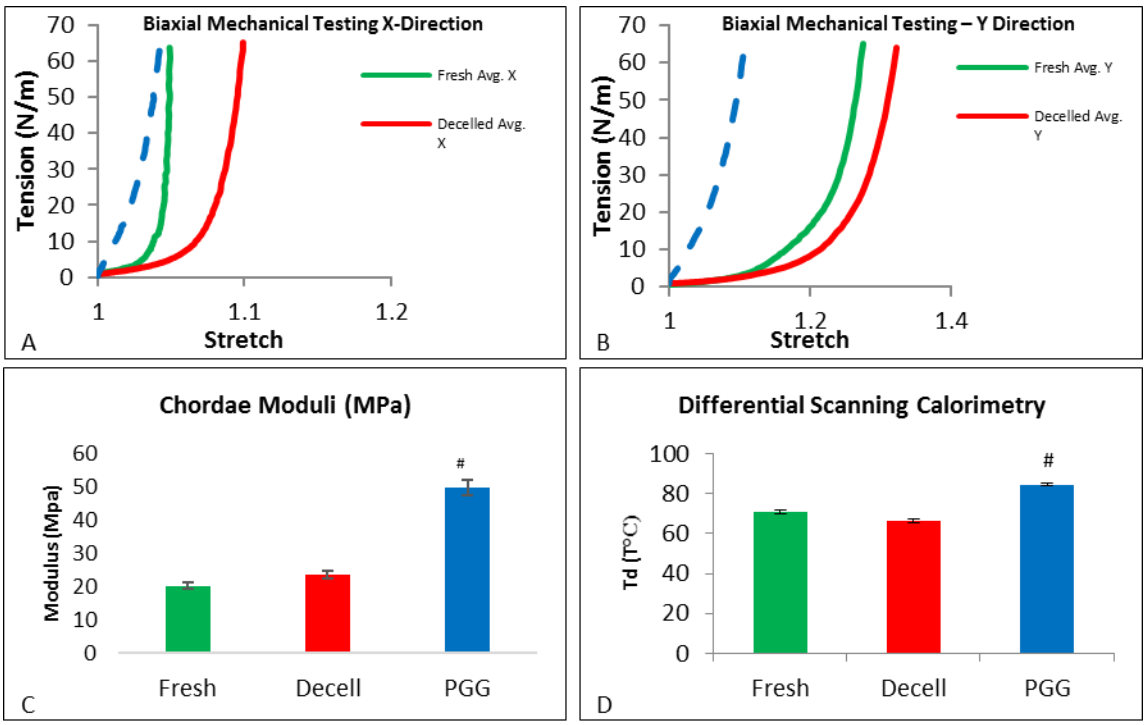

Figure 3.3: Matrix stabilization in acellular mitral valves. Fresh, decellularized, and PGG-treated scaffolds were compared. A, B) biaxial stress-strain analysis of leaflets from each treatment type, were tested in the radial (X) and circumferential (Y) directions. Avg., average values for n=5. C) The elastic moduli of fresh, decelled and PGG-treated chordae were also measured. PGG-treated chordae had a significantly higher moduli than the other two groups. D) Differential scanning calorimetry (DSC) evaluation of fresh, decelled, and PGG-treated acellular leaflets was conducted. This measure of cross-linking in the scaffolds showed

PGG-treated samples to be significantly higher than fresh and decellularized groups. Td is the thermal denaturation temperature. *$p<0.05$ compared to fresh.

Stabilization of the acellular mitral valve leaflet and chordae scaffold with PGG was further evaluated on its resistance to degradation by proteases. PGG-treated scaffolds were treated in collagenase and elastase for 24hr and 48hr treatments. These results were compared to fresh and untreated decellularized leaflet and chordae scaffolds. Results indicate that PGG significantly increases the resistance to degradation. Untreated decelled scaffolds were more readily degradable by both collagenase and elastase even compared to fresh tissues (**Figure 3.4A, B**). Treatment with PGG significantly reduced the scaffolds' susceptibility to enzymes: by 5-fold to collagenase and more than 2-fold to elastase. This trend was true for both the 24 and 48-hour time points, but more pronounced in the 48-hour time point.

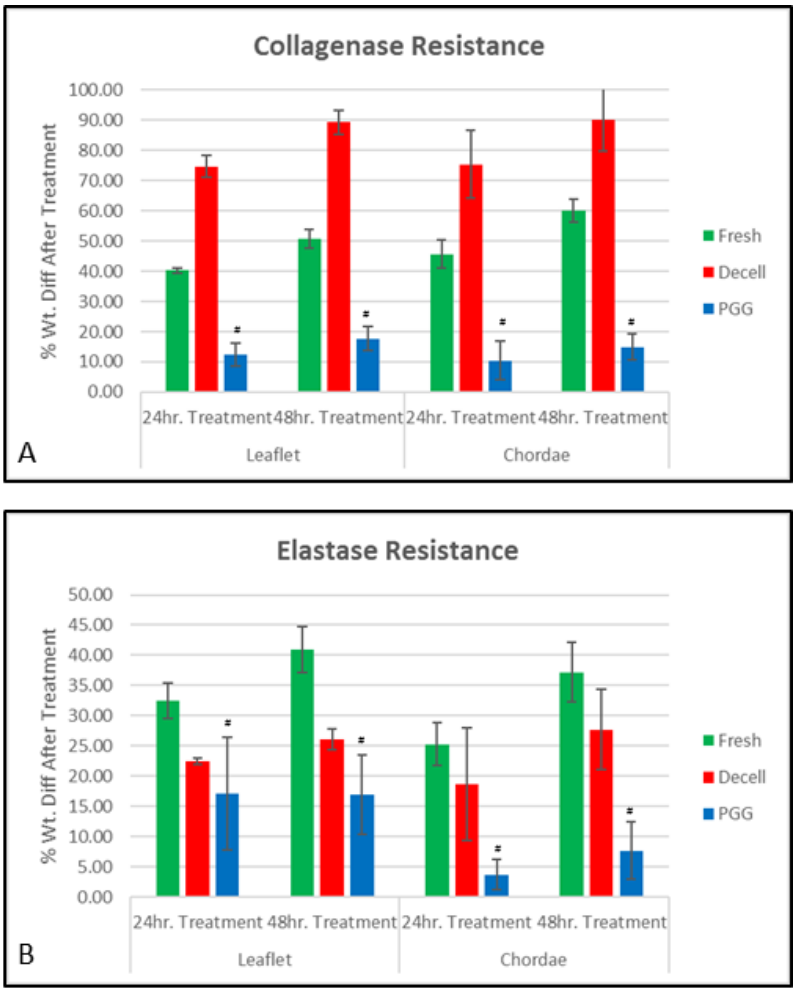

Figure 3.4: Resistance to Proteases. Fresh, decellularized, and PGG-treated acellular mitral valve leaflets and chordae were compared based on their resistance to proteases. There was a 24 hour and 48 hour exposure time and these were compared for each tissue type and group. Values are expressed as percent dry weight loss after exposure to enzyme. # $p<0.05$ compared to fresh. A) Resistance to collagenase was evaluated. PGG-treated tissues showed significantly lower percent weight loss from exposure compared to fresh tissues. Decellularized tissues showed the greatest capacity to degrade for both time points. B) Resistance to elastase was evaluated. PGG-treated tissues also showed significantly lower percent weight loss from exposure to the enzyme when compared to fresh. # $p<0.05$ compared to fresh. Fresh tissues showed the greatest capacity to degrade from elastase for both time points.

3.3.4 Cell Seeding and Cytocompatibility:

To evaluate the capacity for cells to survive on the PGG-treated scaffold, cells were seeded into and on the exterior of the scaffold. The acellular mitral valve scaffolds exhibited excellent compatibility toward hADSCs as demonstrated by the presence of viable cells after 3 days of incubation under static conditions (**Figure 3.5A**). Injected cells spread between the fibers of leaflets, as seen in the DAPI, H&E, and the Movat's Pentachrome stained sections (**Figure 3.5B, C, E**). An IHC for vimentin, a protein known to be secreted by mesenchymal cells also showed positive (**Figure 3.5D**). Cells seeded on the surface maintained their viability and attached to the valve.

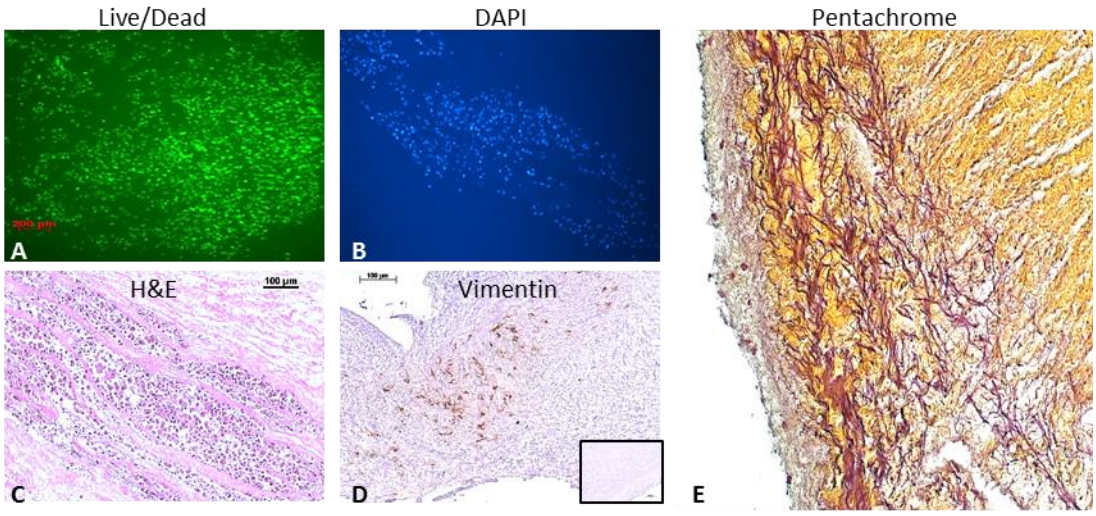

Figure 3.5: Cell Seeding and Cytocompatibility. Cytocompatibility of acellular scaffolds. Representative images of PGG-treated scaffolds seeded with cells and analyzed 3 days after seeding to show cytocompatibility. A) Live/Dead staining was performed with green fluorescence showing living cells and red showing dead cells. B) DAPI nuclear staining to show nuclei within the tissue. C) H&E staining. D) An IHC for vimentin was performed, brown showing a positive stain for the protein. E) A Movat's Pentachrome was also performed.

3.4 Discussion:

3.4.1 Evaluation of Decellularization Efficiency and Characterization:

In this study, we have taken a thorough and systematic approach to establish a method to develop a tissue engineered mitral valve scaffold using decellularized porcine mitral valves. While decellularization of organs and other heart valves, including and especially the aortic valve, is not uncommon, very few groups have sought to develop a decellularized scaffold for mitral valves[6,7]. This is despite a serious need for an improved valvular replacement. Utilization of this niche microstructure as an inductive scaffold has well established potential, however as mentioned a decellularized scaffold must meet several criteria. As mentioned above, the scaffold must remove cellular and nuclear materials according to standards set in current literature, conserve the extracellular matrix and the corresponding mechanical characteristics of native valve, and stability of the scaffold must be ensured.

Our choice of chemical agents was predicated on an already existing aortic valve decellularization protocol[10]. In several pilot studies, we used differing time points and eventually different concentrations of the components of the detergent solutions and increased the concentration of the DNase/RNase solutions described above. Unique to the mitral valve are the four tissue types that one must account for in search for an optimized decellularization that removes xenogeneic cellular and nuclear material while still preserving the ECM. While not definitive, macroscopically there is a marked difference when comparing fresh valves, which have red and brown color to them, with the white and

sometimes translucent coloring of a decellularized valve. In our histological analysis, we sought to show complete removal of the cellular components. Each histological image shows the cross-section of the leaflet or the chordae tendinae. This is to ensure complete view of the ECM, especially to view the three layers of the mitral valve ECM. Lacking in each of the decellularized samples are the cells from the native valves. Pores are now present where these cells used to reside, these pores could eventually be replaced with seeded cells. To further elucidate cellular removal, an IHC for actin, a common cellular protein was shown to have zero expression in the decellularized scaffolds. As part of the criteria established by our group as well as in literature, removal of nuclear material is also essential for a successful decellularization. The ethidium bromide agarose gel electrophoresis performed showed no presence of DNA in both the leaflets and the chordae (**Figure 3.1D**). Densitometry showed about a 96% removal of DNA when compared to fresh controls. To further meet the decellularization criteria, more quantitative analysis was required. Therefore, the Nanodrop was utilized to measure DNA quantities in ng/mg of ECM. From this, we showed significant differences between fresh and decellularized samples when comparing DNA quantities. Badylak and his group have established that complete removal of all DNA from a scaffold would be impossible, but that an amount less than 50ng/mg of ECM would be acceptable. Both of our samples for leaflets and chordae meet these criteria (**Figure 3.1E)**.

3.4.2 Preservation of ECM and Basal Lamina Components:

While the elimination of cellular and nuclear material from the scaffold is paramount for the success of the scaffold, preservation of the existing niche ECM is of

equal importance. The ECM as mentioned is an inductive microstructure that can direct cells to migrate, proliferate, differentiate, or encourage apoptosis and degradation of the scaffold. The mechanotransductive cues delivered to cells via an intact mitral valve microenvironment are extremely significant to the reasoning in choosing this as a scaffold. Simply providing an array of collagen and elastin to seeded cells would inevitably render the scaffold useless and undiscernible as a mitral valve scaffold. Therefore, post-decellularization analysis must evaluate how this process affected the complex collagen and elastin matrix after cellular and nuclear materials were removed. This is true for each tissue type under consideration within the mitral valve apparatus.

Results from several histological stains performed show a preserved mitral valve ECM. Movat's Pentachrome, which stains for many matrix components, showed a loss of GAGs; however, this is expected after using the detergent solution used in the decellularization protocol. The two main structural proteins, collagen and elastin however remained. As seen in the comparison between the fresh and decellularized leaflet and chordae, the structure of collagen and elastin remain. A VVG stain was done specifically to visualize the elastin in the scaffold. Overall, the quantity and quality of the elastin seems to have remained intact after decellularization. This is important because in degenerative valves, elastin, as well as collagen, are fragmented and could lead to mitral valve prolapse and insufficiency[11]. Also pertinent to ECM conservation was retaining the basal lamina predominantly collagen type IV and laminin. Studies have shown that an intact basal lamina provides a scaffold along which cells can migrate, proliferate and regenerate damaged tissues[12–14]. An IHC was performed for both of these basal lamina proteins for

each tissue type in fresh and decelled samples. As expected, the fresh samples stained positively for collagen type IV and laminin. This was also true for the decellularized samples. Therefore, our scaffolds after undergoing decellularization are not only acellular and lack nuclear material, but we were able to retain basal lamina proteins that are essential for a successful recellularization. Not only did we preserve these proteins, but the overall architecture of the heart valve ECM in both the leaflets and the chordae tendinae.

3.4.3 Evaluation of the Scaffold's Durability:

The mitral valve conducts a complex mechanical performance with the mitral valve structures and requires the integrity and durability of strong collagen and resilient elastin fibers[15,16]. As mentioned, a tissue engineered mitral valve would be expected to operate in a harsh environment of continual and repetitive stresses brought on by the demands of the heart. Therefore, a decellularized scaffold must be able to withstand these forces immediately upon implantation. Translatability of this project depends on this immediate functionality for patients. Accordingly, after evaluating the preservation of the ECM, we tested the durability of the decelled scaffold and the effect PGG treatment had on them. PGG, used before for the stabilization of aortic valve scaffolds, was used here for the first time for the stabilization of the complex and heterogeneous structure of the mitral valve. Biaxial mechanical testing was performed on three groups, fresh, decell, and PGG-treated decelled scaffolds (**Figure 3.3A, B**). From this, we can see that the decellularization process does in fact decrease the strength of the tissue when compared to the fresh samples. Treatment with PGG increased the mechanical strength of the scaffolds in both the circumferential and radial direction slightly higher than native valves. PGG also increased

the modulus for the chordae tendinae in comparison to the untreated-decelled chordae. Weak and enlarged "floppy" leaflets are often associated with chordal elongation, thinning, and/or rupture. Therefore, chordal modulus is important for the valve's overall coaptation. Differential scanning calorimetry (DSC) was used to evaluate crosslinking within the scaffolds when compared amongst fresh, decelled, and PGG-treated samples. PGG-treated samples yielded a significantly higher thermal denaturation temperature when compared to the decelled group. This is related to the preservation of the integrity of the collagen and elastin fibers. An evaluation of the scaffold's durability must also consider withstanding a host response from the patient. Most of the natural and untreated tissues used in scaffolds elicit a host response and are prone to degradation post-implantation[17]. Because the mitral must undergo large and repetitious forces during a patient's lifetime, the scaffold must be able to withstand degradation, degenerative pathologies will ensue, or the construct will fail altogether. In either case, failure of valvular coaptation would persist and the multiple mechanisms in the mitral apparatus would fail to operate properly. Treatment with PGG has shown to circumvent these issues. We evaluated (**Figure 3.4A, B**) the effectiveness PGG would have on degradation of scaffolds treated with the proteases collagenase and elastase. Fresh, decelled, and PGG-treated acellular scaffolds were compared at both 24 and 48-hour treatments. Remarkably, PGG-treatment significantly increased resistance to degeneration of the scaffolds at both time points. The untreated decelled scaffolds were the most prone to degeneration when exposed to collagenase, and the fresh tissues were the most prone to degeneration when treated with elastase. It appears the decellularization process does affect a scaffold's degeneration potential and perhaps affects the structural

proteins collagen and elastin differently, as evidenced the differences in degradation. The increased resistance of PGG-treated scaffolds to the activity of proteases confirms the integrity of these macromolecules. These results may be significant as it was demonstrated that fragmented elastin is prone to calcify in cardiovascular tissues, such as the aortic wall[18]. In fact, varying degrees of calcification are found in the mitral valve annulus of degenerating valves. PGG in previous studies has shown to significantly decrease calcification of implanted tissues, and while this was not tested with the present study, we anticipate that the tissue-engineered mitral valve would be protected from in vivo calcification[9].

Besides optimal physical properties and durability, the collagen and elastin-based scaffolds proved to be cytocompatible. The paradigm with which our lab operates advocates for recellularization of the scaffold and construct pre-conditioning in a bioreactor. Therefore, human adipose derived stem cells were seeded into and on the PGG-treated scaffold to assess their potential to survive (**Figure 3.5**). Live/Dead images as well and nuclear staining showed that not only can cells thrive on the scaffold, but we also have the capacity to seed the scaffold interstitially. This was imperative to the further aims presented. In addition to their survival, the cells appeared to synthesize a layer of GAGs, which we interpreted as constructive remodeling of the leaflets (**Figure 3.5E**). This cell-matrix interaction is the key to the success of this scaffold. The positive remodeling observed by the initial cell seeding we believe is a result of the well-preserved biochemical composition of the scaffolds, as well as its architecture.

3.5 Conclusions:

An effort was made to develop an acellular scaffold that provided cells with a tailor-made and inductive scaffold for regeneration of the mitral. To achieve this, porcine mitral valves were rid of cellular and nuclear materials successfully without damaging the existing extracellular matrix composition and structure. DNA levels remaining in the scaffold were well below values established in literature as acceptable. Basal lamina proteins collagen type IV and laminin were preserved which will provide a means for the eventual recellularization of the scaffolds. After the scaffolds were decellularized, they were stabilized with PGG. PGG, by virtue of tis collagen and elastin-stabilizing abilities preserved the composition and structure of the ECM of the acellular leaflets and chordae, required by the valve's complex mechanical effort. In mechanical and DSC testing, PGG-treated scaffolds provided acceptable mechanical and crosslinking characteristics similar to native tissues and statistically different when compared to decellularized scaffolds. Once implanted, these scaffolds would inevitably undergo a host response and exposure to proteases. Treatment with PGG provided significant protection from collagenase and elastase confirming their ability to protect against degradation from an expected host response. PGG-treated scaffolds also were able to support cell survival and remodeling thus confirming their potential as a great mitral valve scaffolds.

3.6 References

1. Crapo, P. M., Gilbert, T. W. & Badylak, S. F. An overview of tissue and whole organ decellularization processes. *Biomaterials* **32,** 3233–43 (2011).
2. Bernard, M. P. *et al.* Nucleotide sequences of complementary deoxyribonucleic acids for the pro alpha 1 chain of human type I procollagen. Statistical evaluation of structures that are conserved during evolution. *Biochemistry* **22,** 5213–5223 (1983).
3. Londono, R. & Badylak, S. F. Biologic Scaffolds for Regenerative Medicine:

Mechanisms of In vivo Remodeling. *Ann. Biomed. Eng.* **43,** 577–592 (2015).
4. Simon, P. Early failure of the tissue engineered porcine heart valve SYNERGRAFT™ in pediatric patients. *Eur. J. Cardio-Thoracic Surg.* **23,** 1002–1006 (2003).
5. Badylak, S. F. Decellularized Allogeneic and Xenogeneic Tissue as a Bioscaffold for Regenerative Medicine: Factors that Influence the Host Response. *Ann. Biomed. Eng.* (2014). doi:10.1007/s10439-013-0963-7
6. Iablonskii, P. *et al.* Tissue-engineered mitral valve: morphology and biomechanics. *Interact. Cardiovasc. Thorac. Surg.* **20,** 1–8 (2015).
7. Grande-Allen, K. J. & Liao, J. The heterogeneous biomechanics and mechanobiology of the mitral valve: implications for tissue engineering. *Curr. Cardiol. Rep.* **13,** 113–20 (2011).
8. Liao, J., Joyce, E. M. & Sacks, M. S. Effects of decellularization on the mechanical and structural properties of the porcine aortic valve leaflet. *Biomaterials* **29,** 1065–74 (2008).
9. Chow, J. P. *et al.* Mitigation of diabetes-related complications in implanted collagen and elastin scaffolds using matrix-binding polyphenol. *Biomaterials* **34,** 685–95 (2013).
10. Sierad, L. N. *et al.* Design and Testing of a Pulsatile Conditioning System for Dynamic Endothelialization of Polyphenol-Stabilized Tissue Engineered Heart Valves. *Cardiovasc. Eng. Technol.* **1,** 138–153 (2010).
11. Salhiyyah, K., Yacoub, M. H. & Chester, A. H. Cellular Mechanisms in Mitral Valve Disease. 702–709 (2011). doi:10.1007/s12265-011-9318-7
12. Vassort, G. & Turan, B. Protective Role of Antioxidants in Diabetes-Induced Cardiac Dysfunction. 73–86 (2010). doi:10.1007/s12012-010-9064-0
13. Tollervey, J. R. & Lunyak, V. V. medicine or an additional piece in the puzzle of Merging Innovations to Advance Stem Cell Research and Therapies © 2012 Landes Bioscience . **4101,** (2017).
14. Rehman, J. *et al.* Human Adipose Stromal Cells. 1292–1299 (2004). doi:10.1161/01.CIR.0000121425.42966.F1
15. Kunzelman, K. S., Quick, D. W. & Cochran, R. P. Altered collagen concentration in mitral valve leaflets: Biochemical and finite element analysis. *Ann. Thorac. Surg.* **66,** (1998).
16. Tamura, K. *et al.* Abnormalities in elastic fibers and other connective-tissue components of floppy mitral valve. *Am. Heart J.* **129,** 1149–1158 (1995).
17. Isenburg, J. C., Simionescu, D. T. & Vyavahare, N. R. Elastin stabilization in cardiovascular implants: improved resistance to enzymatic degradation by treatment with tannic acid. *Biomaterials* **25,** 3293–302 (2004).
18. Simionescu, A., Simionescu, D. T. & Vyavahare, N. R. Osteogenic Responses in Fibroblasts Activated by Elastin Degradation Products and Transforming Role of Myofibroblasts in Vascular Calcification. *Am. J. Pathol.* **171,** 116–123 (2007).

CHAPTER 4 – EVALUATION OF THE HOST RESPONSE TO IMPLANTED MITRAL VALVE SCAFFOLDS

4.1 Introduction:

Mammalian host response is an integral consideration and ultimate determinant of an implantable biomaterial's success; this is especially true with tissue-engineered constructs. In discordance with the conventional goal for a biomaterial's "inertness", a tissue engineered construct instead aims to employ the immune response as a means to integrate these constructs with the patient for repair and ultimately regeneration of the damaged tissue. The advent of tissue engineering has modified the accepted principles for a host's response to implanted materials. These constructs support cellular attachment, migration, viability, growth and encourage differentiation of a variety of cell types. Decellularized matrices, such as our mitral valve scaffold, need to modulate the innate immune response and thereby control the release of bioactive molecules and its own degradation to eventually support functional replacement of the tissue[(1)]. The functional outcome of this scaffold is ultimately determined by the elicited host response and the subsequent effects on the scaffold[(1,2)]. This is especially true for a tissue engineered mitral valve, as it undergoes demanding mechanical loading at the immediacy of its implantation. These arduous and repetitious mechanical forces, when considered in the realm of tissue engineering, are perhaps exclusive to the heart valve. Accordingly, degradation and remodeling of the heart valve scaffold must be evaluated within the innate immune response. Constructive remodeling, as defined by Badylak's group, is the process by which a construct is completely degraded and eventually replaced by appropriate and newly native functional tissue[(2)]. An implanted mitral valve construct must be able to facilitate

gradual constructive tissue remodeling within its environment. This outcome is dependent upon a favorable response from the host's immune system, which is largely a function of macrophage polarization.

Immediately following implantation, the process of tissue remodeling begins and a robust macrophage response ensues beginning with the infiltration of neutrophils and monocytes[2–5]. These monocytes will then differentiate into two broad, polarized categories of macrophages. Differentiation leads to either the pro-inflammatory, M1 macrophage, or the pro-healing, M2 macrophage[1,2,6–9]. A successful functional outcome is conditional upon how these macrophages receive the microstructure they have invaded and their plans for degradation and remodeling. Polarization into either phenotype is context specific and is contingent upon the highly complex ECM scaffold in which the remodeling is taking place. M1 macrophages are the pro-inflammatory and cytotoxic macrophage phenotype and promote pathogen killing within the wound site. They also function to debride the implant site of dead cells and damaged tissues. This phenotype is induced by the well-known pro-inflammatory signals and cytokines IFN-γ and TNF-α.[1,6]. They in turn produce additional pro-inflammatory cytokines IL-1β, IL-6, IL-12, IL-23, and TNF-α[1,8]. These activated macrophages produce high levels of induced nitric oxide synthase (iNOS) and secrete toxic levels of reactive oxygen species (ROS), while also acting as inducer and effector cells for Th1 type inflammatory responses[2]. The M2 macrophage phenotype is characterized as the pro-healing macrophage and is typified by expressing IL-12, IL-23, and IL-10[1,8]. It can be induced by several different factors the most common of which are the cytokines IL-4, IL-13, and IL-10[1,6,8]. These "alternatively

active" macrophages express high levels of receptors that resolve inflammation such as scavenger, mannose, and galactose receptors[2]. More specifically, there are three M2 sub-phenotypes, M2a, M2b, and M2c each with their own inducers and markers[2,6,10,11]. Despite these sub-phenotypes, macrophage polarization generally refers to the polar extremes of the pro-inflammatory M1 and the anti-inflammatory M2 macrophage[10,11]. This polarization is driven by cues in the microenvironment from the ECM scaffold[12]. While the directors of macrophage phenotype are not fully understood, enough is known about these populations that specific markers can identify them. M1 macrophages are distinguished by iNOS, CD80, and CCR7 while M2 macrophages are identified by CD163, CD206, and Fizz1/Ym[7–9]. Macrophages are also a plastic cell population capable of changing their polarization based on the stimuli they receive during the process of wound healing[8]. To date, most strategies that employ a more balanced polarization between M1 and M2 macrophages or a predominantly M2 macrophage presence have shown to illicit the most successful functional outcomes[1]. Therefore, it would greatly benefit a mitral valve construct to tip the scales of immune response to an anti-inflammatory, M2 phenotype. Knowing too that the presence of an M1 phenotype is necessary and not fully discouraged. Therefore to encourage a more desirable and tunable constructive remodeling our group turned to Penta-galloyl glucose (PGG).

PGG, is a well characterized polyphenol which exhibits high affinity for proline-rich proteins like collagen and elastin[13]. PGG has a high affinity towards these proteins due to its polyphenol shape[14]. As mentioned previously, this gravitation towards collagen and elastin made PGG an ideal scaffold stabilizer and actually impeded degradation by a

factor of about 50[15]. PGG has also has been reported to have many beneficial effects such as antioxidant, anti-diabetic, and anti-inflammatory activities[14,16–20]. The protective effects of antioxidants for endothelial and vascular aspects are well known[21–24]. Tannins, like PGG, are also good modulators of antioxidants and it can act as a radical scavenger and sink. Studies have shown that this free radical scavenging ability can inhibit lipid peroxidation induced by hydrogen peroxide[25]. PGG has also been shown to debilitate pro-inflammatory cytokines, TFN-α and IL-6, both of which are pertinent in macrophage polarization[26]. In addition, the antioxidant properties of this multifaceted polyphenol also act as a means of regulating reactive oxygen species (ROS).

Ultimately, the goal of this study was to evaluate our scaffold's potential for a functional outcome, evaluate constructive remodeling of the construct and of course assess biocompatibility of the mitral valve scaffold. This was done by completing a 4 and 8 week rat subdermal implant study using PGG-treated and non-treated decellularized scaffolds. Our group evaluated cellular infiltration to see what types of cells inhabited the scaffolds, macrophage polarization and degradation of the scaffolds. Each of these were compared between the PGG and non-treated scaffolds. The host response in this study the key determinant of the functional outcome and translatability of this scaffold from bench to bedside. By successfully traversing the host response and attenuating a pro-inflammatory response in favor of a pro-healing and remodeling response, this mitral valve scaffold with the aid of PGG has a chance at a successful functional outcome.

4.2 Methods and Materials:

4.2.1 Histology and Immunohistochemistry:

Rehydrated paraffin sections (5μm) were stained with Hematoxylin and Eosin (H&E), and Movat's Pentachrome according to the instructions in the kits purchased from Poly Scientific R&D Corp. (Bayshore, NY). 4',6-diamidino-2-phenylindole (DAPI) was purchased from Sigma-Aldrich Corporation (Lakewood, NJ).

Immunohistochemistry (IHC) was performed on formalin-fixed and paraffin-embedded sections using heat-mediated antigen retrieval (10mM citric acid at pH of 6, for 10 min at 90°C), followed by exposure to 0.025% Triton X-100 for 5 minutes. After incubation in normal blocking serum for 45 minutes, the primary antibodies diluted to 2μg/mL were applied overnight at 4°C in a humidified chamber. The following antibodies were used: mouse anti-α-Smooth Muscle Actin (Abcam, Ab7817), rabbit anti-SM22 (Abcam, Ab14106), rabbit anti-Calponin (Abcam, Ab46794), rabbit anti-Vimentin (Abcam, Ab92547), rabbit anti-HSP-47 (Abcam, Ab77609), rabbit anti-P4HA3 (Abcam Ab101657). Negative controls were obtained by omitting the primary antibodies. The Vectastain Elite kit and the ABC diaminobenzidine tetrahydrochloride peroxidase substrate kit were purchased from Vector Laboratories (Burlingame, CA). Sections were counterstained with a diluted hematoxylin prior to mounting. Images were obtained at various magnifications on a Zeiss Axiovert 40CFL microscope using AxioVision Release 4.6.3 digital imaging software (Carl Zeiss MicroImaging, Inc. Thornwood, NY).

4.2.2 Penta-galloyl glucose (PGG) Treatment:

High-purity 1,2,3,4,6-Penta-O-galloyl-beta-D-glucose (PGG) was a generous gift from N.V. Ajinomoto OmniChem S.A., Wetteren, Belgium (www.omnichem.be). The acellular scaffolds were treated with sterile 0.3% PGG in 50mM Na_2HPO_4, 0.9% NaCl, pH

5.5 containing 20% isopropanol overnight at room temperature under agitation and protected from light. Scaffolds were then rinsed with sterile PBS 3 times, and then stored in sterile PBS with 1% protease inhibitors and 1% antibiotic/antimycotic (Pen-Strep).

4.2.3 In vivo Biocompatibility:

Acellular leaflet and chordae scaffold samples, treated with PGG and non-PGG treated, were prepared as described above. A 10mm diameter sterile biopsy punch was then used to cut equally, sized biopsy punch was then cut equally sized leaflet samples for implantation. Equally sized chordae samples were also chosen. Before implantation, the samples were sterilized in 0.1% (w/v) peracetic acid in PBS for 1h, followed by rinsing in four changes of sterile PBS.

In accordance with an IACUC-approved animal use protocol, 52 juvenile Sprague-Dawley rats were anesthetized with buprenorphine at 0.03-0.05 mg/kg and acepromazine at 0.5 mg/kg administered subcutaneously. A small incision was made in the center of the dorsal area of each rat about 2 cm inferior to the scapulae, and, using blunt dissection, two pockets were created between the dermis and fascia lateral to the incision (one pocket in each direction). A scaffold sample was placed into each pocket, and the incision was closed using staples. Thirteen rats received non-treated, decellularized scaffolds, and the remaining 13 received PGG-treated decellularized scaffolds. This was true for both tissue types, mitral valve leaflet and chordae tendinae. Rats were allowed to recover and were housed individually for the remainder of the study. At 4 weeks 24 rats were euthanized and at 8 weeks, the remaining 28 were euthanized, both via CO2 gas (Euthanex system) followed by pneumothorax. Scaffold samples and small amounts of their adjacent host

tissues were excised and fixed in 10% neutral buffered formalin and processed for histological examination.

4.2.4 Gelatin Zymography:

MMP activity was determined by gelatin zymography: 6µg proteins/lane were loaded in triplicated on ready to use BioRad gels, alongside pre-stained molecular weight standards. After development and staining with Coommassie Blue, the MMP clear bands on a dark blue background were evaluated by densitometry and expressed as relative density units. Electrophoresis apparatus and imager, chemicals, and molecular weight standards were all purchased from BioRad.

4.2.5 IHC Quantification:

Relative quantification for immunohistochemistry stains were performed on ImageJ (provided by NIH) using the ImmunoRatio plugin. This was developed by Touminen and Isoloa, University of Tampere, Finland. The quantities expressed here are a percentage of DAB expressed to the nuclear area or ECM area shown. This depends on the stain type used, i.e. a cellular or matrix stain. Each image was individually adjusted for the blue threshold (nuclei) and brown threshold (DAB) to fine-tune each component. Instructions for how to use this plugin were provided and followed.

4.2.6 Statistical Analysis:

Results are expressed as means ± standard deviation (SD). Statistical analysis was performed using one-way analysis of variance (ANOVA). Differences between means were determined using the least significant difference (LSD) with an alpha value of 0.05.

4.3 Results:

4.3.1 Explantation and Histological Evaluation of the ECM:

Decellularized scaffolds, both untreated and PGG-treated, were explanted from the 52 rats at 4 and 8-week time points. At explantation, there was a marked difference in degradation between the PGG-treated and untreated samples with the greatest visible difference at the 8-week time point. Macroscopic evaluation of the explanted tissue, as shown in **Figure 4.1**, displays this difference in degradation of the scaffolds. It is also apparent that PGG-treatment leaves a distinct coloration of the tissue. This was true at both the 4 and 8-week time points.

Figure 4.1: Macroscopic Evaluation of Explants. Following explantation, non-treated and PGG-treated groups for each tissue type were examined. PGG-treated groups appeared less degraded and noticeably colored as compared to the non-treated samples. This coloration made the PGG-treated groups easier to find and retrieve at the end of the in vivo study.

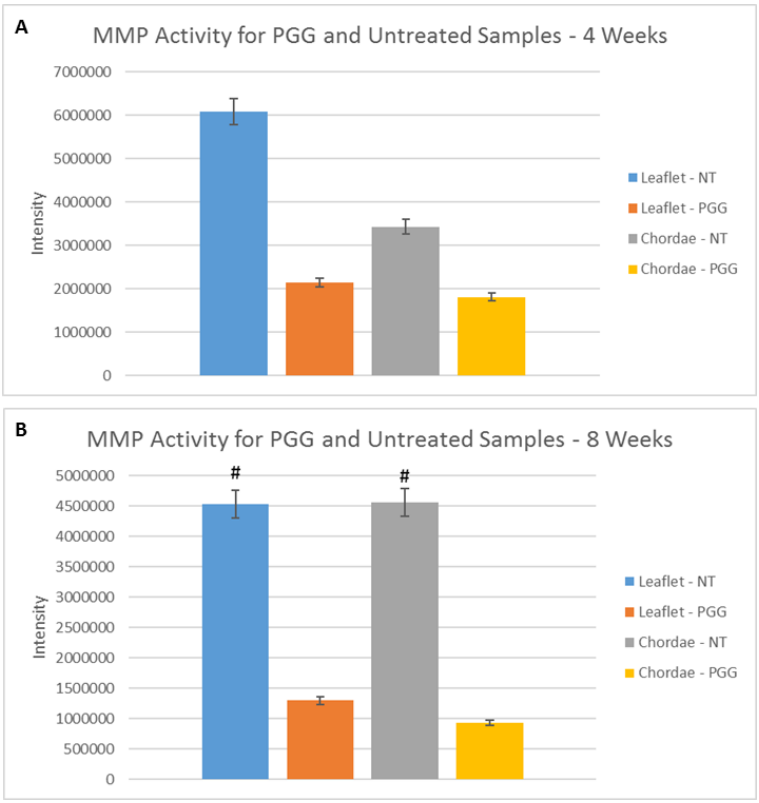

Figure 4.2: MMP Activity of Implanted Scaffolds. To evaluate degradation of the non-treated and PGG-treated acellular scaffolds, a gelatin zymography was performed. Quantities of band volume were determined and plotted. At 4 weeks, non-treated samples have a higher MMP activity than PGG-treated samples. Similarly, at 8 weeks, non-treated leaflets and chordae are significantly higher than PGG-treated tissues. It is apparent that at longer time points the difference in degradation increases as scaffolds are subject to a longer exposure to the host response.

Figure 4.3 displays the zymography gels that were quantified in **Figure 4.2**. As evidence by the gel, non-treated samples expressed both MMP9 and MMP2. However, in the PGG-treated tissues, only bands for MMP9 were detected. This is in congruence with the quantified data presented above describing the MMP expression to be signifincalty higher in the non-treated samples when compared to the PGG-treated groups.

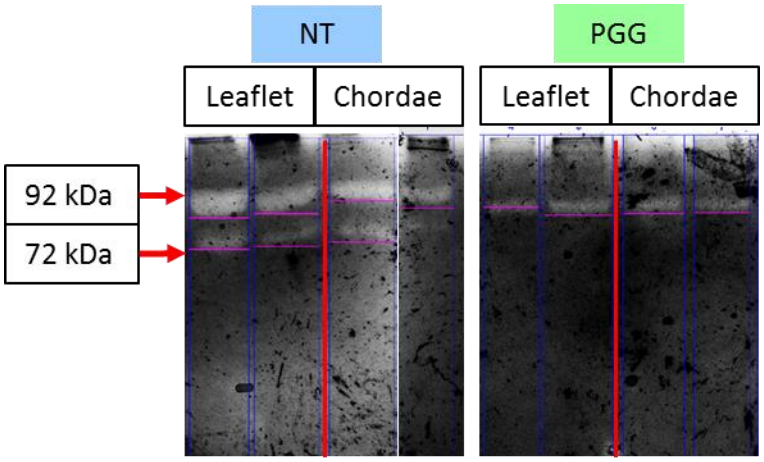

Figure 4.3: Gel Zymography for Non-treated and PGG-Treated Implanted Scaffolds. A gel zymography was done and quantified in Figure 4.2. The non-treated (NT) samples clearly show presence of both MMP9 and MMP2 markers. PGG-treated samples display only the expression of MMP9 markers.

Most scaffolds treated with PGG were easily recoverable, however some untreated scaffolds were difficult to find due to their reduced size. Although not shown here, PGG-treated samples had a brown residue around it from the PGG, while untreated samples did not. Aside from this macroscopic evaluation of degradation, a gelatin zymography was performed to determine and quantify MMP activity within the scaffolds at each time point. As seen in **Figure 4.2A, B**, non-treated acellular scaffolds exhibit significantly higher MMP activity when compared to PGG-treated scaffolds. This was especially true for the 8-week time points.

Histological analysis using H&E and Movat's Pentachrome staining was used to evaluate the integrity of the ECM after implantation. As seen in **Figure 4.4**, PGG-treated tissues were well preserved at both the 4 and 8-week time points. Movat's Pentachrome shows good preservation of elastin bands and of the collagen. Similarly, non-treated samples largely showed a good preservation of both collagen and elastin.

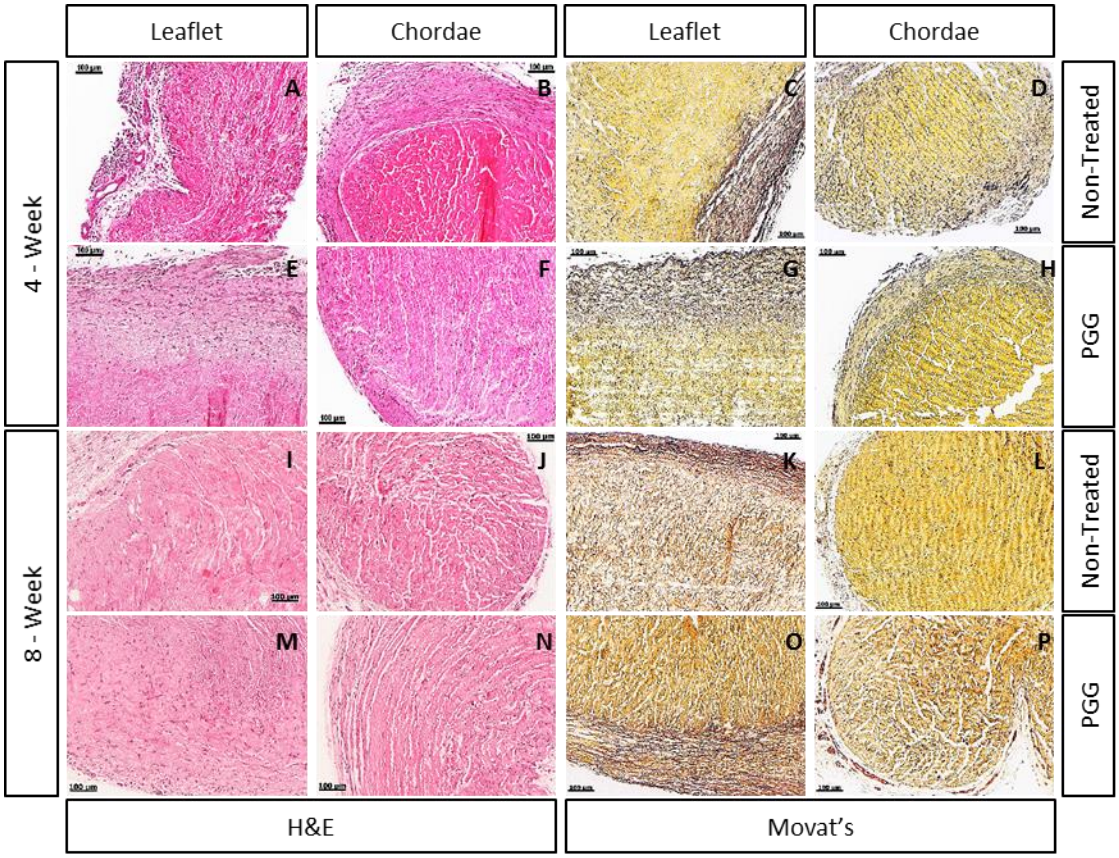

Figure 4.4: Histological Evaluation of Scaffold ECM Post-Implantation. H&E and Movat's Pentachrome were performed on explanted scaffolds. Leaflet and chordae sections are shown here. These scaffolds were implanted as either non-treated or PGG-treated acellular scaffolds. Both 4 and 8-week time points are also shown here. As evidence by these histological stains, ECM were largely preserved in both the non-treated and PGG-treated scaffolds for both tissue types and at both time points. Also, as these were originally acellular scaffolds, cellular invasion is apparent in these histological images.

The presence of cells is clearly visible from each section in **Figure 4.4**. Since these scaffolds were implanted as acellular, it is apparent that invasion of host cells has taken place at each time point. **Figure 4.5** shows a semi-quantitative measure of the amount of cells invading each scaffold, represented as a normalized percentage of the area of the section imaged.

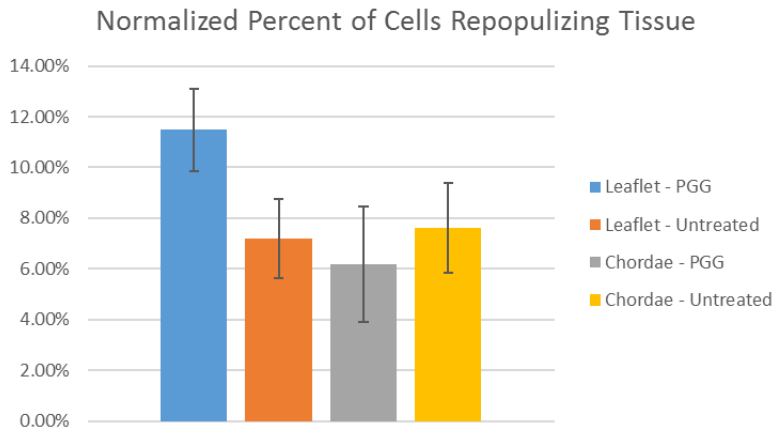

Figure 4.5: Cellular Infiltration into Scaffolds. A semi-quantitative measure was taken to evaluate quantity of cells invading into the implanted scaffolds due to the normal host response. Values here are represented as a normalized percentage of the collective area of the cells as compared to the area of the tissue in each section imaged. Overall, there were no significant differences between PGG and non-treated groups for each tissue type.

As evidenced by **Figure 4.5** there is no significant difference between PGG and non-treated scaffolds. Therefore, PGG treatment of our acellular scaffolds did not hinder infiltration of cells from the host response.

4.3.2 Histological Evaluation and Identification of Cellular Presence:

To garner a better understanding of how the host cells reacted to the implanted scaffolds and whether PGG treatment affects inflammatory cell infiltration, we analyzed the scaffolds and stained with CD8, a marker for T-cells, and CD68, a pan-macrophage marker. IHC for CD8 showed a presence of T-cells in each scaffold type and under each treatment type (**Figure 4.6**). Although there was a significant difference found between non-treated and PGG-treated groups. In both 4 and 8-week time points, CD8 expression was found to be significantly higher in non-treated scaffolds. This was especially apparent

during the 4-week time point because, while still statistically significant, at 8 weeks the contrasting levels of CD8 expression were not so wide. PGG treatment of scaffolds appeared to strongly discourage T-cell infiltration, but it did not completely inhibit it. CD68 expression for macrophages was also found in all scaffolds and treatment types. There were not significant differences between groups (**Figure 4.7**). While not statistically significant, there was a lower overall expression of CD68 in PGG-treated tissues.

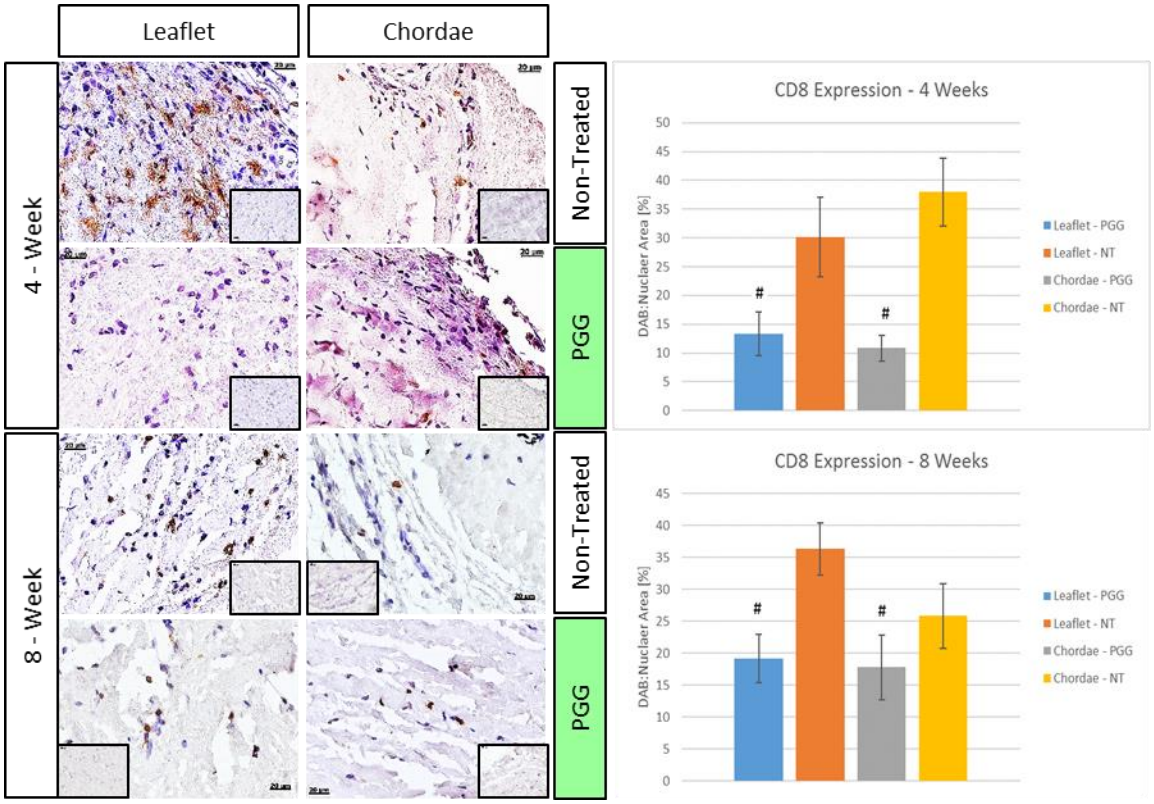

Figure 4.6: Histological Evaluation and Semi-Quantitative Analysis of CD8 Expression. T-cell infiltration was determined using an IHC for CD8. Expression of CD8 at both the 4 and 8-week time points is shown as well as each treatment type and tissue type. A semi-quantitative analysis of these images (n=6) showed significant differences in CD8 expression. PGG-treated scaffolds showed significantly less expression of CD8 at both the 4 and 8-week time points.

Expression of smooth muscle cell marker, α-Smooth Muscle Actin (α-SMA), was evaluated to determine the infiltration of smooth muscle cells into the scaffolds and PGG's effect on this infiltration. Overall, PGG-treated scaffolds showed a markedly lower expression of α-SMA at both time points in the leaflets and chordae when compared to treated samples (**Figure 4.8**). While not shown, similar results for other smooth muscle cell markers, SM22 and calponin were found, with PGG treatment significantly reducing their expression. Markers for fibroblasts such as vimentin (**Figure 4.9**), HSP-47, and prolyl 4-hydroxylase were also shown to be expressed at significantly higher levels in PGG-treated tissues as compared to their untreated counterparts at both time points. It is important to note that these differences in expression do not mean that expression of each of the aforementioned markers did not occur. In each of the histological figures presented in herein, expression of each marker is clearly present.

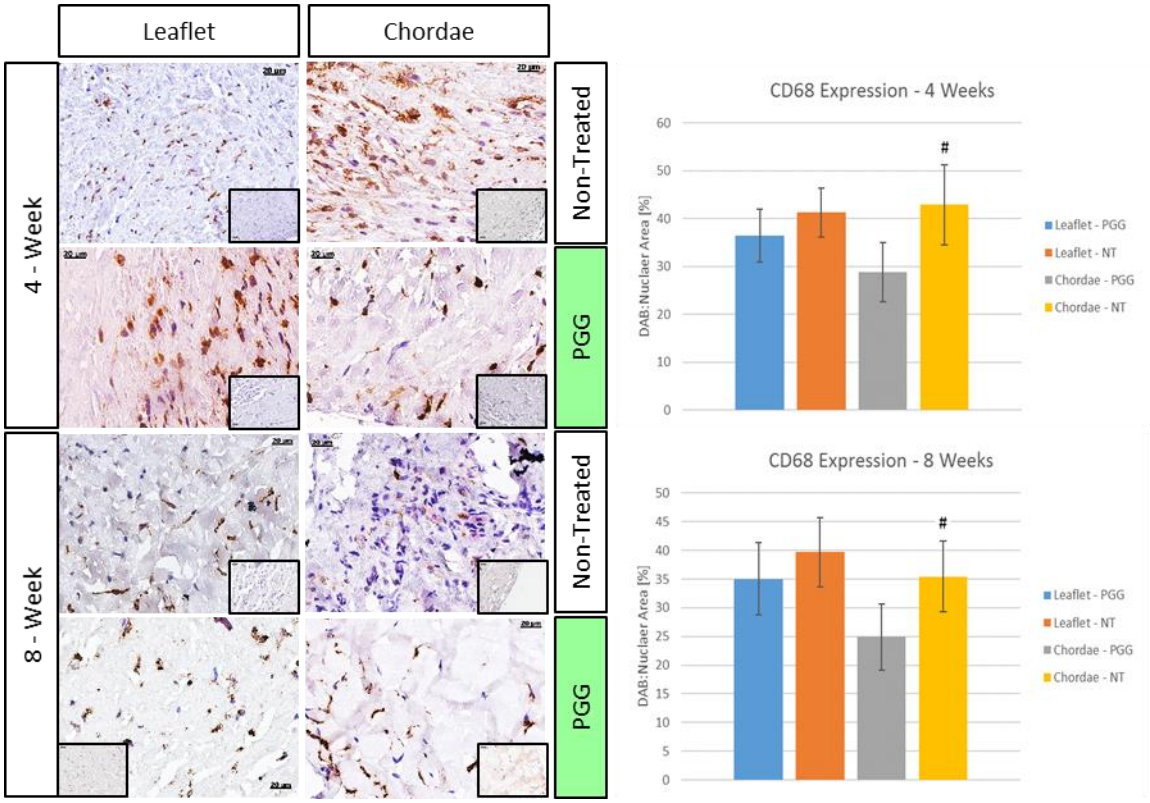

Figure 4.7: Histological Evaluation and Semi-Quantitative Analysis of CD68 Expression. Macrophage infiltration was determined using an IHC for CD68. Expression of CD68 at both the 4 and 8-week time points is shown as well as each treatment type and tissue type. A semi-quantitative analysis of these images (n=6) showed no significant differences in CD68 expression. PGG-treatment did not seem to hinder infiltration of macrophages into the scaffolds at either time point.

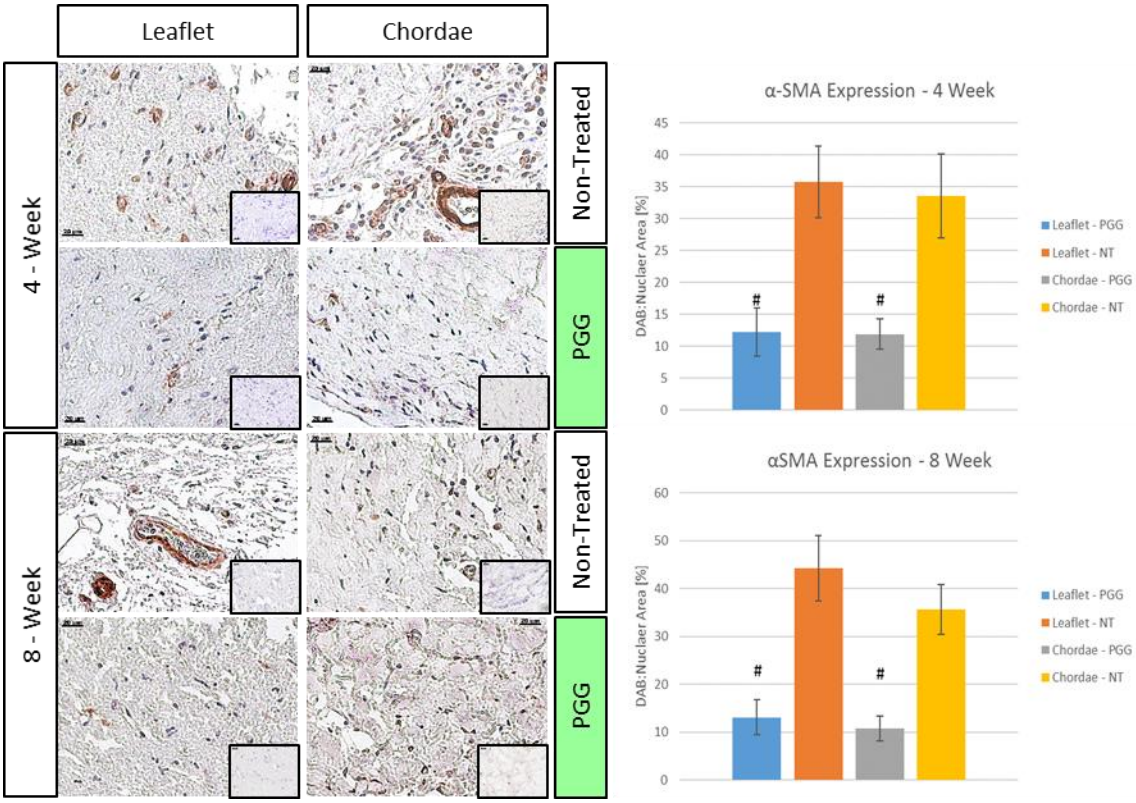

Figure 4.8: Histological Evaluation and Semi-Quantitative Analysis of α-SMA Expression. α-SMA expression was determined using an IHC. Expression of α-SMA at both the 4 and 8-week time points is shown as well as each treatment type and tissue type. A semi-quantitative analysis of these images (n=6) showed significant differences in α-SMA expression. PGG-treated scaffolds showed significantly less expression of α-SMA at both the 4 and 8-week time points.

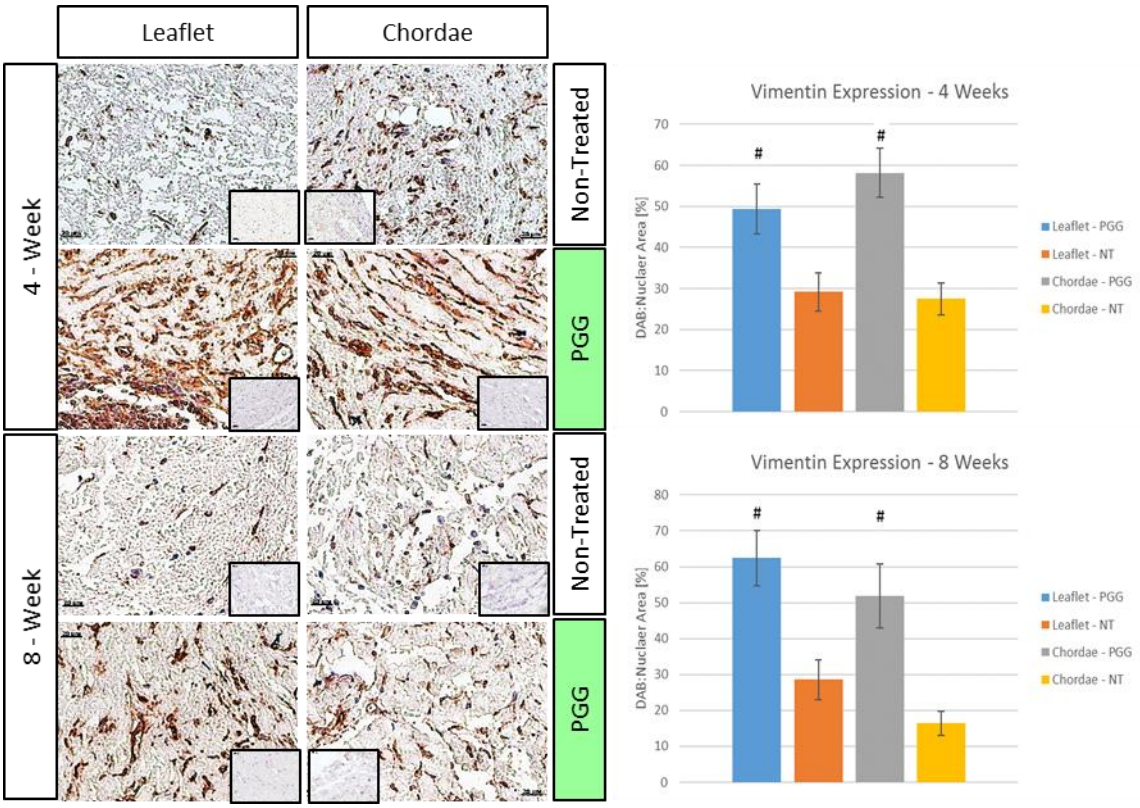

Figure 4.9: Histological Evaluation and Semi-Quantitative Analysis of Vimentin Expression. Vimentin expression was determined using an IHC. Expression of vimentin at both the 4 and 8-week time points is shown as well as each treatment type and tissue type. A semi-quantitative analysis of these images (n=6) showed significant differences in vimentin expression. PGG-treated scaffolds showed significantly greater expression of vimentin at both the 4 and 8-week time points.

4.3.3 Histological Evaluation of Macrophage Polarization:

As mentioned above, a statistically significant difference was not found between groups using the pan-macrophage marker, CD68. This however does not mean that the treatment groups experience the same inflammatory response. Therefore to illustrate the different macrophage phenotypes present within each treatment type, an IHC and semi-quantitative analysis for iNOS (M1) and CD163 (M2) were performed. As seen in **Figure 4.10**, expression of the M1 macrophage, with the iNOS marker, was significantly higher in

untreated groups at both the 4 and 8-week time points. PGG seems to discourage macrophage polarization towards the M1, or pro-inflammatory phenotype. In comparison, PGG-treated groups showed significantly higher expression of the M2 marker, CD163 at both time points (**Figure 4.11**). While discouraging the M1 macrophages, treatment with PGG seems to encourage the pro-healing M2 macrophages.

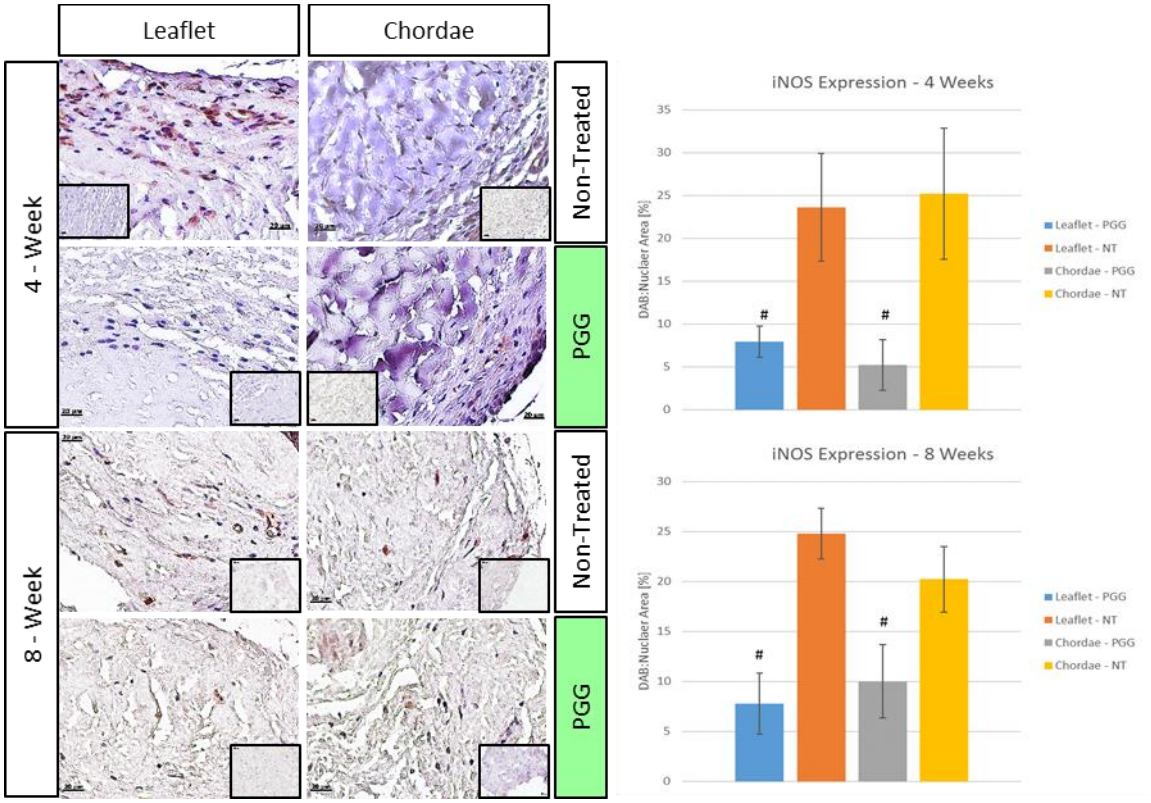

Figure 4.10: Histological Evaluation and Semi-Quantitative Analysis of iNOS Expression. iNOS expression was determined using an IHC. Expression of iNOS at both the 4 and 8-week time points is shown as well as each treatment type and tissue type. A semi-quantitative analysis of these images (n=6) showed significant differences in iNOS expression. PGG-treated scaffolds showed significantly less expression of iNOS at both the 4 and 8-week time points.

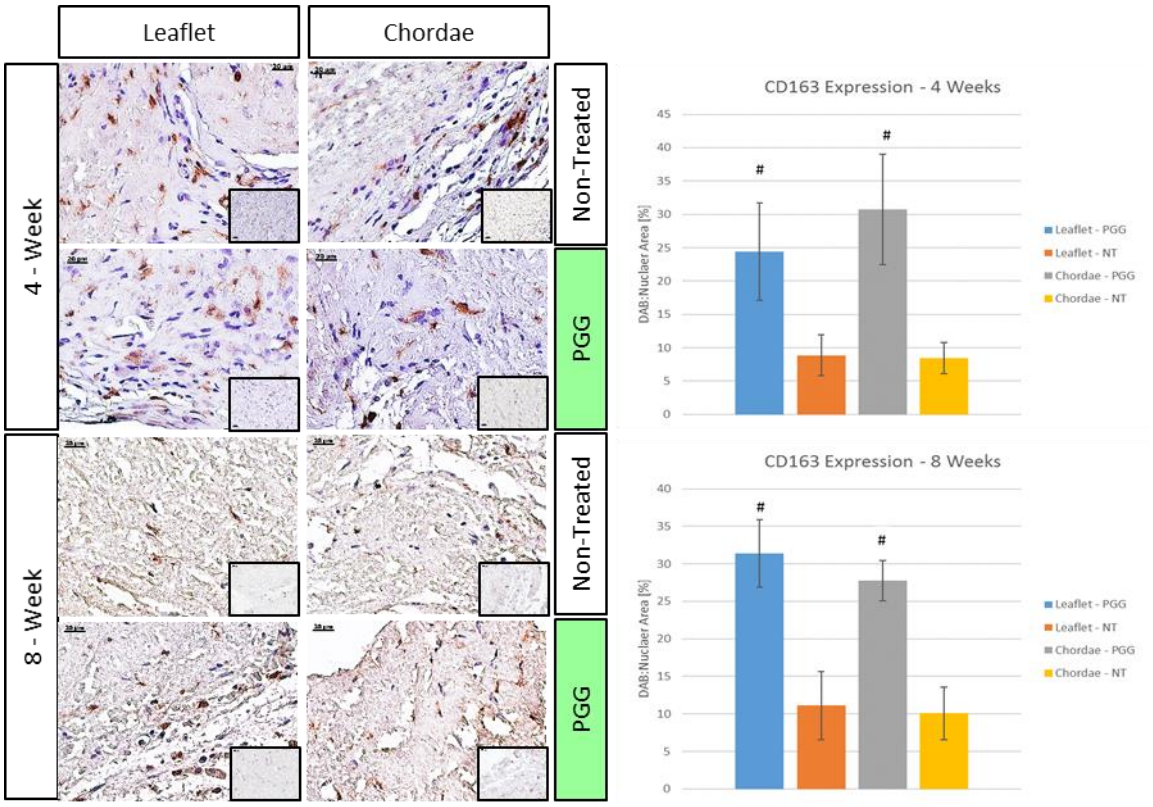

Figure 4.11: Histological Evaluation and Semi-Quantitative Analysis of CD163 Expression. CD163 expression was determined using an IHC. Expression of CD163 at both the 4 and 8-week time points is shown as well as each treatment type and tissue type. A semi-quantitative analysis of these images (n=6) showed significant differences in CD163 expression. PGG-treated scaffolds showed significantly greater expression of CD163 at both the 4 and 8-week time points.

4.4 Discussion:

4.4.1 General Observations and Integrity of the Scaffolds:

Biological scaffolds comprised of niche ECM proteins have been used in a wide variety of tissue engineering applications[2,27]. The combination of natural components and specific microstructure assist in cell attachment and proliferation while promoting distinct functionalities relevant to that tissue type. Cellular residents in the ECM structure are depended upon to remodel the scaffold during development and wound repair. As such,

matrix composition and organization are a function of the adaptation of the cells and their reaction to the mechanical and chemical cues they are receiving from the microenvironment[28]. This interaction between matrix and cells is crucial for the success of the construct due to their codependency[28]. Investigating biocompatibility in an in vivo study, would allow for an evaluation on how infiltrating host cells respond to an ECM scaffold. As mentioned earlier, this reaction between host cells with the ECM scaffold is the predominant determinant for the scaffold's success[2]. Biocompatibility is a term that has evolved during the advancement of biomaterials from inert to bioactive implants. For regenerative medicine applications, biocompatibility could be defined as "the ability of a biomaterial to perform its desired function with respect to a medical therapy, without eliciting any undesirable local or systemic effects in the recipient or beneficiary of that therapy, but generating the most appropriate beneficial cellular or tissue response in that specific situation, and optimizing the clinically relevant performance of that therapy"[29]. In our mitral valve scaffold specifically, a balance must be achieved between slight degradation and remodeling by cells. In the studies presented here, we show the critical relationship between our mitral valve scaffold and the host cellular response in an in vivo rat study.

Macroscopically, non-treated scaffolds were noticeably more difficult to retrieve upon explantation. This was in large part due to their degradation while subcutaneously implanted. PGG-treated samples in contrast, were easy to recover and were significantly less degraded at both the 4 and especially the 8-week time point. To obtain a finer understanding of the quality of the ECM scaffold after each time point, each sample was

examined microscopically. As evidenced in **Figure 4.4**, when examined histologically, overall the ECM quality did not appear to be significantly disturbed. H&E and Movat's Pentachrome staining showed decent preservation of collagen microstructure. On the whole, PGG-treated leaflets and chordae did look the least degraded. Regardless of treatment, this is important for the scaffold and its influence on the incorporated cells. As mentioned ECM quality is crucial as it acts as an inductive scaffold[28]. Upon further examination of the ECM in this figure, elastin quality seems to have diminished in the non-treated samples. This is important to note because degradation of elastin in cardiovascular tissues, has shown to encourage calcification at these sites[15,30,31]. While we did not find evidence of calcification (not shown), it is likely a different model, particularly one with mechanical stimulation, would have shown calcification in these non-treated groups.

Degradation of an ECM scaffold, such as our own, is an inevitable if not necessary outcome for the eventual success of the scaffold. Constructive remodeling, as defined earlier, is a process which must occur for our mitral valve scaffold to be successful[6]. However, for heart valves, this process must be gradual. Upon implantation, tissue engineered valves would be expected to face the strong and repetitive forces experienced by this tissue. To survive this, degradation of the scaffold must be limited and gradual over time. Therefore, we incorporate PGG as a treatment to hinder degradation of the scaffold. Several papers from our group alone have shown the benefits of treating with PGG, especially its ability to significantly reduce degradation[20,30,32–34]. Matrix degradation can lead to several compounding effects on the infiltrating host cells and of course the matrix itself. Circulating immune cells rely upon matrix degradation for access into the

microstructure to encourage an inflammatory response. As such, these cells release enzymes called matrix metalloproteases, or MMPs. There are several MMP phenotypes, but common types are secreted by T-cells[35–37]. Inflammatory mediators like TNF-α also stimulate expression of MMP's in macrophages[38,39]. During degradation of the matrix by MMPs, many matrikines and cytokines are released upon ECM molecule degradation or conformation change. These matrikines have been shown to increase TGF-β1 expression, a known activator of fibroblasts, as well as further expression of MMPs[34,35]. When examining our samples for degradation, a zymography gel was run with PGG and non-treated samples (**Figure 4.2**) to examine MMP quantities. Overall, levels of MMP's were significantly higher in untreated samples when compared to PGG-treated samples. PGG, while not able to completely inhibit MMP degradation, which we were not aiming to do, was able to decrease the amount of degradation by decreasing the expression of these matrix-degrading enzymes. A decreased level of MMP could also be indicative of decreased levels of T-cells and other inflammatory markers such as TNF-α. The stabilization effect of PGG also decreased the availability of degrading matrikines and cytokines, which as a result were not able to encourage further degradation of our ECM mitral valve scaffold.

As shown in **Figure 4.4**, host cells were in fact able to penetrate the scaffolds at each time point and for each treatment of the scaffold. Cellular infiltration is indicative of many things including cytocompatibility, porosity, and migration potential with the scaffold. Quantification of the infiltrating cells (**Figure 4.5**), showed no significant difference between treatment groups. This was true at both time points. Therefore, PGG-

treatment of our scaffold does not hinder infiltration of host cells after implantation, thus allowing for a normal host response. In this subdermal study, repopulation of these acellular scaffolds with host cells is needed for remodeling.

While no significant difference was found between the PGG and non-treated samples regarding the infiltration of cells, there did seem to be a difference in cell quantity between the 4 and 8-week time points. The decrease found for the 8 week time points is most likely due to the shift in pro-healing phase of the macrophage polarization. At this later time point, most of the initial cellular infiltration and inflammatory response to the foreign scaffold had completed and the transition to a pro-healing, and the majority of macrophages displayed an M2 phenotype.

4.4.2 Evaluation of Immune Response:

An immune response to an implanted device or material is a key component to evaluating biocompatibility. Immune responses can initiate or propagate inflammatory action from the host. Significant or prolonged inflammation for an ECM scaffold would undoubtedly yield failing results. In our study, macroscopically (**Figure 4.4**), cardinal signs of inflammation were not present. We did not see an extreme density of invading cells in the scaffolds, nor did we see the presence of foreign giant body cells (FGBCs). PGG-treated samples did not see a significant increase in vascularity either. Decellularized ECM scaffolds can induce an inflammatory response due to improper or incomplete decellularization resulting in the presence of xenogeneic antigens like α-gal. Also, an incomplete removal of the treatments used for decellularization can lead to failure of the scaffold due to inflammation. Overall, however we did not see any indications of an

aggressive inflammatory response from the host. One measure we also looked at was the presence of T-cells in the scaffolds. These T-cells or lymphocytes are present in and play important roles in the inflammatory response. These T-cells increase MMP's within the tissue they are invading, actively recruit macrophages to the site, and as a result, a cascade of reactions including degradation of the tissue ensues. To investigate whether PGG treatment had an effect on T-cell recruitment we looked for CD8 expression, a marker for T-cells. As seen in **Figure 4.6**, at both the 4 and 8-week time points, PGG consistently and significantly reduced CD8 expression in the scaffolds. Non-treated scaffolds on the other hand showed significantly higher expression of CD8. This correlates with the results previously which PGG-treatment decreased MMP expression. Since T-cells and MMPs can induce expression of, or recruit the other, these results agree. It is possible that due to the treatment with PGG and the resistance it provides scaffolds to degradation, the host was presented with less cytokine and matrikines that would invoke an inflammatory response. Because of the stability of our mitral valve scaffold, T-cell recruitment was discouraged, as were the compounding effects on inflammation and degradation that would have ensued. Also examined was the expression of CD68, a pan-macrophage marker (**Figure 4.7**). There were no significant differences between the treatment groups found. As discussed earlier, there are differing macrophage phenotypes; therefore, what is more important is the ratio of M1 to M2 macrophages. We still however wanted to identify what infiltrating cells were macrophages and this figure accomplishes this. Infiltration from macrophages was clear in all treatment groups.

4.4.3 Histological Identification of Infiltrating Cells:

Other than identify degradation and immune-related cells, many other cells did not stain positive for these markers, thus more cell types are present with the explanted scaffolds. As mentioned earlier, the complexity and specificity of the ECM scaffold is critical in cell proliferation, migration, differentiation, etc. Therefore, the types of cells that infiltrated our scaffolds in this subdermal study should be indicative of their potential to attract the appropriate cell types. These infiltrating cells are the ones that actively remodeling the scaffolds in vivo and play an important role in the scaffold's long term success. They can affect matrix remodeling as well as degradation. We looked at several markers for smooth muscle cells and fibroblasts. Expression levels for α-SMA, SM22, and calponin were evaluated for our smooth muscle cells markers, while vimentin, HSP-47, and prolyl-4-hydrosylase were examined for our fibroblast markers. Only results for α-SMA and vimentin are shown for each of the cell types investigated, however results for each are discussed due to the consistency across groups. Overall, expression of α-SMA was significantly increased in non-treated samples when compared to the PGG-treated groups (**Figure 4.8**). This was also true for SM22 and calponin expression at each time point. We also quantified expression of common fibroblast markers. Vimentin (**Figure 4.9**), showed significantly higher expression in PGG-treated groups than non-treated at both time points. This fibroblast maker expression was also consistent with HSP-47 and prolyl-4-hydroxylase. Therefore, from these results, PGG-treated tissues encourage infiltration of fibroblasts over smooth muscle cells, and the opposite is true for non-treated groups. A possible explanation for this could be that non-treated samples have shown higher expression of CD8, a sign of inflammation and a higher expression of MMPs. This

in turn could be activating fibroblasts infiltrating the non-treated scaffolds into myofibroblasts. Myofibroblasts are known to cause fibrosis and overproduction of ECM[40]. They can also increase TGF-β1 levels. Histological inspection revealed more vessel formation appearing in the non-treated samples post-explantation. This is not normally seen in mitral valve leaflets or chordae. Therefore, it is possible these vessels are attributing to some of the rise in inflammatory makers and myofibroblasts. A large expression of fibroblast markers in the PGG-treated leaflets we would consider normal and beneficial to the matrix remodeling in these scaffolds. Mitral valve leaflets and chordae are largely populated by VICs, which are fibroblast-like. Therefore infiltration of similar cell-types may be an indication that PGG-treated ECM scaffold encourages appropriate cell type infiltration.

4.4.4 Macrophage Polarization:

Macrophages play a critical role in the success of ECM scaffolds. Macrophages are classically known to play a central role in host defense and inflammatory response. However, beyond defense these cells orchestrate tissue remodeling and other crucial metabolic functions[41]. M1 macrophages are characterized by the expression of high levels of pro-inflammatory cytokines such as TNF-α, IL-6, and iNOS[2,6,11,35,41]. M1 macrophages are also responsible for generating large amounts of reactive oxygen species (ROS) which caused further oxidative stress on implants. In ECM scaffolds, this oxidative stress along with other factors affective degradation (MMPs, etc.) may induce the formation of oxidants since ECM fragments promote immune cell recruitment. Also ROS has been shown to recruit additional macrophages and leukocytes[42]. M2 macrophages operate as the pro-

healing phenotype and are characterized by expression of IL-10 and CD163[1,11,28,41]. M2 macrophages have poor antigen presenting potential and possess immunoregulatory functions such as actively scavenging debris, tissue remodeling, promoting wound healing, and suppression of Th1[41]. Two commonly used markers for M1 and M2 macrophages were iNOS and CD163 respectively. Using these markers, it was observed that iNOS expression was significantly higher in untreated samples at both time points (**Figure 4.10**). Meaning there was a greater presence of M1 macrophages in the untreated samples. In contrast, CD163 was expressed in significantly higher quantities in PGG-treated samples as compared to non-treated groups (**Figure 4.11**). This was true at both the 4 and 8-week time points. Therefore, M2 macrophages appear in greater quantities in PGG-treated scaffolds. As mentioned before, the pan-macrophage expression (CD68) was not significantly different between groups, however it appears that the ratios of M1 and M2 macrophages for the treatment groups was significantly different. PGG's ability to encourage the M2 phenotype is critical for the success of this scaffold. By depressing the pro-inflammatory M1 macrophage, further degradation of the scaffold was prevented, oxidative stress reduced, significantly less pro-inflammatory cytokines were released and more M1 macrophages were not recruited.

PGG has shown to have anti-inflammatory qualities and therefore has some effect on macrophage polarization due the fact that PGG-treatment greatly encourages M2 macrophages over M1[13]. One possibility for this is due to the antioxidant properties of PGG. Antioxidants have been shown to scavenge ROS which are known to increase inflammation and oxidative stress in tissues[43]. Antioxidants block oxidant-mediated

pathways by scavenging ROS. It has also been shown that PGG can significantly reduce the expression of TNF-α, which is a major determinant in macrophage polarization[20]. It has also been seen that ROS production is a function of TNF-α expression[44]. By decreasing the expression of this pro-inflammatory cytokine, PGG may reduce M1 polarization. In accordance with our results, we also saw PGG's effect on scaffold degradation and how this affected expression of CD8, smooth muscle cell markers, fibroblast markers, as well as vascularity and MMP expression. Combined, we have seen that ECM fragments and degradation can encourage inflammation of the scaffold and even fibrosis. Each of these factors seem to compliment and encourage the other in the untreated samples. M1, macrophages which are associated with increased vascularity, may coincide with the higher expression of CD8 and the delivery of these T-cells to non-treated samples[45].

4.5 Conclusion:

The host response and biocompatibility of any biomaterial are the most crucial factors in determining the success or failure of an implant. As researchers have progressed past the use of "inert" biomaterials and into the realm of bioactive scaffolds made from natural substances like ECM, there are many questions not only on how a bioactive material will respond to the host, but more importantly how the implant will utilize the host response to its advantage. For tissue engineered applications, scaffolds derived from ECM have become popular due the familiar proteins that make up the scaffold and its ability to incorporate cells to eventually become a regenerated tissue. We must understand that the cells and their interaction with the ECM scaffold are the only way to remodel and integrate

the biomaterial into the host. Therefore, we must appreciate and discover the mechanisms by which the host's cells mediate the immune response around our scaffold. By doing so, we will have a better understanding of the effectiveness and potential for our tissue engineered mitral valve scaffold.

The studies discussed above were all attributed to the scaffold developed in chapter 3. Our aim was to better understand how our scaffold would affect the immune response of the rats and how this in turn affected our scaffolds. We examined our scaffolds at both 4 and 8-weeks and had two treatment groups, PGG-treated and non-treated scaffolds. Results were shown for the leaflets and the chordae tendinae. We focused our results on the degradation of the scaffolds, the immune response, overall ECM quality, and identification and polarization of macrophages.

Our results led us to conclude that PGG-treatment of our scaffolds has many benefits to our scaffold. We knew PGG significantly decreased degradation with proteases in vitro, however the same was true in vivo. PGG also decreased expression of CD8 an immune cell marker and promotor of inflammation. Smooth muscle cell markers were also expressed at significantly lower levels in PGG-treated groups. These cells may have been fibroblasts that were activated and became myofibroblasts, which can lead to over-production and mismanagement of ECM remodeling. Fibroblast markers were also significantly higher in PGG-treated tissues. Importantly, the M2 phenotype was highly encouraged and showed significantly more expression in the PGG-treated tissues. This predominance of the pro-healing phenotype of macrophages discourages further inflammation and allows for remodeling of the scaffold.

Overall, it is evident that treatment with PGG has significant beneficiary effects on our mitral valve scaffold. Any tissue engineered ECM scaffold needs to undergo constructive remodeling to become a healthy and regenerated tissue. While the same is true for the heart valve scaffold, extra precautions must be taken due to the high stress environment the valve resides in. Because this valve is expected to function immediately and ideally for the life of the patient, PGG allows for a more gradual remodeling, while also discouraging inflammation and degradation of the scaffold.

4.6 References:

1. Brown, B. N. & Badylak, S. F. Expanded applications , shifting paradigms and an improved understanding of host – biomaterial interactions. *Acta Biomater.* **9,** 4948–4955 (2013).
2. Badylak, S. F. Decellularized Allogeneic and Xenogeneic Tissue as a Bioscaffold for Regenerative Medicine: Factors that Influence the Host Response. *Ann. Biomed. Eng.* (2014). doi:10.1007/s10439-013-0963-7
3. Medicine, R. Extracellular Matrix Bioscaffolds for Orthopaedic Applications. 2673–2686 (2006).
4. Anderson, J. M. Inflammatory response to implants. *Am. Soc. Artif. Intern. Organs* 101–107 (1988).
5. Badylak, S. *et al.* Morphologic Study of Small Intestinal Submucosa as a Body Wall Repair Device. **202,** 190–202 (2002).
6. Brown, B. N., Ratner, B. D., Goodman, S. B., Amar, S. & Badylak, S. F. Macrophage polarization: an opportunity for improved outcomes in biomaterials and regenerative medicine. *Biomaterials* **33,** 3792–802 (2012).
7. Brown, B. N. *et al.* Macrophage phenotype as a predictor of constructive remodeling following the implantation of biologically derived surgical mesh materials. *Acta Biomater.* **8,** 978–987 (2012).
8. Brown, B. N., Valentin, J. E., Stewart-akers, A. M., Mccabe, G. P. & Badylak, S. F. Macrophage phenotype and remodeling outcomes in response to biologic scaffolds with and without a cellular component. *Biomaterials* **30,** 1482–1491 (2009).
9. Badylak, S. F. *et al.* Macrophage Phenotype as a Determinant of Biologic Scaffold Remodeling. **14,** (2008).
10. Stout, R. D., Watkins, S. K. & Suttles, J. Functional plasticity of macrophages : in situ reprogramming of tumor-associated macrophages. *J. Leukoc. Biol.* **86,** 1105–1109 (2017).

11. Olefsky, J. M. & Glass, C. K. *Macrophages , Inflammation , and Insulin Resistance*. (2010). doi:10.1146/annurev-physiol-021909-135846
12. Lawrence, T. & Natoli, G. Transcriptional regulation of macrophage polarization : enabling diversity with identity. *Nat. Rev. Immunol.* **11,** 750–761 (2011).
13. Zhang, Li Li, Sung-Hoon Kim, Ann E. Hagerman, J. L. Anti-Cancer, anti-diabetic and other pharmacologic and biological activities of penta-galloyl-glucose. *Pharm. Res.* **26,** 1–27 (2010).
14. Charlton, A. J. *et al.* Tannin interactions with a full-length human salivary proline-rich protein display a stronger affinity than with single proline-rich repeats. **382,** 289–292 (1996).
15. Isenburg, J. C., Karamchandani, N. V, Simionescu, D. T. & Ã, N. R. V. Structural requirements for stabilization of vascular elastin by polyphenolic tannins. **27,** 3645–3651 (2006).
16. Pan, M., Ho, C., Lin, J. & Lin, J. Suppression of Lipopolysaccharide-Induced Nuclear Factor- B Activity by Theaflavin-3 , 3 J -Digallate from Black Tea and Other Polyphenols through Down- regulation of I B Kinase Activity in Macrophages. **59,** 357–367 (2000).
17. Feldman, K. S. BETWEEN TUMOR NECROSIS FACTOR-tx PRODUCTION AND TANNIN G • C. **9,** 985–990 (1999).
18. Feldman, K. S. *et al.* In Vitro and In Vivo Inhibition of LPS-Stimulated Tumor Necrosis Factor- Secretion by the Gallotannin - D -Pentagalloylglucose. **11,** 1813–1815 (2001).
19. Li, Y. *et al.* -glucopyranose binds to insulin receptor and activates insulin-mediated glucose transport signaling pathway. **336,** 430–437 (2005).
20. Chow, J. P. *et al.* Mitigation of diabetes-related complications in implanted collagen and elastin scaffolds using matrix-binding polyphenol. *Biomaterials* **34,** 685–95 (2013).
21. Vassort, G. & Turan, B. Protective Role of Antioxidants in Diabetes-Induced Cardiac Dysfunction. 73–86 (2010). doi:10.1007/s12012-010-9064-0
22. Oxidative stress in vascular disease_ causes, defense mechanisms and potential therapies.pdf.
23. Statements, P. New Insights on Oxidative Stress and Diabetic Complications May Lead to a ‘ Causal ’ Antioxidant Therapy. **26,** (2003).
24. Johansen, J. S., Harris, A. K., Rychly, D. J. & Ergul, A. Oxidative stress and the use of antioxidants in diabetes : Linking basic science to clinical practice. **11,** 1–11 (2005).
25. Abdelwahed, A. *et al.* Study of antimutagenic and antioxidant activities of Gallic acid and Confirmation by microarray expression profiling. **165,** 1–13 (2007).
26. Wu, M. & Gu, Z. Screening of Bioactive Compounds from Moutan Cortex and Their Anti-Inflammatory Activities in Rat Synoviocytes. **6,** 57–63 (2009).
27. Badylak, S. F., Freytes, D. O. & Gilbert, T. W. Extracellular matrix as a biological

scaffold material: Structure and function. *Acta Biomater.* **5,** 1–13 (2009).
28. Brown, B. N. & Badylak, S. F. Extracellular Matrix as an Inductive Scaffold for Functional Tissue Reconstruction. *Transl. Res.* (2013). doi:10.1016/j.trsl.2013.11.003
29. Williams, D. F. On the mechanisms of biocompatibility. *Biomaterials* **29,** 2941–2953 (2008).
30. Isenburg, J. C., Simionescu, D. T., Starcher, B. C. & Vyavahare, N. R. Elastin stabilization for treatment of abdominal aortic aneurysms. *Circulation* **115,** 1729–37 (2007).
31. Simionescu, A., Simionescu, D. T. & Vyavahare, N. R. Osteogenic Responses in Fibroblasts Activated by Elastin Degradation Products and Transforming Role of Myofibroblasts in Vascular Calcification. *Am. J. Pathol.* **171,** 116–123 (2007).
32. Chuang, T.-H., Stabler, C., Simionescu, A. & Simionescu, D. T. Polyphenol-stabilized tubular elastin scaffolds for tissue engineered vascular grafts. *Tissue Eng. Part A* **15,** 2837–51 (2009).
33. Tedder, M. E. *et al.* Stabilized collagen scaffolds for heart valve tissue engineering. *Tissue Eng. Part A* **15,** 1257–68 (2009).
34. Deborde, C. *et al.* Stabilized Collagen and Elastin-Based Scaffolds for Mitral Valve Tissue Engineering. *Tissue Eng. Part A* **22,** 1241–1251 (2016).
35. Lopresti, S. T. & Brown, B. N. in *Host Response to Biomaterials: The Impact of Host Response on Biomaterial Selection* (ed. Badylak, S. F.) 53–79 (2015).
36. Fox, F. E. & Billings, P. C. Induction of metalloproteinase activity in human T-lymphocytes. **1177,** 174–178 (1993).
37. Leppert, D., Waubant, E. & Galardy, R. T cell gelatinases mediate basement membrane transmigration in vitro. (2017).
38. Hanemaaijer, R. *et al.* Matrix Metalloproteinase-8 Is Expressed in Rheumatoid Synovial Fibroblasts and Endothelial Cells. **272,** 31504–31509 (1997).
39. Unemori, E. N., Hibbs, M. S. & Amento, E. P. Constitutive Expression of a 92-kD Gelatinase (Type V Collagenase) by Rheumatoid Synovial Fibroblasts and Its Induction in Normal Human Fibroblasts by Inflammatory Cytokines. **88,** 1656–1662 (1991).
40. Duffield, J. S., Lupher, M., Thannickal, V. J. & Wynn, T. A. Host Responses in Tissue Repair and Fibrosis. doi:10.1146/annurev-pathol-020712-163930
41. Galdiero, M. R. & Mantovani, A. in *Host Response to Biomaterials: The Impact of Host Response on Biomaterial Selection* (ed. Badylak, S. F.) 117–130 (2015).
42. Mouthuy, P. *et al.* Biomaterials Biocompatibility of implantable materials : An oxidative stress viewpoint. **109,** (2016).
43. Levi, R., Barbee, K., Golomb, G., Spijler, K. L. & Systems, H. Effects of radical oxygen species and antioxidants on macrophage polarization. 5–6 (2015).
44. Gotoh, Y. & Cooper, J. A. Reactive Oxygen Species- and Dimerization-induced Activation of Apoptosis Signal-regulating Kinase 1 in Tumor Necrosis Factor- ⎵

Signal Transduction *. **273,** 17477–17482 (1998).
45. Piller, K. A. R. A. L. S., Reytes, D. O. O. F. & Ovakovic, G. O. V. U. Macrophages Modulate Engineered Human Tissues for Enhanced Vascularization and Healing. **43,** 616–627 (2015).

CHAPTER 5 – DEVELOPMENT OF A MITRAL VALVE BIOREACTOR AND CHARACTERIZATION OF DYNAMIC CELL SEEDING IN MITRAL VAVLE CONSTRUCTS

5.1 Introduction:

Scaffold characterization and evaluation of host response are two critical landmarks for a tissue engineered solution. In fact, they are literally the foundation for creating a living tissue construct capable of regenerating diseased tissue. However, despite their importance, the scaffold is only a part of the larger tissue engineering paradigm[(1)]. To develop a living construct these scaffolds must be repopulated with relevant cell types capable of remodeling and sustaining the tissue during growth and would healing. The incorporation of cells and their process of remodeling the scaffold are important pillars in the world of tissue engineering. The scaffold provides the cells with specific biochemical and biomechanical signaling which directs cell growth, migration, proliferation and differentiation. Recellularization of the scaffold presents unique challenges towards the development of a tissue engineered valve. There are roughly two methods to repopulate the scaffolds with cells, in vitro cell seeding prior to implantation, or implanting an acellular scaffold and waiting for repopulation with endogenous cells. The latter option relies heavily on the fact that relevant cell types will infiltrate the scaffold, that the host response, which would occur during full operation of the scaffold, would not limit or degrade the scaffold, that the remodeling process would not hinder coaptation of the valvular apparatus, and that these repopulating cells would be able to function effectively and efficiently while under extreme repetitious forces. In fact it has been shown that placing

acellular constructs in human patients failed to result in success due to limited to no infiltration by host cells into the construct[2]. Therefore, to exert more control over the recellularization process, in vitro cell seeding of the scaffolds prior to implantation should result in a more successful tissue engineered mitral valve. Cell seeding strategies should be optimized and the infiltrating cells should be characterized to understand the tissue remodeling response[3].

Static cell culture methods are limited in their capacity to produce the complex three-dimensional cues required to develop functioning tissue. Two dimensional cell culture also cannot reproduce the physical demands placed on the tissues in vivo. The human body, especially the human heart is a harsh environment for healthy tissue to survive. In normal activity, the mitral valve experiences pressure changes from 10 to 120mmHg in less than 0.1 seconds and continues to repeat this for an average of 3 billion times in one lifespan. It is important to remember these rigorous conditions as design criteria for creating functional tissue. In order to mimic the pressures and flow conditions present in vivo, bioreactors have been developed to “pre-condition” seeded constructs. Dynamic seeding in a bioreactor has also shown to produce significantly better seeding results when compared to statically seeded constructs[4]. By exposing cells and scaffolds to these relevant forces, remodeling of the scaffold and maturation of the cells can take place before being implanted. Bioreactor design is critical for the success of the pre-conditioning process in which they must apply proper pH, oxygen concentration, nutrient supply, sustained sterility, and mechanical forces.

Before mechanical pre-conditioning can be delivered via a bioreactor, the cell type for scaffold seeding needs to be determined. The ideal choice of cell would be VICs, as they are prevailing cell type in the heart valves and are found within each fibrosa, spongiosa, and ventricularis layer of the valve [5–10]. They are a dynamic population of valvular-specific cells and are the living component of heart valves. VICs are responsible for synthesizing and preserving the composition of the valve matrix, which largely determines the valve's ability to function as well as its material behavior[5]. The central role of the VIC is to maintain the structural integrity of the valve and to act when the valve is in need of repair. These responsibilities are extremely important as heart valves are the most mechanically stressed tissue found in the body. VICs also function as key role players in the body's pathological response to heart valve disease as well as regulating processes following valve injury. Current literature supports five heterogeneous VIC phenotypes[5,11]. Quiescent VICs, or qVICs, are the predominant VIC phenotype in healthy valves and are thought to maintain the valves overall structure and function[5,6,9,12–14]. In this resting state of VICs they act similar to fibroblasts[15,16]. It is from this phenotype that VIC plasticity stems. In response to injury or disease, qVICs become activated VICs (aVICs) and take on the features of myofibroblasts. This phenotype is characterized by increased α-smooth muscle actin (α-SMA) expression, contractility, stress fiber formation, secretion of matrix remodeling enzymes (MMP-1, MMP-2, MMP-9, MMP-13), cytokines (TGF-β), and cathepsins[5,13,17,18]. aVICs also exhibit heterogeneity in their morphologies. Many pathologies result in high cellularity and abnormal changes in ECM content; these are often

caused by the dysregulation of aVICs. Activation of qVICs is brought on by changes in the mechanical environment or from several cytokines, often TGF-β.

For a tissue engineered solution, adipose tissue derived stem cells (ADSCs) show excellent potential for use in heart valve tissue engineering. ADSCs have the ability to differentiate into endothelial cells, providing a non-thrombogenic blood tissue interface critical to regulating activity of interstitial cells, smooth muscle cells, and fibroblasts, which are involved in synthesis of collagen, elastin, and proteoglycans[19–21]. ADSC's also have immunomodulatory properties and are able to suppress T-cell proliferation, reduce inflammatory cytokines, and stimulate production of anti-inflammatory cytokines[22]. They are also able to promote regeneration of tissue via expression of VEGF, IGF-1, TGF-β1, and hematopoietic factors[19,23,24]. Additionally these stem cells are able to suppress M1 type macrophages, which provide classic macrophage activity and alternatively activate M2 macrophages which promote wound healing[23]. Due their ability to differentiate into smooth muscle cells (SMCs) and fibroblasts, which are both similar to VICs, differentiation of ADSC's into these cell types would be critical for our construct[25,26]. The niche, valvular microstructure provided from our scaffold should provide cues for differentiation along with physiological stresses provided by a bioreactor. However, it may also be prudent to pre-differentiate these stem cells using appropriate growth factors to encourage specific differentiation of the ADSCs.

Recellularization of decellularized scaffolds of any tissue, but particularly heart valve scaffolds, has been difficult to say the least[4,27]. To date, static seeding of scaffolds is the most frequent method used in the construction of tissue. However, efficiencies using

this technique range only between 10 -25%[28]. Static seeding onto scaffolds leads to minimal cell infiltration into the scaffolds and has shown low cell seeding competence[28]. To achieve better results, many groups have started directly placing cells interstitially using a variety of methods including perfusion, direct injection, vacuum and centrifugal seeding[29]. In synthetic and hydrogel scaffolds where material properties such as pore size are more customizable, interstitial cell seeding strategies can be more efficient. However when using an ECM scaffold which is already customized for specific tissues, preservation of the native matrix is paramount. Some groups, such as ours, have found some success in direction injection of cells into the scaffolds[28–32]. However, this often creates a bolus of cells which many times do not migrate into the ECM they were injected to. Therefore, many groups have employed growth factors and other cell-homing strategies to encourage migration and proliferation within the scaffolds with some success[28,30,31,33,34]. One novel idea is the use of hydrogels as a means of delivering the cells. These hydrogels provide a customizable way to deliver cells and growth factors into a scaffold. Encapsulation of cells in a hydrogel also aids during injection due to the rheological properties of the gel. Due to their high viscosity, hydrogels exhibit stress-thinning and therefore can protect cells from high shear stress during injection[35,36].

Fibrin hydrogels have been explored for use in cell seeding applications for tissue engineering. Fibrin is a natural product of the coagulation cascade and functions as temporary scaffold during wound healing. It is formed through the polymerization of fibrinogen, which is initiated by the protease thrombin[37]. Due to its autologous derivation, fibrin gels possess excellent biocompatibility[38]. In fact, it can be produced from a patient's

own blood, thereby eliminating the risk of infection or foreign body reaction[39]. Due to its natural origins and function as a cell-binding matrix, fibrin gels could be used as an injectable cell delivery system for interstitial seeding. Well known for its ability to attract cells, it is also known to encourage cell migration and adhesion[37,39,40]. Fibrin can also bind several growth factors, through heparin. Growth factors and cytokines have been used in tissue applications to encourage cell migration into more uniform distributions within scaffolds[30,33,34,41–43]. Therefore, the ability to bind growth factors, both directly and indirectly, is a great attribute for cell seeding. One noted disadvantage of fibrin is its rapid degradation profile. Fibrin gels, unless chemically inhibited, will undergo degradation within several days after implantation. However because fibrin would be used as an injectable hydrogel, the relevance of this rapid degradation is questioned. Cells have easily been encapsulated in fibrin gels and when incorporated in scaffolds, can rely on the mechanical properties of the matrix in which it was injected[40]. Therefore, the fibrin gel serves only to provide a uniform cell distribution and more efficient seeding. Degradation of the fibrin allows for the accumulation of newly synthesized ECM components generated by the encapsulated cells. In addition, degradation of fibrin exhibits minimal inflammation. In fact, culturing macrophages in fibrin gels stimulates anti-inflammatory cytokines and encourages M2 polarization[44]. Fibrin has shown to encourage more new collagen and elastin production from seeded cells than from other gels such as collagen[37,40,45,46]. Fibrin has also been shown to be a potent recruiter of endothelial cells and also has potential as a means of encouraging endothelial to adhere to the scaffold surface[47].

In tissue engineering, the cell seeding of scaffolds is a very complicated process. Due to this complexity, static seeding still remains one of the most common methods to incorporate cells into scaffolds. As mentioned, dynamic seeding by use of a bioreactor, has shown to encourage significantly improved cellular distribution within scaffolds while also providing relevant mechanotransductive signals to the cells. Bioreactor design is centered upon providing a physiological environment in vitro for the cell-seeded construct. Heart valves are dynamic tissues composed of specialized cells and an extracellular matrix that responds to these mechanical demands. Beginning at implantation and continuing indefinitely after that, the tissue engineered valve must accommodate for these mechanical demands but also have ongoing strength, flexibility, and especially durability[(1)]. Therefore, the goal to engineer a tissue engineered mitral valve presents unique hurdles to overcome. Immediately placing a recellularized construct into a patient would most likely fail due to these complex and harsh mechanical conditions. Therefore, pre-conditioning of the MV construct is essential preparation for eventual implantation. By providing a physiological-like environment for the seeded constructs to develop, allows the cells to adhere to and remodel the scaffold so that the living construct can withstand the forces and pressures expected of it. Our laboratory has developed a pulse-duplicating heart valve bioreactor capable of subjecting heart valves to physiological pressures and flows. It consists of a three-chambered heart valve bioreactor (1), an optional pressurized compliance tank (2), a reservoir tank (3) with sterile filter (4) for gas exchange, one-way valves (5), resistance valves (6), pressure transducers (7), a flow meter, a webcam (8), and an air supply that cyclically pumps fluid through the heart valve[(48)].

Creation of a mitral valve bioreactor presents unique challenges due to the unique anatomy and multiple components of this valvular machine. Shape of the annulus, which establishes the form and function of the valve, must be taken into account as it provides optimal force distribution to the leaflets and chordae below. The geometric shape of the annulus approximates to that of a hyperbolic paraboloid[49–53]. Although this nonplanar shape's origins are not fully described in literature, it is understood that this shape is the determinant of optimal force distribution in the leaflets and chordae tendinae[50,53,54]. Chordal attachment is also crucial to provide the necessary tension on the posterior side of the leaflets, as well as the chordae themselves. Few groups have been able to produce an anatomically correct mitral valve bioreactor, accounting for each of these four major components.

5.2 Methods and Materials:

5.2.1 Histology and Immunohistochemistry:

Rehydrated paraffin sections (5μm) were stained with Hematoxylin and Eosin (H&E), Masson's Trichrome and Movat's Pentachrome according to the instructions in the kits purchased from Poly Scientific R&D Corp. (Bayshore, NY). 4',6-diamidino-2-phenylindole (DAPI) was purchased from Sigma-Aldrich Corporation (Lakewood, NJ).

Immunohistochemistry (IHC) was performed on formalin-fixed and paraffin-embedded sections using heat-mediated antigen retrieval (10mM citric acid at pH of 6, for 10 min at 90°C), followed by exposure to 0.025% Triton X-100 for 5 minutes. After incubation in normal blocking serum for 45 minutes, the primary antibodies diluted to 2μg/mL were applied overnight at 4°C in a humidified chamber. The following antibodies

were used: mouse anti-αSMA (Abcam, Ab7817), rabbit anti-HSP-47 (Abcam, Ab77609), rabbit anti-von Willebrand Factor (vWF) (Abcam, Ab9378), rabbit anti-VE cadherin (Abcam, Ab33168), rabbit anti-P4HA3 (Abcam, Ab101657), rabbit anti-calponin (Abcam, Ab46794), rabbit anti-iNOS (Abcam, Ab15323) rabbit anti-Vimentin (Abcam, Ab92547). Negative controls were obtained by omitting the primary antibodies. The Vectastain Elite kit and the ABC diaminobenzidine tetrahydrochloride peroxidase substrate kit were purchased from Vector Laboratories (Burlingame, CA). Sections were counterstained with a diluted hematoxylin prior to mounting. Images were obtained at various magnifications on a Zeiss Axiovert 40CFL microscope using AxioVision Release 4.6.3 digital imaging software (Carl Zeiss MicroImaging, Inc. Thornwood, NY).

5.2.2 Cell Culture and Pre-Differentiation of hADSCs:

Human adipose derived stem cells (hADSCs) (#R7788-110, Fisher Scientific, Life Technologies, passage 0) were obtained and expanded in StemPro Human Adipose-Derived Stem Cell Kit with 1% antibiotic solution (#30-004-CI, Corning – Cellgro). hADSC's were maintained and subcultured at subconfluent conditions on tissue culture plastic with Trypsin-EDTA 1X (#25-053-CI, Corning - Cellgro).

For differentiation of hADSCs to endothelial-like cells, ASCs were cultured for up to 4 weeks in EC differentiation media comprised of DMEM, 2% FBS, and 1% antibiotic solution supplemented with 0.5 ng/mL vascular endothelial growth factor (VEGF, #100-20B, PeproTech Inc) and 20 ng/mL insulin-like growth factor-1 (IGF-1, #AF-100-11, PeproTech Inc). Growth factors were freshly added to the media at the time of each media change.

For differentiation of hADSC's to fibroblast-like cells, hADSC's were cultured for up to 4 weeks in fibroblast differentiation media comprised of DMEM, 5% FBS, and 1% antibiotic solution supplemented with 5ng/mL transforming growth factor beta-1 (TGF-β1, #100-21C, PeproTech Inc.). Growth factors were freshly added to the media at the time of each media change.

5.2.3 Cell Seeding and Fibrin Fabrication:

Pre-differentiated fibroblasts and endothelial cells were seeded into and on the scaffolds respectfully. Before seeding, PGG-treated valves underwent a neutralization step where the mitral valves were incubated in DMEM/10% FBS with 1% antibiotic/antimycotic and Stromal Derived Factor-1α (SDF-1α, #300-28A, PeproTech, Inc.) at 100ng/mL overnight. For seeding, pre-differentiated cells at a density of about 2 million cells per mL were prepared. To facilitate seeding, about 1mL of sterile air was injected into each leaflet through a 33G X 0.5inch needle. The pre-differentiated fibroblasts were resuspended in 250µL thrombin (#T7009-250UM, Sigma) and $CaCl_2$(#BP510-100, Fisher) and mixed with a sterile 250µL aliquot of fibrinogen (#F4129-1G, Sigma) to get final concentrations of 0.5U/mL thrombin, 4mg/mL fibrinogen, and 2mM $CaCl_2$. Cells were injected into each leaflet (0.5mL per leaflet) before mixture could become a fibrin gel. Seeded valves were placed into mounting rings for the bioreactor with a static control. Interstitially seeded constructs were then drop-seeded with pre-differentiated endothelial cells, 200µL of thrombin/$CaCl_2$/fibrinogen at the same concentrations, onto each leaflet and the chordae tendinae of each valve. Seeded constructs were placed in the incubator for

15minutes without media to allow fibrin to gel. After seeding, valves were left in DMEM/10% FBS with 1% antibiotic/antimycotic overnight.

5.2.4 In Vitro Conditioning:

For pulsatile bioreactor conditioning, valves (n=2) were mounted in the sterile mitral valve bioreactor systems in DMEM/10% FBS with 1% antibiotic/antimycotic and pressures progressively increased from 10mmHg to 120mmHg over 21 days to reach physiological conditions (120/10mmHg) at 70 mL ejection fraction and 65 bpm. Valves were kept at these conditions for 7 days and the study concluded after 28 total days in the bioreactor. Media was changed once a week, and 5mL of additional antibiotic/antimycotic was added in between media changes.

5.2.5 Mechanical Testing:

Rectangular 2.5 x 1 cm specimens of tissue from the bioreactor and the static control (n=2) were cut. Specimens were secured to a frame with a 10N load cell (MTS Systems), and preconditioned for 10 cycles between 0-15% strain at a rate of 3.0 mm/min. After 2 minutes rest, samples were pre-strained at 0.2N of load then brought to 10N of stress. The stress/strain curve was taken and the Young's modulus was evaluated for each stress/strain curve between the 10-20% strain and were averaged (n=3).

5.2.6 Penta-galloyl glucose (PGG) Treatment:

High-purity 1,2,3,4,6-Penta-O-galloyl-beta-D-glucose (PGG) was a generous gift from N.V. Ajinomoto OmniChem S.A., Wetteren, Belgium (www.omnichem.be). The acellular scaffolds were treated with sterile 0.3% PGG in 50mM Na_2HPO_4, 0.9% NaCl, pH 5.5 containing 20% isopropanol overnight at room temperature under agitation and

protected from light. Scaffolds were then rinsed with sterile PBS 3 times, and then stored in sterile PBS with 1% protease inhibitors and 1% antibiotic/antimycotic (Pen-Strep).

5.2.7 Development of Mitral Valve Mounting System:

The shape of the annular mounting ring was started using a combination of measurements reported in literature as well as a 3D-scan of a mitral annuloplasty ring. This scan was then imported into SolidWorks where it was modeled and fitted to existing parameters for the aortic valve bioreactor. After consulting with Aptus Bioreactors, chordal attachment was designed with the mounting system. These pieces were then 3D-printed and used in the bioreactor experiments. Several bioreactor chambers and other consumable materials were purchased from Aptus Bioreactors: Mitral valve clamping holder, lower (MA386), Mitral valve clamping holder, upper (MA396), Bioreactor membrane with installation kit (KT430), and the Mitral fittings consumables kit (KT485).

5.2.8 Statistical Analysis:

Results are expressed as means ± standard deviation (SD). Statistical analysis was performed using one-way analysis of variance (ANOVA). Differences between means were determined using the least significant difference (LSD) with an alpha value of 0.05.

5.3 Results:

5.3.1 Recellularization Studies Using Fibrin:

Recellularization of decellularized scaffolds is a difficult but necessary step producing a translatable tissue engineered mitral valve. Several pilot studies were implemented to gain insight into how to encourage migration of directly injected cells throughout the matrix. Fibrin was used as this vehicle to deliver cells more uniformly

interstitially. To aid in this migration, SDF-1, a cytokine well known to encourage migration of cells, was used in the scaffolds[55–57]. After allowing two weeks for cells to spread, various histological stains were performed to evaluate this process. As seen in **Figure 5.1**, an H&E, Masson's Trichrome, and IHC's for vimentin and CXCR4 were conducted. From the H&E staining it is evident that cells spread from the injection site outward into the scaffold. It was also found that cells were spreading in areas away from the injection site. In addition, cells were drop-seeded on the scaffold, also using fibrin, and a nice monolayer of cells is shown here. Trichrome staining similarly displays the improved migration of cells, but more importantly displays remaining fibrin within the scaffolds. These pink areas, in a normally collagen (blue) dominated region, designate where fibrin spread in the scaffolds and remained during the seeding studies. A small monolayer of cells is also found externally as before. IHC's for vimentin and CXCR4 were also conducted. Vimentin stain was positive for all seeded cells. Also identified positively was CXCR4, the receptor on the cell for SDF-1, which regulates the cells homing ability and affects their migration[33,55,57].

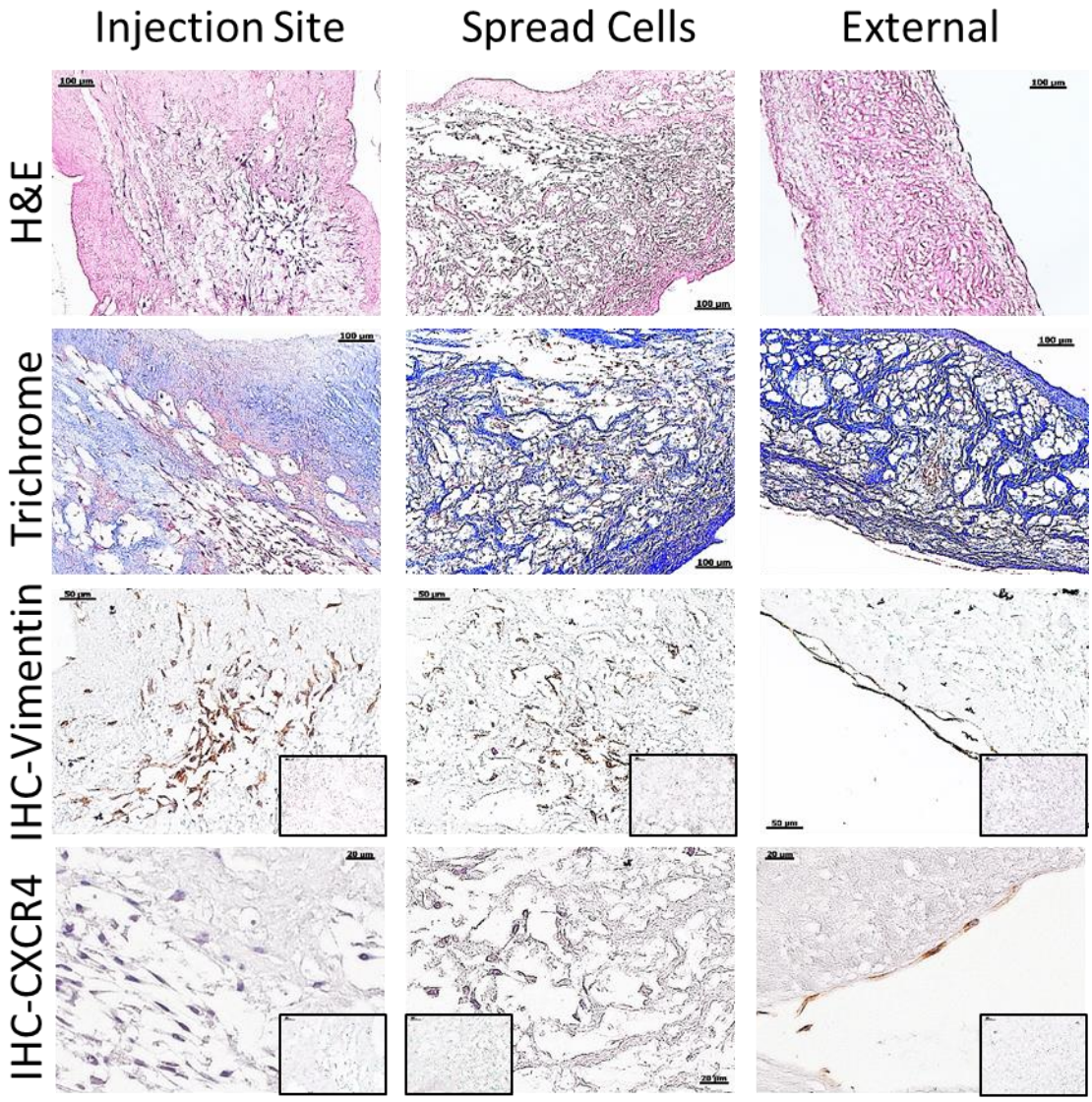

Figure 5.1: Cell Seeding Using Fibrin and SDF-1. Scaffolds immersed in SDF-1, a well-known cytokine, were injected with fibrin gel. This fibrin gel was used as a carrier to introduce cells into the acellular mitral valve scaffolds. Noticeable spreading of cells can be seen. Injection spots, while distinct, did not house a bolus of cells as in previous studies. Cells were also found apart from these injection spots indicating migration. Cells also readily attached externally after being statically seeded, also with fibrin. An IHC for vimentin was positive, as was the expression for CXCR4, an indication that the SDF-1 incorporated into the scaffolds had an effect on cell migration.

5.3.2 Pre-Differentiation of hADSCs to Fibroblasts and Endothelial Cells:

After these positive results in encouraging cell migration after injection, we decided that instead of injecting hADSCs directly in to the scaffolds, that we would pre-differentiate the hADSCs using specific growth factors. To verify their differentiation into endothelial cells and fibroblasts, an immunofluorescence was performed for various markers. Endothelial cells, which used IGF and VEGF, were stained for VE-cadherin and vWF. Fibroblasts, which used TGF-β for pre-differentiation, were stained for HSP-47, prolyl-4-hydroxylase, and vimentin. In **Figure 5.2**, these immunofluorescence stainings are shown.

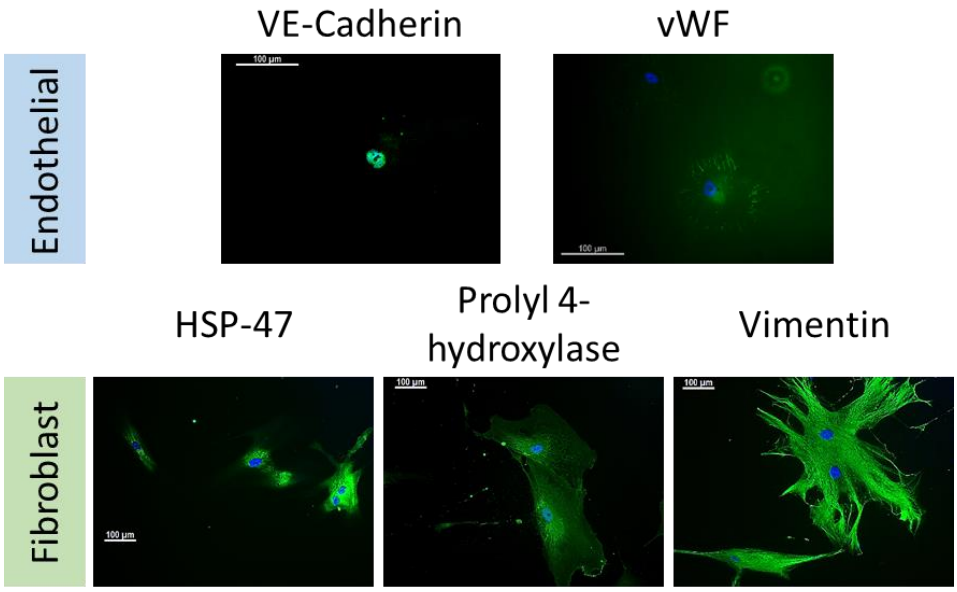

Figure 5.2: Pre-Differentiation of hADSCs into Endothelial Cells and Fibroblasts. hADSCs were pre-differentiated into fibroblasts due to their similarity to VICs. To confirm their differentiation an immunofluorescence for fibroblast markers HSP-47, prolyl 4-hydroxylase, and vimentin all showed

positively. Likewise, pre-differentiated endothelial cells were confirmed by a positive stain for each VE-cadherin and vWF.

5.3.3 Design of a Mitral Valve Mounting Ring for Placement in Bioreactor:

After approving of cell types and a recellularization protocol, design of the mitral valve bioreactor was completed. Our group has already designed an aortic valve bioreactor of which we made modifications to fit the mitral valve and its complex geometry[48]. Developing a mounting system for the mitral valve was perhaps one of the most crucial design criteria. As seen in **Figure 5.3**, a two-piece mounting system was developed. The first criteria met for this design was the use of a hyperbolic paraboloid to mount the mitral annulus. As mentioned several times, this unique shape provides optimal force distribution throughout the valve. Dimensions for this shape were taken from literature and from existing annuloplasty rings which were 3D scanned. Also apparent in this design is the "D" shape. This allows proper placement of the anterior and posterior sides of the annulus and leaflets. Lastly in this design is the incorporation of several bars below the annular clamp which was used for chordal attachment. Springs were attached to the papillary muscles and then were hooked to these bars. This allowed for proper coaptation of the leaflets and provided tension on their ventricular surface.

Figure 5.3: Development of the Mitral Valve Mount for Bioreactor Testing. A mounting ring was developed for the mitral valve as a modification to the already existing aortic valve bioreactor. The natural shape of the annulus was incorporated in this design to provide optimal force distribution throughout the valve during in vitro bioreactor testing. Also included were bars used to attach springs to the papillary muscles. This spring system allows for coaptation of the mitral valve at physiological pressures, while also providing proper tensile forces on the leaflets. This tension is also important for proper force applications in the chordae as well.

5.3.4 Cell Seeding Protocol, Mounting of Seeded Mitral Valve, and Placement in Bioreactor:

In **Figure 5.4**, the protocol for how recellularization takes place up until placement in the bioreactor is shown. After starting with an acelluar scaffold and neutralized overnight

in DMEM (10%FBS, and 1% AbAm) with SDF-1, valves were then taken out and directly injected with cells (Panel C). From here, the annulus is placed by properly aligning the posterior and anterior sides according to the mounting ring shape (Panel D). After locking the annulus in place, metal rings for eventual placement in the bioreactor are positioned around the mounting system (Panel E). Then papillary muscles and chordae tendinae are attached to springs, which are attached to the lower bars of the mitral mount (Panel F). Finally, this completely seeded and mounted mitral apparatus is placed within the bioreactor and media is added (Panel G).

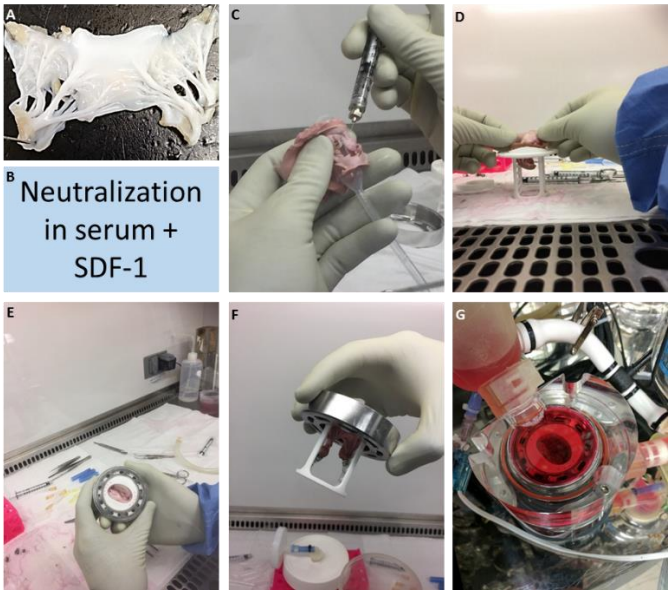

Figure 5.4: Mitral Valve Seeding and Mounting for Bioreactor Testing. Recellularization and mounting of the seeded scaffold is a several step process. Panel A shows our decellularized mitral valve scaffold. As described in panel B, these valves are then treated overnight in serum with 100ng/mL SDF-1. Cells were then directly injected into the scaffolds. Pre-differentiated endothelial cells were then seeded drop-wise on the scaffold. After allowing the fibrin and cell mixtures to gel in the incubator, the construct is mounted in the mounting rings and springs are attached to the papillary muscles (panels D-F). Finally, after allowing cells to attach to the scaffold overnight, the mounted mitral valve construct is placed within the bioreactor.

5.3.5 Design and Assembly of the Mitral Valve Bioreactor:

While the existence of the aortic valve bioreactor provided a foundation to work with, the mitral valve the physiological demands it undergoes are different. As a result, parts and assembly of the mitral valve bioreactor are unique. **Figure 5.5** shows a complete mitral valve bioreactor system. In this system are several chambers which are essential for holding anatomical pressures. The atrial chamber, significantly shorter than the aortic atrial chamber, acts as the atrium for the heart valve. Due to the very low pressures in the atrium experienced by the mitral valve (about 10mmHg), this chamber is small to decrease pressure here. The valve rests between the atrial chamber and two chambers beneath which act as the ventricle. It is here that the high pressures are placed on the valve during systole (120mmHg). The extra ventricular chamber is needed here to ensure that the mounting system which holds the papillary muscles, is not hit by the silicone membrane below. This membrane caps off an air chamber. Air is pumped into this chamber, which forces the silicone membrane upwards into the ventricular chamber. This forces flow and pressures into the system. **Figure 5.5** also shows proper closing of the mitral valve as well as the springs of the mounting ring in action.

Figure 5.5: Assembly of the Mitral Valve Bioreactor. The overall structure of the mitral valve bioreactor is a modification of an aortic valve bioreactor. There are four chambers, an atrial chamber, ventricular chamber, air chamber, and an additional ventricular chamber. Also, present in this set-up is a large glass reservoir chamber, flow meter and two pressure transducers, which measure pressures in the atrial and ventricular chambers. In the center of the bioreactor is the mounted and seeded mitral valve construct. Pressure and flow is originated in the air chamber where air is pumped in, thus moving a silicone membrane. This membrane creates the flows and pressures desired for experimentation. Gas exchange is allowed through a sterile filter. The incubator in which this mitral valve bioreactor is placed controls all temperature, CO_2 levels, and humidity. Flow rate is also measured and can be adjusted using clamps.

5.3.6 Mechanical Testing of the Seeded Leaflets After Bioreactor Completion:

After 4 weeks of preconditioning in the bioreactor, the tissue underwent tensile testing to determine the young's modulus. This was compared to the static control. As seen

in **Figure 5.6**, the static control had a higher modulus of elasticity when compared to the leaflets from the bioreactor. This difference was not statistically significant however.

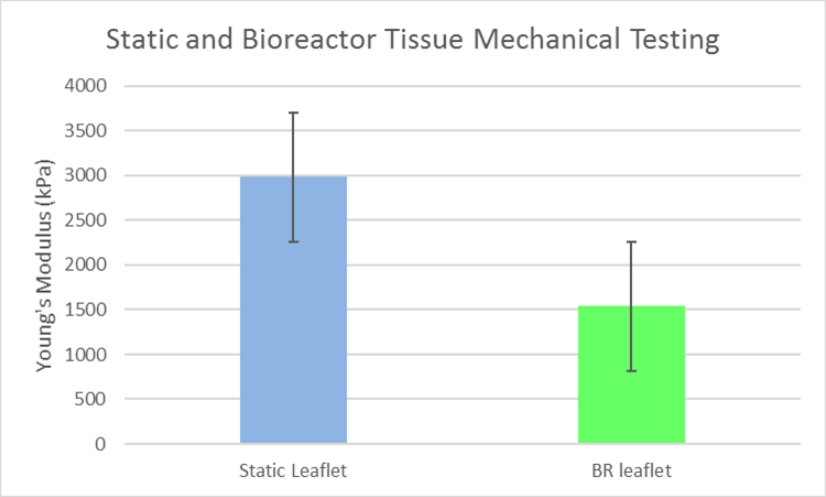

Figure 5.6: Uniaxial Tensile Testing of Static and Bioreactor Conditioned Tissues. Mechanical testing was performed on the leaflets and chordae for both static and bioreactor conditioned groups. From this data, modulus of elasticity was determined between the range of 10-20% strain. Young's modulus was calculated for both the static control and the bioreactor tissue. Young's modulus was higher for the static control, but not significantly.

5.3.7 Live/Dead Staining of Static and Pre-Conditioned Tissue:

A Live/Dead stain was used to evaluate the amount of living and dead cells present within each treatment group. As evidenced by **Figure 5.7**, living cells (indicated with green fluorescence) were difficult to find. Dead cells were indicated using black arrows. Before these cells died, it is apparent that there are more cells spread in the pre-conditioned construct when compared to the static control. It is possible that more cells could be found from other tissue sections within each group.

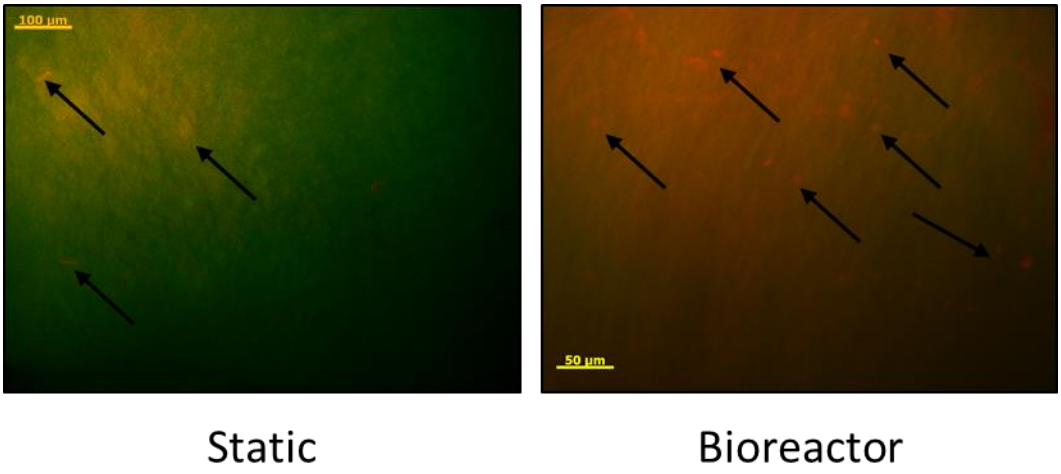

Figure 5.7: Live/Dead Images of Tissue from Static Control and Bioreactor. Small sections of tissue from both the static control and the pre-conditioned tissue from the bioreactor were stained with Live/Dead solution to visualize dead and living cells. Dead cells are much more apparent within each tissue type, however more spreading of the cells is apparent in the tissue from the bioreactor. These cells are indicated with black arrows.

5.3.8 Histological Evaluation of Recellularized Scaffolds Post-Bioreactor Conditioning:

After 4 weeks of preconditioning in the bioreactor, cell seeding and migration were evaluated histologically in the bioreactor tissue and the static control. As seen in **Figure 5.8**, an H&E and DAPI stain were used to identify nuclei. As before, Masson's Trichrome was used to show ECM content, but more importantly any remaining fibrin within the constructs. Movat's Pentachrome was used to show ECM content, but especially GAG deposition. Overall, cells did not migrate as well as before. Both static and preconditioned tissue show boluses of cells. Bioreactor tissue does show more cells than the static control. Areas injected with fibrin are obvious due the contrasting colors in the trichrome stain. GAG deposition was found, which is an improvement from previous seeding attempts. Few endothelial cells remained after bioreactor conditioning, but this is still an improvement

over previous bioreactor studies. A clear dark monolayer is present on the H&E and some in the DAPI. Trichrome and pentachrome stains also show similar results here.

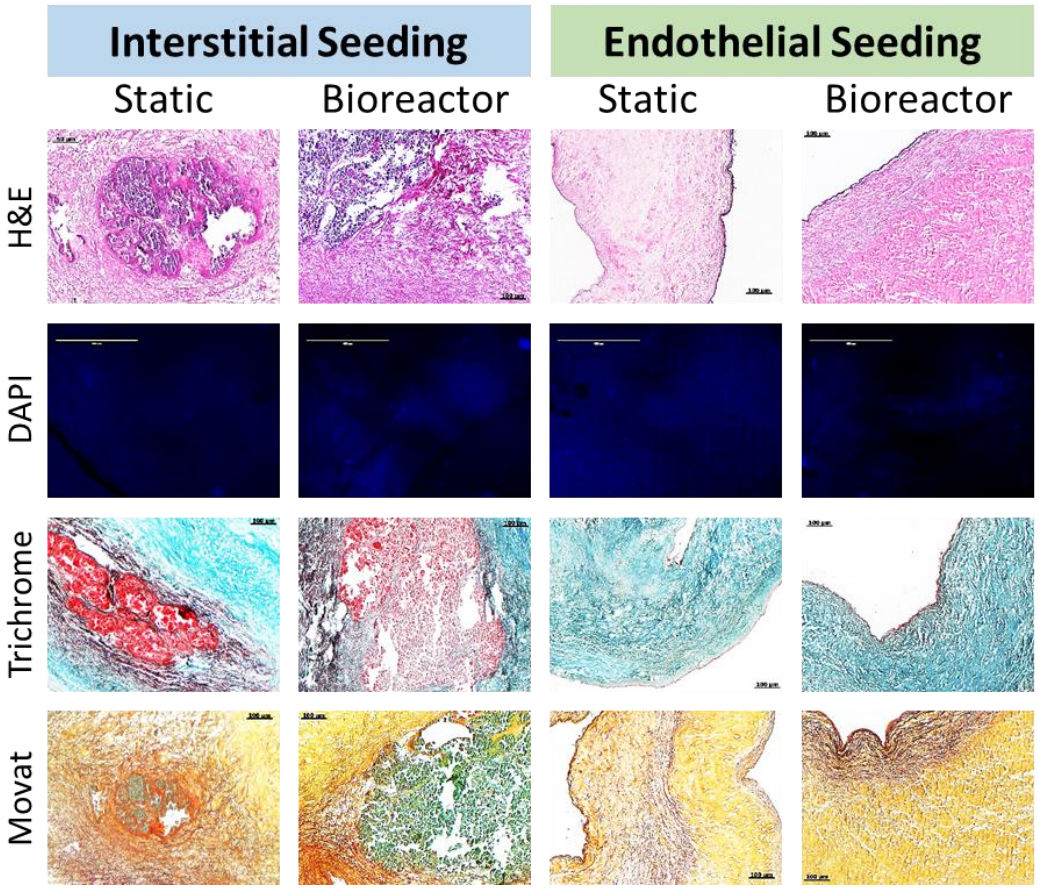

Figure 5.8: Recellularization of Acellular Scaffolds. To show revitalization of our acellular mitral valve scaffolds, several histological stains were performed. Images shown are from both the static control and the tissue preconditioned in the bioreactor. Pre-differentiated fibroblasts and pre-differentiated endothelial cells were seeded interstitially and externally respectively. An H&E and DAPI stain were performed to highlight nuclei in the tissue. Leaflet tissue are represented in this image since no cells were injected in the chordae, only externally. A Masson's Trichrome was performed to visualize remaining fibrin. Lastly, a Movat's Pentachrome was performed to view ECM quality and deposition of GAGs.

5.3.9 Characterization of Cells in Bioreactor and Static Control Tissues:

Immunohistochemistry was used to determine expression of smooth muscle cell, fibroblast, and endothelial cell markers. In **Figure 5.9**, some expression is observed for α-SMA and calponin. An overwhelming positive stain here would have been indicative of activation of our seeded cells into myofibroblasts.

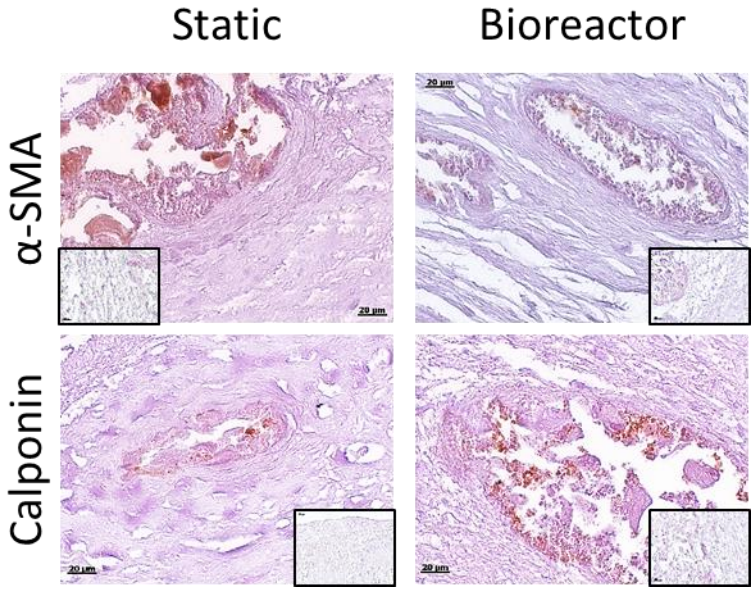

Figure 5.9: Characterization of Seeded Cells with Smooth Muscle Cell Markers. The static control and bioreactor tissues were stained to see if the seeded cells expressed smooth muscle markers. A positive stain here would be indicative of fibroblasts becoming activated within the tissue. Positive expression for markers α-SMA and calponin did appear, but were minimal in known injection spots within the tissue sections.

Figure 5.10 shows an IHC for fibroblast markers vimentin, prolyl-4-hydroxylase (P4HA3), and HSP-47. Strong expression for each of these markers, especially vimentin, was observed in both the static and bioreactor-conditioned groups. Vimentin expression was more spread throughout the ECM in some sections possibly indicating an improved migration.

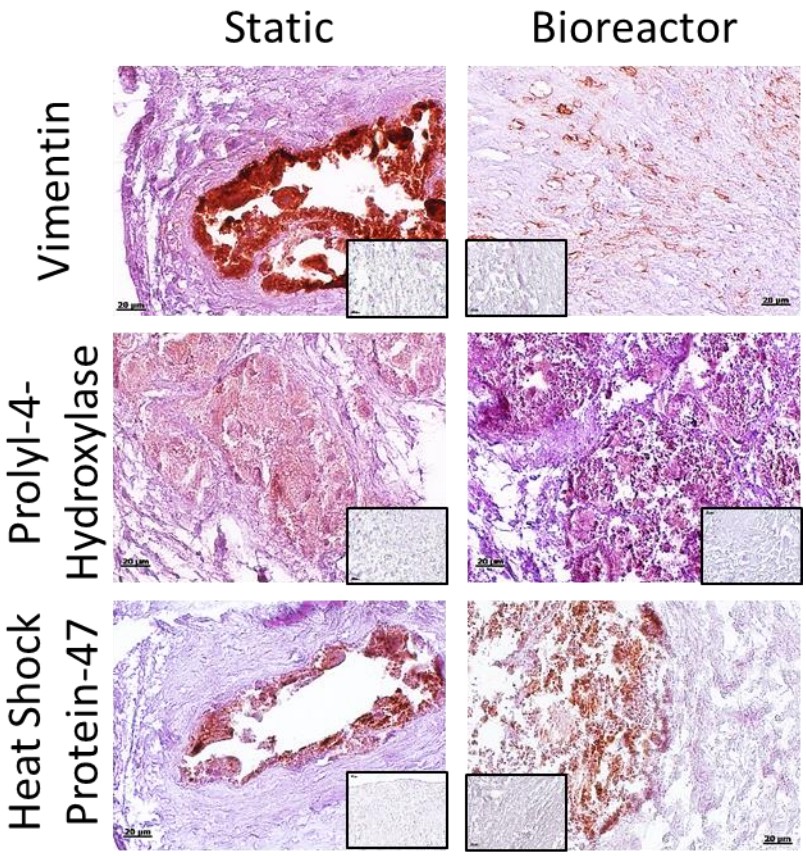

Figure 5.10: Characterization of Seeded Cells with Fibroblast Markers. Seeded constructs were evaluated on their expression of fibroblast markers vimentin, HSP-47, and prolyl-4-hydroxylase. Positive expression was observed in both the static control and bioreactor tissue sections. Expression was clearly higher than smooth muscle cell marker expression.

Lastly, expression of endothelial cell markers vWF, VE-cadherin, and iNOS were evaluated. Although not much clear expression was observed, some cells on the construct's exterior did survive and expressed positively for each marker. In **Figure 5.11**, you can see this expression as well as the expression of these markers on the chordae tendinae. This was the only cell type seeded on the chordae tendinae and thus they only appear in this figure.

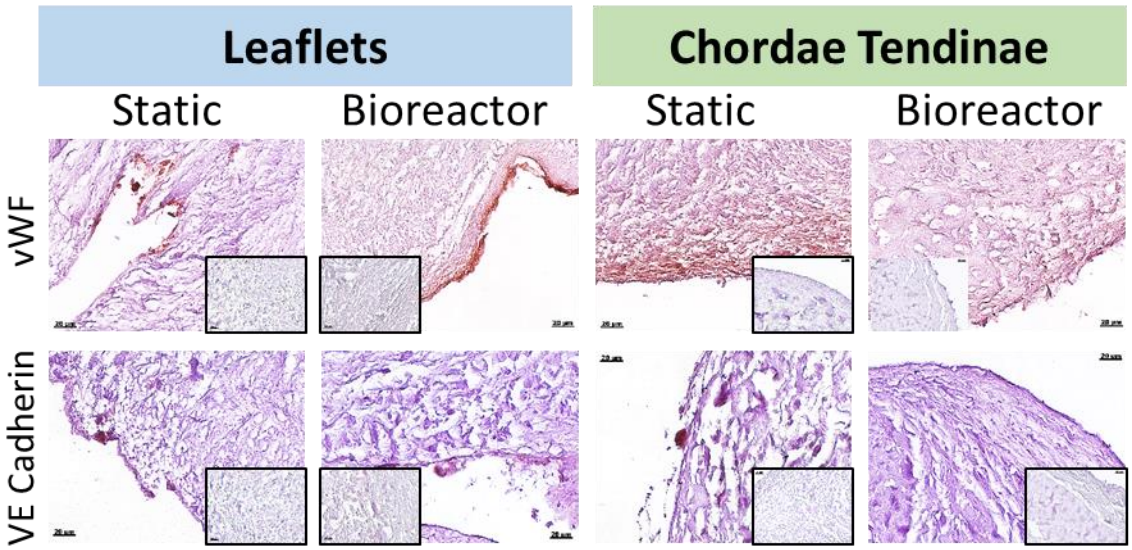

Figure 5.11: Characterization of Seeded Cells with Endothelial Cell Markers. Scaffolds were seeded with pre-differentiated endothelial cells. Markers for von Willebrand Factor (vWF), VE cadherin, and iNOS were evaluated. A slight, but obvious staining was observed on both the leaflets and chordae tendinae. Chordae, shown here, were only seeded with endothelial cells.

5.4 Discussion:

5.4.1 Progress Towards Recellularization of the Mitral Valve Scaffold:

Recellularization of an acellular scaffold, perhaps especially ECM scaffolds, is difficult to achieve. Ideally, appropriate cells are introduced to the scaffold and they are able to repopulate and remodel the scaffold. It is important to note that many groups understand the importance of recellularization, but their statically seeded methods take many weeks to achieve an acceptable result, which is not translatable for clinical purposes. Therefore, we sought to improve this process by incorporating cells into the scaffolds and promoting migration throughout. In the past, our group has found that direct injection of the cells into the scaffold is a better method to introduce cells interstitially as opposed to drop seeding them on the scaffold and waiting for them to migrate throughout. Direct

injection however is by no means a successful for producing a revitalized construct flush with cells. While cells are inserted within the scaffold, a bolus of cells is created at the injection site and these cells do not migrate out either because they physically cannot or because there is no reason for them to alter their current dense state within the scaffold.

Fibrin, a well-known and natural hydrogel, has been used as cell carrier to seed stem cells for various cardiovascular applications[40,58]. Also, as mentioned before utilizing the increased viscosity of a hydrogel like fibrin significantly improves the survivability of cells being injected into a matrix compared to just using cell culture media[35,36]. Therefore, we decided to take advantage of these properties and the natural cell binding ability of fibrin as a means to better deliver cells to the scaffold. To enhance migration into the scaffold, we employed stromal cell derived factor-1 (SDF-1). SDF-1 is a well-known and powerful recruiter of cells in injury. As a pro-inflammatory cytokine, it is said to be the most potent chemoattractive signal for the CXCR4 receptor, which is considered a major stem cell homing factor[33]. Translationally speaking, usage of an inflammatory cytokine sounds incongruous with typical biocompatibility doctrine. However, SDF-1 has a short half-life so as to limit over-recruitment of cells to the injury site in vivo[55]. Therefore, we chose to incorporate this powerful cytokine in the matrix before seeding in hopes that the cells in the fibrin gel would be encouraged to venture into the remaining acellular scaffold.

Based on the results presented in **Figure 5.1**, overall cell seeding efficiency was significantly improved when compared to previous seeding studies. While an injection site was still clearly visible, for the first time we were able to observe a marked improvement in migration of these seeded cells into the scaffold. Also important to note is that many of

these cells spreading throughout the matrix were not necessarily close to the migration site, leaving us to conclude that they had migrated quite far from their original insertion into the scaffold. We believe that this success can be attributed to both the fibrin gel and the SDF-1.

After this two week seeding study, fibrin remained within the scaffold. The gel did not create a bolus of its own; it did seem to perfuse throughout some of the scaffold near the injection sites. This is evidence by the pink stain in the Masson's Trichrome. Fibrin does degrade quickly, but it does appear to reside long enough in the scaffolds after two weeks. Vimentin stained positive for the seeded cells. Also important to note is there was a positive stain for CXCR4, indicating that the cell receptor was in fact engaged most likely due to the presence of SDF-1 within the scaffold. Migration of the cells from these injection sites is a huge step in the right direction towards complete recellularization.

5.4.2 Pre-Differentiation of hADSCs into Appropriate Cell Types:

As described in our tissue engineering paradigm, an appropriate choice of cells should be incorporated into the tissue. Originally, we opted to use hADSCs due to their ease of obtainment, ability to harvest large quantities, and their large capacity for differentiation. However, recently we decided to alter this approach. By using specific growth factors, we can guide these hADSCs toward specific phenotypes. This pre-differentiation allows one to ensure commitment towards the desired cell type. In our case, this ensures that differentiation will be not solely be determined by interactions with the ECM microstructure. Pre-differentiation provides more assurance that the desired cell types will be achieved. VICs and VECs are the most appropriate cell types for the mitral

valve. VECs are endothelial cells and VICs are fibroblast-like in their ability to remodel and produce matrix proteins. After treating hADSC's with TGF-β for fibroblast differentiation and VEGF and IGF for endothelial differentiation, an immunofluorescence revealed positive expression for markers found in each of the desired cell types.

5.4.3 Mitral Valve Bioreactor Design:

Designing of a mitral valve bioreactor provided many obstacles with the valve's complex anatomy and many moving parts. Some groups have been able recreate some aspects of a functioning mitral valve in vitro, but they cannot use these devices sterilely or cannot provide anatomical pressures[59,60]. Design criteria was also narrowed due to the existence of an already well-functioning aortic valve bioreactor from our group. The first, and possibly most crucial, design element for the mitral valve bioreactor was establishing an approach to mount the valve. As mentioned before, the unique shape of the annulus provides optimal force distribution to the other functioning parts of the mitral valve. Therefore, dimensions of the annulus were found in literature[61,62]. Also, a mitral annuloplasty ring was 3D scanned and placed within a CAD program (Solidworks) where modifications could be made and other design criteria implemented.

One of these other design criteria designing a system for attachment of the chordae tendinae. To expect correct differentiation from the seeded valves, the proper forces must be observed in the bioreactor. To achieve this, tensile forces must be placed on the ventricular side of the leaflets and the chordae themselves. To achieve these tensile loads, as seen in **Figure 5.3**, bars were placed below the annulus mount. Springs were placed on the remaining papillary muscles and then attached to these bars. After the recellularization

process and placement within the bioreactor, the chordae in conjunction with the springs, provided a functioning mitral valve without prolapse into the atrial chamber.

5.4.4 The Current Recellularization Process and Placement into the Bioreactor:

Figure 5.4 illustrates the general approach taken for seeding of the valve and the corresponding placement into the bioreactor. As seen, SDF-1 was again used to assist in migration of the seeded cells. It is important to note that during seeding, time was allowed for the fibrin gel and cell mixture to solidify. Once complete, cells, delivered using fibrin again, were drop-seeded on the outside of the interstitially-seeded mitral valve. Springs were attached onto the papillary muscles and secured to the bars below the mounting ring. After which the entire mounting element easily placed within the bioreactor.

5.4.5 Overall Bioreactor Design and Testing:

Aside from the specific mounting system for the mitral apparatus, several other design criteria were used or modified from the aortic valve bioreactor. Readouts and raw data on flow rate, heart rate, atrial pressure and ventricular pressure are monitored using flow meters and pressure transducers. The pressure transducers are located next to chambers that mimic conditions in the atrium of the heart and the ventricle of the heart. Unique to the mitral valve bioreactor is an extra chamber attached to the ventricular chamber to add room for the chordal attachment on the valve mounting system. Also, as noted, the atrial chamber for the mitral valve bioreactor is shorter to allow for the very low pressures experience in the atrium. To ensure continued coaptation of the valve in case of a spring failure, a suture ring was wrapped around one bar of the mounting system and the papillary muscles. Enough slack was allowed in this suture ring so as not to interfere with

the movement of the papillary muscles or the corresponding chordae. The valve pressures overtime were slowly increased to allow time for adaptation and maturation of the seeded cells. During this pressure ramp-up, the leaflets open and closed properly throughout indicating that the chordae were providing enough pull-back on the leaflets for proper function.

5.4.6 Mechanical Testing of the Bioreactor Treated Leaflets:

A comparison between seeded and preconditioned leaflets from the bioreactor and a seeded, static control was completed. From **Figure 5.6**, it is shown that the modulus of elasticity for the static control is higher than that for the preconditioned tissue. This difference however is not statistically significant. We believe the explanation for this difference however is due to the forces and repetitious extension this valve underwent in the bioreactor. These forces acted on the collagen and elastin matrix, most likely straightening out these fibers over time.

5.4.7 Histological Characterization of the Seeded Mitral Valve Tissues:

After removal from the bioreactor, several histological stains were performed to gain insight into how the cells reacted to the physiological conditions in the bioreactor and compare these with the static control. As evidenced by **Figure 5.8**, an H&E, DAPI, Masson's Trichrome, and Movat's Pentachrome were performed. Unfortunately, cells spreading throughout the matrix was not nearly as successful as the pilot studies discussed earlier. While more cells were present and in larger areas in the preconditioned leaflets, boluses were still found in both groups. Each histological stain shows these boluses within the leaflets. The only condition that differed between the seeding results discussed

previously and these results from the bioreactor was the treatment with PGG. It is possible that while PGG possesses many properties that have provided significantly improved the quality of the mitral valve scaffold, that it may also be hindering migration of seeded cells. We have mentioned previously that PGG stabilized the scaffold by binding to the collagen and elastin. This increased the young's modulus for all PGG-treated tissues. This increase could be making it physically impossible for the cells to spread from the injection sites. Perhaps in the future, steps should be taken to porate the scaffold before treatment with PGG to allow a stable scaffold, which also provides avenues for cellular infiltration.

Regardless of the lack of migration within the tissue, the pentachrome stain did indicate the deposition of GAGs within the scaffold, which is a marked improvement. Also of note are the possibility that some endothelial cells did survive the shear stresses from the bioreactor treatment. While it is apparent that most of these externally seeded cells did not attach or survive, here is some evidence here that certain areas of construct did retain the pre-differentiated endothelial cells. Future work should be placed in furthering the ability to keep these cells attached to the surface.

5.4.8 Evaluation of Differentiation and Activation of Seeded Cells:

As mentioned, VICs and VECs are the ideal source of cells for mitral valve scaffold repopulation. Pre-differentiated fibroblasts and endothelial cells were seeded into and onto the scaffolds respectively. To evaluate their continued differentiation or activation several IHC's were conducted looking at smooth muscle cell markers for activated fibroblasts, fibroblast markers, and of course endothelial cell markers. These can be seen in **Figure**

5.9-5.11. It is important to note that literature has not provided a sure means of identifying VICs. However, many papers insist that due to their similarity to fibroblasts, that these markers are suitable. Also, markers for smooth muscle cells are indicative of fibroblasts that are activated. In the mitral valve these cells, called aVICs, or activated VICS, are important players in several mitral valve pathologies as they can quickly deposit ECM, which easily disrupts normal valve function. At the injections sites, a slight positive stain was found for α-SMA and calponin as seen in **Figure 5.9**. In contrast to these faint stains, expression of fibroblast markers vimentin, HSP-47, and prolyl-4-hydroxylase were quite strong as shown in **Figure 5.10**. This would suggest that most of the interstitially seeded cells remained quiescent and non-active despite all of the forces they experienced. Lastly, for any remaining endothelial cells, expression of vWF, VE cadherin, and iNOS were evaluated. While few in number, **Figure 5.11** clearly shows some expression of these endothelial markers on both the leaflets and the chordae. This is positive that some endothelial cells were able to resist detachment even at physiological pressures.

5.5 Conclusion:

The paradigm of tissue engineering in which we model and operate under, describes the combination of scaffold, cells, and bioreactor to develop a living construct capable of regenerating diseased tissues. As scaffold characterization was described in great detail, it was then time to turn to the implementation of cells into the scaffolds and precondition these constructs in the bioreactor. Recellularization remains a difficult barrier to cross. As mentioned earlier, many criteria must be evaluated for a proper and translatable

recellularization strategy. Cells will eventually repopulate a scaffold if given time. However, as many papers have reported this process taking months, the time required for revitalization of the scaffold is not acceptable for patients in great need of a tissue engineered replacement. By directly injecting cells into the scaffold, cells can be incorporated immediately; however, these cells often do not migrate from these injection sites and create boluses of cells. To combat this, we incorporated a well-known hydrogel, fibrin, with great cell attachment properties as a carrier for the cells. We also utilized SDF-1, a potent cytokine, to encourage migration into the scaffolds. Overall, this process greatly improved the recellularization effort in the mitral valve scaffold.

To disallow seeded cells time to adapt to a harsh heart valve environment before implantation invites sure failure of the construct. Therefore, a mitral valve bioreactor was developed and modified from an aortic valve bioreactor to provide physiologic conditions for the seeded construct. Shape and function of each distinct tissue type had to be considered, none more than the unique annular shape and the need for tension in the chordae tendinae. By recreating a mitral valve annulus for mounting of the valve, optimal force distribution could be achieved during bioreactor testing. In addition, by using a spring and attachment system for the chordae, tension could be felt through the chordae through to the leaflets, providing correct anatomical cues to seeded cells and the ECM. Evaluation of the constructs post-bioreactor showed limited migration of the cells throughout the tissue. This could be a result of PGG stabilization creating a scaffold too strong to allow cells to physically migrate into. Therefore, PGG's role in this process should be evaluated. In addition, slight poration of the tissue may provide the necessary avenues for which cells

can travel. Despite this insufficiency, IHCs for various markers showed a significant expression for fibroblast markers and only a slight positive stain for smooth muscle cell markers indicating that these cells were not activated and remained mostly quiescent during the bioreactor process. Also important to note were the existence, while small in quantity, of endothelial cells along the leaflets and chordae. Positive stainings for several endothelial markers were found for preconditioned tissues.

5.6 References:

1. Mendelson, K. & Schoen, F. J. Heart valve tissue engineering: concepts, approaches, progress, and challenges. *Ann. Biomed. Eng.* **34,** 1799–819 (2006).
2. Voges, I. *et al.* Adverse results of a decellularized tissue-engineered pulmonary valve in humans assessed with magnetic resonance imaging. **44,** 272–279 (2013).
3. Fioretta, E. S., Dijkman, P. E., Emmert, M. Y. & Hoerstrup, S. P. The future of heart valve replacement: recent developments and translational challenges for heart valve tissue engineering. *J. Tissue Eng. Regen. Med.* (2016). doi:10.1002/term.2326
4. Amrollahi, P. & Tayebi, L. Bioreactors for Heart Valve Tissue Engineering: A Review. *J. Chem. Technol. Biotechnol.* **49,** n/a-n/a (2015).
5. Liu, A. C., Joag, V. R. & Gotlieb, A. I. The emerging role of valve interstitial cell phenotypes in regulating heart valve pathobiology. *Am. J. Pathol.* **171,** 1407–18 (2007).
6. Chester, A. H. & Taylor, P. M. Molecular and functional characteristics of heart-valve interstitial cells. *Philos. Trans. R. Soc. Lond. B. Biol. Sci.* **362,** 1437–43 (2007).
7. Taylor, P. M., Batten, P., Brand, N. J., Thomas, P. S. & Yacoub, M. H. The cardiac valve interstitial cell. *Int. J. Biochem. Cell Biol.* **35,** 113–8 (2003).
8. Brand, N. J., Roy, A., Hoare, G., Chester, A. & Yacoub, M. H. Cultured interstitial cells from human heart valves express both specific skeletal muscle and non-muscle markers. *Int. J. Biochem. Cell Biol.* **38,** 30–42 (2006).
9. Blevins, T., Peterson, S. & Lee, E. Mitral valvular interstitial cells demonstrate regional, adhesional, and synthetic heterogeneity. *Cells Tissues …* **187,** 113–122 (2008).
10. Fayet, C., Bendeck, M. & Gotlieb, A. Cardiac valve interstitial cells secrete fibronectin and form fibrillar adhesions in response to injury. *Cardiovasc. Pathol.* **16,** 203–211 (2007).
11. Grande-Allen, K. J. & Liao, J. The heterogeneous biomechanics and mechanobiology of the mitral valve: implications for tissue engineering. *Curr.*

Cardiol. Rep. **13,** 113–20 (2011).
12. Gould, S. T., Matherly, E. E., Smith, J. N., Heistad, D. D. & Anseth, K. S. The role of valvular endothelial cell paracrine signaling and matrix elasticity on valvular interstitial cell activation. *Biomaterials* **35,** 3596–606 (2014).
13. Hjortnaes, J. *et al.* Directing Valvular Interstitial Cell Myofibroblast-Like Differentiation in a Hybrid Hydrogel Platform. *Adv. Healthc. Mater.* 1–10 (2014). doi:10.1002/adhm.201400029
14. Han, L. & Gotlieb, A. I. Fibroblast growth factor-2 promotes in vitro mitral valve interstitial cell repair through transforming growth factor-β/Smad signaling. *Am. J. Pathol.* **178,** 119–27 (2011).
15. Duan, B., Hockaday, L. A., Kapetanovic, E., Kang, K. H. & Butcher, J. T. Stiffness and adhesivity control aortic valve interstitial cell behavior within hyaluronic acid based hydrogels. *Acta Biomater.* **9,** 7640–7650 (2013).
16. Stephens, E. H., Durst, C. a, West, J. L. & Grande-Allen, K. J. Mitral valvular interstitial cell responses to substrate stiffness depend on age and anatomic region. *Acta Biomater.* **7,** 75–82 (2011).
17. Rabkin-Aikawa, E., Farber, M., Aikawa, M. & Schoen, F. J. Dynamic and reversible changes of interstitial cell phenotype during remodeling of cardiac valves. *J. Heart Valve Dis.* **13,** 841–7 (2004).
18. Rabkin, E. *et al.* Activated Interstitial Myofibroblasts Express Catabolic Enzymes and Mediate Matrix Remodeling in Myxomatous Heart Valves. *Circulation* **104,** 2525–2532 (2001).
19. Gimble, J. M., Katz, A. J. & Bunnell, B. a. Adipose-derived stem cells for regenerative medicine. *Circ. Res.* **100,** 1249–60 (2007).
20. Gimble, J. & Guilak, F. Adipose-derived adult stem cells: isolation, characterization, and differentiation potential. *Cytotherapy* **5,** 362–9 (2003).
21. Zuk, P. Review Article Adipose-Derived Stem Cells in Tissue Regeneration : A Review. *ISRN Stem Cells* **2013,** 1–36 (2013).
22. Surgery, R., Force, D. & Yokosuka, H. Concise Review : Adipose-Derived Stem Cells as a Novel Tool for Regenerative Medicine. *Stem Cells* **30,** 804–810 (2012).
23. Francesco, F. De, Ricci, G., Andrea, F. D., Nicoletti, G. F. & Ferraro, G. A. Human Adipose Stem Cells : From Bench to Bedside. *Tissue Eng. Part B* **21,** 572–585 (2015).
24. Zuk, P., Zhu, M. & Ashjian, P. Human adipose tissue is a source of multipotent stem cells. *… Biol. cell* **13,** 4279–4295 (2002).
25. Tedder, M. & Simionescu, A. Assembly and testing of stem cell-seeded layered collagen constructs for heart valve tissue engineering. *… Eng. Part …* **17,** (2010).
26. Huang, W. *et al.* Fn14 promotes differentiation of human mesenchymal stem cells into heart valvular interstitial cells by phenotypic characterization. *J. Cell. Physiol.* 1–20 (2013). doi:10.1002/jcp.24480
27. Badylak, S. F., Taylor, D. & Uygun, K. Whole Organ Tissue Engineering:

Decellularization and Recellularization of Three-Dimensional Matrix Scaffolds. *Annu. Rev. Biomed. Eng.* **13,** 110301095218061 (2010).
28. Fu, R. *et al.* Review Decellularization and Recellularization Technologies in Tissue Engineering. *Cell Transplant.* **23,** 621–630 (2014).
29. Villalona, G. A. *et al.* Cell-Seeding Techniques in Vascular Tissue Engineering. *Tissue Eng. Part B* **16,** (2010).
30. Lee, K., Silva, E. a & Mooney, D. J. Growth factor delivery-based tissue engineering: general approaches and a review of recent developments. *J. R. Soc. Interface* **8,** 153–170 (2011).
31. Momtahan, N., Sukavaneshvar, S. S. T. C., Roeder, B. L. & Cook, A. D. Strategies and processes to decellularize and recellularize hearts to generate functional organs and reduce the risk of thrombosis. *Tissue Eng. Part B. Rev.* 1–58 (2014). doi:10.1089/ten.TEB.2014.0192
32. Kennamer, A. *et al.* Bioreactor Conditioning of Valve Scaffolds Seeded Internally with Adult Stem Cells. 507–515
33. Rybalko, V. Y. *et al.* Controlled delivery of SDF-1α and IGF-1: CXCR4 $^{+}$ cell recruitment and functional skeletal muscle recovery. *Biomater. Sci.* **3,** 1475–1486 (2015).
34. Tayalia, P. & Mooney, D. J. Controlled growth factor delivery for tissue engineering. *Adv. Mater.* **21,** 3269–85 (2009).
35. Mesenchymal, H. *et al.* Effect of Needle Diameter and Flow Rate. **16,** (2010).
36. Matter, S., Guvendiren, M., Lu, H. D. & Burdick, J. A. Shear-thinning hydrogels for biomedical applications. (2012). doi:10.1039/c1sm06513k
37. Brown, A. C. & Barker, T. H. Fibrin-based biomaterials : Modulation of macroscopic properties through rational design at the molecular level. *Acta Biomater.* **10,** 1502–1514 (2014).
38. Zhao, H., Gong, Y., Gao, C. & Shen, J. A polylactide / fibrin gel composite scaffold for cartilage tissue engineering : fabrication and an in vitro evaluation. 135–143 (2009). doi:10.1007/s10856-008-3543-x
39. Ahmed, T. a E., Dare, E. V & Hincke, M. Fibrin: a versatile scaffold for tissue engineering applications. *Tissue Eng. Part B. Rev.* **14,** 199–215 (2008).
40. Mol, A. *et al.* Fibrin as a cell carrier in cardiovascular tissue engineering applications. *Biomaterials* **26,** 3113–3121 (2005).
41. Sahni, A., Francis, C. W. & Dc, W. Vascular endothelial growth factor binds to fibrinogen and fibrin and stimulates endothelial cell proliferation Vascular endothelial growth factor binds to fibrinogen and fibrin and stimulates endothelial cell proliferation. **96,** 3772–3778 (2013).
42. Rhee, S., Ho, C. & Grinnell, F. Promigratory and procontractile growth factor environments differentially regulate cell morphogenesis. *Exp. Cell Res.* **316,** 232–244 (2009).
43. Martino, M. M., Briquez, P. S., Ranga, A., Lutolf, M. P. & Hubbell, J. a. Heparin-

binding domain of fibrin(ogen) binds growth factors and promotes tissue repair when incorporated within a synthetic matrix. *Proc. Natl. Acad. Sci. U. S. A.* **110,** 4563–8 (2013).
44. Hsieh, J. Y. *et al.* Differential regulation of macrophage inflammatory activation by fibrin and fibrinogen. *Acta Biomater.* **47,** 14–24 (2017).
45. Li, Y., Meng, H., Liu, Y. & Lee, B. P. Fibrin gel as an injectable biodegradable scaffold and cell carrier for tissue engineering. *Sci. World J.* **2015,** (2015).
46. Il, W., Yameen, B., Vilos, C. & Sahu, A. Optimization of fibrin gelation for enhanced cell seeding and proliferation in regenerative medicine applications. (2017). doi:10.1002/pat.3866
47. Caiado, F. *et al.* The role of fibrin E on the modulation of endothelial progenitors adhesion, differentiation and angiogenic growth factor production and the promotion of wound healing. *Biomaterials* **32,** 7096–7105 (2011).
48. Sierad, L. N. *et al.* Design and Testing of a Pulsatile Conditioning System for Dynamic Endothelialization of Polyphenol-Stabilized Tissue Engineered Heart Valves. *Cardiovasc. Eng. Technol.* **1,** 138–153 (2010).
49. Silbiger, J. J. & Bazaz, R. Contemporary insights into the functional anatomy of the mitral valve. *Am. Heart J.* **158,** 887–95 (2009).
50. Silbiger, J. J. Anatomy, mechanics, and pathophysiology of the mitral annulus. *Am. Heart J.* **164,** 163–76 (2012).
51. Timek, T. a *et al.* Annular height-to-commissural width ratio of annulolasty rings in vivo. *Circulation* **112,** I423-8 (2005).
52. Jensen, M. O. *et al.* Saddle-shaped mitral valve annuloplasty rings experience lower forces compared with flat rings. *Circulation* **118,** S250-5 (2008).
53. Jimenez, J. H., Soerensen, D. D., He, Z., He, S. & Yoganathan, A. P. Effects of a saddle shaped annulus on mitral valve function and chordal force distribution: An in vitro study. *Ann. Biomed. Eng.* **31,** 1171–1181 (2003).
54. Salgo, I. S. *et al.* Effect of Annular Shape on Leaflet Curvature in Reducing Mitral Leaflet Stress. *Circulation* **106,** 711–717 (2002).
55. Marquez-Curtis, L. A. & Janowska-Wieczorek, A. Enhancing the migration ability of mesenchymal stromal cells by targeting the SDF-1/CXCR4 axis. *Biomed Res. Int.* **2013,** (2013).
56. Zhou, J. *et al.* Development of decellularized aortic valvular conduit coated by heparin-sdf-1α multilayer. *Ann. Thorac. Surg.* **99,** 612–618 (2015).
57. Yu, J., Sievers, R. E. & Lee, R. J. Effects of scaffold-delivered SDF-1 alpha protein in chronic rat myocardial infarction model. *J. Med. Biol. Eng.* **34,** 224–229 (2014).
58. Whelan, D., Caplice, N. M. & Clover, A. J. P. Fibrin as a delivery system in wound healing tissue engineering applications. *J. Control. Release* **196,** 1–8 (2014).
59. Barzilla, J. E., McKenney, A. S., Cowan, A. E., Durst, C. a & Grande-Allen, K. J. Design and validation of a novel splashing bioreactor system for use in mitral valve organ culture. *Ann. Biomed. Eng.* **38,** 3280–94 (2010).

60. Ritchie, J., Warnock, J. N. & Yoganathan, A. P. Structural characterization of the chordae tendineae in native porcine mitral valves. *Ann. Thorac. Surg.* **80,** 189–197 (2005).
61. Mahmood, F. *et al.* Mitral annulus: an intraoperative echocardiographic perspective. *J. Cardiothorac. Vasc. Anesth.* **27,** 1355–63 (2013).
62. Mahmood, F. *et al.* Three-dimensional echocardiographic assessment of changes in mitral valve geometry after valve repair. *Ann. Thorac. Surg.* **88,** 1838–44 (2009).

CHAPTER SIX: CONCLUSIONS AND RECOMMENDATIONS FOR FUTURE WORK

6.1 Summary of Project Development:

There is a clear and significant gap in our ability to care for patients with cardiovascular diseases. On the whole, cardiovascular disease is the largest consumer of human life in the country. Overall, cardiovascular disease cost the United States about $316.1 billion in 2013. By 2030, this cost is expected to rise to about $918 billion. By this time, almost half of the population of the United States is expected to have some form of cardiovascular disease[1]. Diseases and deficiencies of the mitral valve affect a large percentage of those sufferers. In fact, of all patients with valvular diseases, 72% have a mitral valve disease[1]. As is evident, mitral valve disease is a frequent cause of heart failure and death[2]. The age of the patient is also a critical factor. Most mitral valve diseases are associated with some form of degeneration with leads to a malfunctioning heart valve. Therefore, older patients, those 75 and older, are especially affected. In fact, about 10% of the US population has mitral regurgitation[1,3]. The elderly however are not the only patient group suffering from mitral valve diseases. Mitral stenosis, caused by acute rheumatic fever, is the leading cause of heart disease in children worldwide[4]. Prosthetic heart valves have remained a constant in patient care, however their design and the issues that follow them have largely lasted unchanged since their conception in the 1960's. Repair of the mitral valve has shown improved success, however results are palliative and revisional surgery is often required to re-repair the dysfunctional heart valve.

The limitations of treatment and lack of permanent solutions available to patients represented an enormous opportunity to innovate. Within the paradigm of tissue engineering, we set to develop a novel yet translational approach to replace the diseased mitral valve with a living construct, thereby allowing patient-tailored tissue regeneration of the valve. Successful strategies as well as failed designs were reviewed and studied not only in heart valve tissue engineering but across the entire field to develop our unique approach. We sought to develop a stable, fully recellularized and mechanically preconditioned tissue engineered mitral valve construct. Our tissue engineered valve criteria demanded a design that allowed for repopulation with cells and remodeling of an ECM scaffold derived from porcine tissue. This scaffold had to withstand appropriate mechanical pressures and degradation from proteases. All of this of course using translational approaches that would allow an easy adaptation from the lab bench to the hospital bedside.

6.2 Progress Toward Achievement of Specific Aims:

In an attempt to lessen this clear gap in patient care mentioned above, three overlaying and specific aims were established to direct our research towards a permanent tissue engineered solution. While these aims were discussed in more detail in Chapter Two, they are presented here in brief:

Aim 1 *(Chapter 3)***: Develop an acellular scaffold with ECM and mechanical properties similar to the human mitral valve.**

Hypothesis*: A detergent based decellularization method will remove all cellular materials from a porcine mitral valve while retaining sufficient extracellular matrix*

content, including basal lamina proteins. Chemical treatment with PGG will stabilize the matrix scaffold and yield physiologically similar mechanical strength.

Aim 2 *(Chapter 4)***: To characterize host response and determine resistance to degradation of the scaffold treated with PGG.**

Hypothesis*: The stabilizing, anti-inflammatory, anti-calcification function of PGG will limit scaffold degradation and mitigate immune rejection.*

Aim 3 *(Chapter 5)***: Develop a mitral valve bioreactor able to provide physiological loading and biochemical environment characteristic to mitral valves.**

Hypothesis: *Optimally seeded constructs will flourish under physiologic conditions provided by a bioreactor that provides correct anatomical positioning and force distribution from annulus to papillary muscles.*

Each of these aims add cohesively towards the development of a tissue engineered mitral valve. Each has been discussed at length in the above chapters, but a summary of the work and major takeaways from each chapter is as follows:

6.2.1 Aim 1 (Chapter 3): Develop an acellular scaffold with ECM and mechanical properties similar to the human mitral valve:

1. We developed and optimized a decellularization process that removed all cellular and nuclear material from the scaffold. Histological analysis showed complete removal of xenogeneic cells and gel electrophoresis and nanodrop show significant removal of nuclear material. We showed levels less than 50ng/dry tissue of nuclear material remaining in our scaffold, which is under the acceptable limit established in literature.

2. After development of an acellular mitral valve scaffold, we sought to characterize the scaffold and evaluate the effects the decellularization process had on the niche ECM. Overall, the ECM was well preserved, with all four layers of the heart valve visibly present and intact. We were not able to retain GAGs post decellularization. However, we were able to conserve basal lamina proteins collagen type IV and laminin which are essential for cell attachment and migration.
3. Further characterization of the mitral valve scaffold showed that decellularization did have an effect on the mechanical properties of the scaffold when compared to fresh tissue. PGG, a well-known and well-characterized polyphenol, was used to shore up any lost mechanical strength during decellularization. As a result, mechanical properties returned significantly closer to fresh mechanical properties.
4. PGG was also used as a treatment for the scaffold to evaluate the scaffolds potential for degradation when in the presence of proteases. If implanted in vivo, our scaffold would inevitably be encountered by similar proteases and therefore we evaluated our scaffolds at 24 and 48 hours in treatments of collagenase and elastase. PGG significantly improved the resistance of the scaffold to degradation.
5. Lastly, the scaffold was evaluated on its potential for allowing cell growth and proliferation. Cytocompatibility results turned out positive in that cells were able to survive within and on the scaffold. It was also shown that cells could in fact be incorporated within the scaffold via direct injection. This proved vital for the other aims in the project.

6.2.2 Aim 2 (Chapter 4): To characterize host response and determine resistance to degradation of the scaffold treated with PGG:

1. Host response to an implanted biomaterial is perhaps the most important determinant of success or failure of the implant. After conducting4 and 8 week time points with PGG-treated and non-treated groups we evaluated how these once acellular scaffolds degraded overtime. In looking at MMP levels within the tissue, there was a significant difference between the PGG and non-treated tissues. PGG-treated scaffolds showed much less expression of MMPs, indicating a much lower rate of degradation.
2. The microstructure of our ECM scaffold is perhaps its most important feature. Therefore, we sought to evaluate its preservation after implantation. Histological results indicate that the ECM was highly preserved at both time points. Clear fibers and layers of collagen and elastin were present.
3. Infiltration with autologous cells from the host are inevitable. Therefore, we wanted to evaluate if PGG affected the ability of these cells to infiltrate the scaffolds and begin remodeling of the tissue. We found no significant difference between treatment groups at both time points. PGG did not have an effect on cells' ability to infiltrate the scaffolds.
4. An inflammatory response was investigated using CD8, a marker for T-cell lymphocytes. Non-treated scaffolds showed a significantly higher expression of CD8 than PGG-treated groups at both time points. This is not to say that CD8 expression in PGG groups was eliminated but the expression of the pro-

inflammatory marker was significantly lower. Accordingly, PGG is able to decrease infiltration of CD8-positive cells, hindering inflammation.

5. Next, we wanted to identify the cell types that had infiltrated the scaffold. In PGG-treated samples expression of fibroblast markers, vimentin, prolyl-4-hydroxylase, and HSP-47 all showed significantly higher expression when compared to non-treated groups. In the non-treated groups, expression of smooth muscle cell markers α-SMA, calponin, and SM22 showed significantly higher expression compared to the PGG-treated groups. PGG seems to encourage fibroblast infiltration as opposed to smooth muscle cells. On the other hand, perhaps both scaffolds allow for fibroblast infiltration, but PGG is able to hinder their activation into myofibroblasts.
6. Lastly, we wanted to understand PGG's effect on macrophage polarization. M1, the pro-inflammatory macrophage, showed significantly higher expression in the non-treated groups. The opposite was true for PGG-treated groups. M2, the pro-healing macrophage, showed significantly higher expression in PGG-treated groups. Therefore, PGG encourages M2 macrophage polarization as opposed to the pro-inflammatory M1 macrophage.

6.2.3 Aim 3 (Chapter 5): Develop a mitral valve bioreactor able to provide physiological loading and biochemical environment characteristic to mitral valves:

1. In a cumulative effort to revitalize the acellular scaffold with cells, the reseeding strategy needed to be more effective. In an effort to avoid creation of boluses of cells within the scaffold, fibrin, a well-known hydrogel, was used to assist in the seeding efficiency as well as a means to aid in migration of the cells into the

scaffold. Also utilized to coax cell migration was the cytokine SDF-1. Efforts for a more efficient recellularization were largely successful. Cells noticeably migrated from the injection site into the tissue.

2. Prior to this work, our group developed an aortic valve bioreactor, which provided a sterile environment for testing aortic valves at physiological conditions. The mitral apparatus having a unique structure required several design points that had to be addressed to produce a functioning bioreactor. A system to mount a recellularized mitral valve construct into a bioreactor was designed based on the particular shape of the mitral annulus. Using this as the foundation for optimal force distribution, attachment of the chordae tendinae was also addressed. Springs were chosen and wrapped around the papillary muscles to provide appropriate tension required for physiological testing.
3. Overall, the bioreactor and the tissue inside of it ran well. The valve was able to properly open and close at physiological pressures. These pressures were slowly ramped up for several weeks to assure cell maturation, migration, and differentiation. Sterility of the bioreactor was maintained throughout as well as conditions such as temperature, CO_2 levels and humidity.
4. After histological analysis, cells were found within the constructs in both the bioreactor tissue as well as the static control. More cells were found within the bioreactor-seeded constructs. There is a possibility that some of the endothelial cells that were seeded on the outside of the scaffolds were able to survive the

physiological pressures that the valves endured. Seeding efficiency with the use of PGG as well the added forces in the bioreactor was significantly lessened.

5. Several markers for fibroblasts and smooth muscle cells were used to evaluate the phenotypes of the cells after being placed in the bioreactor. While results showed positive markers for both, fibroblast markers showed significantly stronger than the smooth muscle cell markers. This implies that the majority of the seeded pre-differentiated fibroblasts remained quiescent ever during bioreactor testing.

6.2.4 Prospective on Progress Made and Comments on Potential Continued Research:

The studies and aims described here were modeled after the general tissue engineering paradigm in an attempt to successfully combine an ECM scaffold, appropriate cell types and a condition this living construct in a bioreactor. Three aims were established from this paradigm and significant progress was achieved if not completed with each aim. Aim 1 and 2, largely based on scaffold characterization both in vitro and in vivo, are mostly complete. The scaffold itself, along with PGG treatment, yielded successful results in creating a stable scaffold capable of supporting cellular proliferation. More studies continuing to analyze PGG's role and longevity within the scaffold would prove to be useful information for Aim 1. In addition, the in vivo reaction towards the scaffold was successful in limiting an inflammatory response and as a result directing macrophage polarization towards a pro-healing phenotype. Continued studies of host response may lead to a better understanding of PGG's biochemical role in direction macrophage polarization as well as its hindrance of inflammatory markers. Further studies may highlight PGG's longevity in vivo as well. Information could also be extrapolated here in understanding cell

migration into the scaffold. This information could be used to optimize cell-seeding experiments in the future.

Development of the mitral valve bioreactor presented several difficulties due to the complexity of the mitral apparatus. With its hyperbolic paraboloid shape, the mitral annulus forms the foundation for force distribution. From this particular geometry, and fitting this to the other existing bioreactor system, originally fit for the aortic valve, was difficult. Despite these, coaptation of the valve was achieved and we believe optimal force distribution was as well. However, significant improvements could be made to optimize the process by which the mitral valve bioreactor is set up and run during experimentation. These could include an easier mechanism for mounting the valve in the mounting rings and attachment of the papillary muscles and chordae to this as well. Despite these challenges, this system, now equipped for the mitral valve, should become a valuable tool in working toward completion of Aim 3. Recellularization of the scaffolds to create a living valve also proved difficult despite the advances made using fibrin as a seeding conduit. More evaluation should be taken as to why migration out of the scaffold did not occur. And if it did in fact occur, why did these cells not survive the bioreactor process? Overall, as studies continue, avoidance of a bolus of cells within the constructs and encouragement of cell migration should be prioritized.

Regardless of the directions this project will take, overall it is the belief of this author that the studies and progress herein have had a positive impact upon the development of a tissue engineered mitral valve. This valve, whose pathological prevalence is evident, needs a tissue engineered solution in the future to provide permanent and patient specific solution.

6.3 Recommendations for Future Work:

6.3.1 Aim 1:

As previously mentioned the goals set in Aim 1 were largely completed. Characterization of the scaffold proved that we were able to sufficiently remove xenogeneic cellular and nuclear material while still preserving the ECM. Cells were also able to survive within on the exterior of the scaffold. Moving forward, quantifiable characterization of the scaffold should be acquired. Several methods can be used to quantify the amount of collagen and elastin in scaffolds. This should be done and compared to fresh vs. decellularized scaffolds for both leaflets and chordae tendinae. In addition, while not examined before, levels of fibronectin should be explored as well to confirm further existence of basal lamina proteins present after decellularization. Most of the IHC's used to establish preservation of ECM quality, should be quantified as done in Chapter 2 to compare fresh vs. decellularized scaffolds. Also worth evaluating would be to examine our current decellularization protocol and seek further optimization of this process. Some groups are able to completely decellularize their heart valve scaffolds without removing GAG content which would be of serious benefit moving forward[5]. Therefore, we believe that the decellularization protocol, while it has proven successful by most current parameters, could always be improved.

The following is a suggested study to establish a better understanding of PGG's staying power within the scaffolds. This information, which is regularly requested by other researchers, would provide some insight into how the scaffold retains PGG over time.

6.3.1.1 In Vitro Longevity of PGG within Decellularized Scaffolds

6.3.1.1.1 Scaffold Preparation and Design

Decellularization of the scaffolds will utilize the protocol described in Chapter 3. After the decellularization process is complete, four groups will be established at differing concentrations of PGG. See **Figure 6.1** for the study design. Concentrations of zero PGG (treated with sterile 1 x PBS), 0.15% PGG, 0.3% PGG, and 0.6% PGG will be used on four scaffolds (using an n=6 for each of these groups). Treated leaflets can be placed in 6-well plates and covered with basic cell culture media (DMEM, 10% FBS, and 1% AbAm). These treated scaffolds will be placed on a shaker at low speeds and allowed to shake for several weeks. Media will be changed regularly for each group and saved to evaluate leeching of PGG into the media. For each group we will collect samples at each week for 4 weeks. At these time points, histological evaluation will be used to determine any loss of PGG within the scaffolds. Mechanical data could also be obtained from each of these time points.

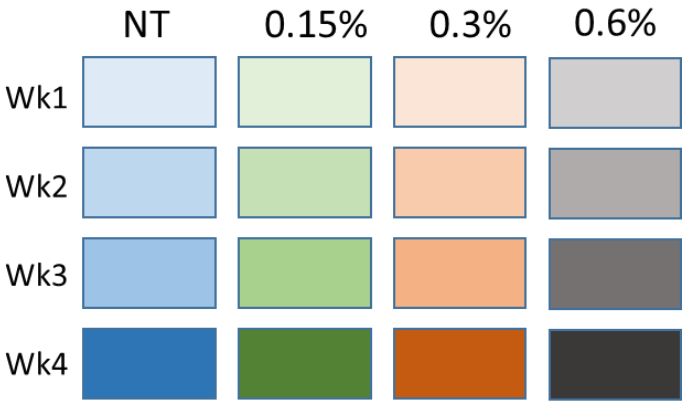

Figure 6.1: Design for Evaluation of PGG Retention in Scaffolds. Several concentrations of PGG as well as a negative control could be used to evaluate PGG's staying power within the decellularized scaffolds. Each of these groups (n=6) will be evaluated at four different time points.

6.3.2 Aim 2:

Biocompatibility and host response are critical barriers that a biomaterial must pass to be successful. Overall, in Aim 2, it was shown that our PGG-treated scaffolds limited inflammatory responses, had decreased degradation, and polarized macrophages towards the M2 phenotype. While these benchmarks were considerable and overall successful, there are a number of IHC and IF stainings that could be done to look further at other areas of interest. In further studies, we would particularly like to look further into how PGG decreases expression of TNF-α in these constructs. This well-known, pro-inflammatory cytokine is expressed by M1 macrophages as well encouraging other macrophages to polarize towards the M1 phenotype. PGG, a well-characterized phenotype has shown antioxidant properties. Antioxidants have shown to decrease expression of TNF-α[6,7]. Also important in macrophage polarization is the production of ROS. These reactive oxygen species can damage tissue if over expressed, but due to their presence in tissue play an important role in changing the macrophage phenotype from M1 to M2. However, antioxidants are known to cleave ROS production, leaving one to question how, if expression of ROS eventually leads to the M2 phenotype, how then would decreased levels of ROS due to treatment with PGG, lead to the M2 macrophage[7]. This conundrum would be worth evaluating and would provide key details into how PGG biochemically affects inflammation and macrophage polarization.

It might also be interesting to evaluate what stems cells, if any, infiltrated the scaffold. An IHC for CD34 or CD29 could be used to identify mesenchymal stem cells infiltrating into the scaffold. Other signs of inflammation, other than CD8 and CD68 could

be evaluated. In Aim 3, fibrin was used as a cell-seeding conduit. Fibrin has also been shown to discourage the M1 phenotype. Seeded scaffolds with fibrin and autologous rat cells could provide an interesting insight into this study and its combined anti-inflammatory effort with PGG[8]. Knowing this, there are several different groups that could be tested using a similar biocompatibility study that was done in Aim 2.

The following is a suggested study to further evaluate PGG's role in diminishing inflammation and encouraging M2 macrophages. This study would also be used to determine how fibrin, as a cell carrier for seeding, acts in vivo. We would also seed these scaffolds without fibrin to determine if any differences take place after the study.

6.3.2.1 Study Design and Groups:

The design parameters will be similar to the subdermal rat study conducted and described in Aim 2. In accordance with an IACUC-approved animal use protocol, juvenile Sprague-Dawley rats will be anesthetized with buprenorphine at 0.03-0.05 mg/kg and acepromazine at 0.5 mg/kg administered subcutaneously. A small incision will be made in the center of the dorsal area of each rat about 2 cm inferior to the scapulae, and, using blunt dissection, two pockets created between the dermis and fascia lateral to the incision (one pocket in each direction). A scaffold sample will placed into each pocket, and the incision closed using staples. Rats will receive non-treated, decellularized scaffolds, and the remaining will receive PGG-treated decellularized scaffolds. This will be true for each overarching group of which there are four. The first group will comprise of acellular scaffolds, the second will be scaffolds seeded with autologous ADSC's taken from the rats previously, the third group will have the same cell types seeded using fibrin, and the fourth

group will also utilize fibrin, but the cells will be pre-differentiated into fibroblasts and endothelial cells. This is true for both tissue types, mitral valve leaflet and chordae tendinae. Rats would be allowed to recover and housed individually for the remainder of the study. At 4 weeks rats will be euthanized and at 8 weeks, the remaining rats will be euthanized, both via CO2 gas (Euthanex system) followed by pneumothorax. Scaffold samples and small amounts of their adjacent host tissues will be excised and fixed in 10% neutral buffered formalin and processed for histological examination.

In **Figure 6.2**, the one group example is shown. This map would be the same for each of the four groups, which reiterated are:

1. Decellularized scaffolds
2. Scaffolds recellularized with autologous rat ADSCs
3. Scaffolds recellularized with autologous rat ADSCs using fibrin as a carrier
4. Scaffolds recellularized with pre-differentiated autologous rat ADSCs using fibrin as a carrier.

From these four groups and time points, we will be able to evaluate further how our final scaffolds, seeded with cells would survive in vivo.

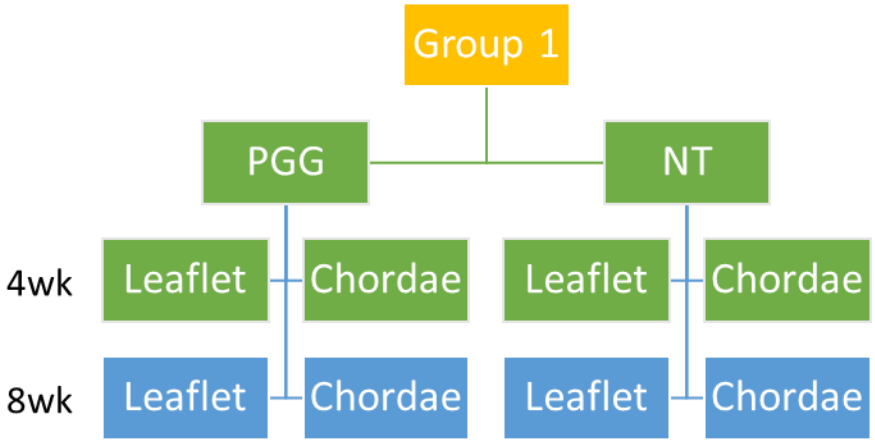

Figure 6.2: Schematic Design of Group Organization. Each of the identified groups would utilize this organizational map. Each group has PGG-treated and non-treated groups, time points at both 4 and 8 weeks, and each of these uses both leaflets and chordae scaffolds.

6.3.2.1.1 Scaffold Preparation:

All scaffolds will be prepared using the decellularization protocol described in Aim 1. Before implantation, the samples were sterilized in 0.1% (w/v) peracetic acid in PBS for 1h, followed by rinsing in four changes of sterile PBS. Sterile PGG treatment will use a concentration of 0.3% as seen in each aim described.

6.3.2.1.2 Cell Culture and Seeding:

To obtain autologous ADSCs, a small amount of belly fat would be harvested from each rat. The tissue would be minced, washed with ammonium chloride to remove red blood cells, incubated in collagenase, and centrifuged. The stromal vascular fraction pellet would be plated in tissue culture flasks and cultured for 2 weeks to propagate the cells. ADSCs would then be seeded into each scaffold at a concentration of $1x10^6$ cells per

scaffold. According to the group, this may or may not include fibrin as a cell carrier. For group 4, cells will be pre-differentiated using several growth factors.

For differentiation of ADSCs to endothelial-like cells, ADSCs would be cultured for 2 weeks in EC differentiation media comprised of DMEM, 2% FBS, and 1% antibiotic solution supplemented with 0.5 ng/mL vascular endothelial growth factor and 20 ng/mL insulin-like growth factor-1. Growth factors would be freshly added to the media at the time of each media change.

For differentiation of ADSC's to fibroblast-like cells, ADSC's were cultured for 2 weeks in fibroblast differentiation media comprised of DMEM, 5% FBS, and 1% antibiotic solution supplemented with 5ng/mL transforming growth factor beta-1. Growth factors would be freshly added to the media at the time of each media change.

Fibrin would be made at a concentration of 0.5U/mL thrombin, 4mg/mL fibrinogen, and 2mM $CaCl_2$. After seeding, these recellularized scaffolds would then be left overnight in media to allow for cellular adhesion.

6.3.2.1.3 Characterization of Explanted Constructs:

After each respective time point has ended, histological evaluation will be utilized. H&E, Masson's Trichrome, Movat's Pentachrome, and DAPI staining will be used to evaluate cellular infiltration and ECM integrity. To evaluate inflammation, CD68 and CD8 expression will be evaluated using IHC. To identify cell types, fibroblast makers HSP-47, prolyl-4-hydroxylase, and vimentin will be used. Smooth muscle markers to be used would be α-SMA, calponin, and SM22. To evaluate macrophage polarization, CD163 will be used as a marker for M2, and iNOS as a marker for M1 macrophages. Proteins will be isolated

from each scaffold and a zymography performed to determine MMP expression. Mechanical testing will also be performed. From the isolated proteins, an ELIZA will be performed to measure TNF-α expression within each group. ROS expression will also be determined for each treatment group to evaluate PGG's role in scavenging it.

We will attempt to evaluate how infiltrating cells migrate into the tissue. A better understanding of this migration within the scaffolds could shed light on a more optimized cell seeding protocol. We would also be interested in seeing how the fibrin affected the cellular infiltration or if it encouraged a larger inflammatory response. How would the host respond to the seeded cells? Another graduate student in our lab found that seeded ADSC's encouraged a lower inflammatory response. How would pre-differentiated cells affect this outcome? How will PGG affect ROS production and will this correlate with TNF-α expression?

6.3.2.1.4 Outcome Success Measures:

A continued resistance to inflammation and a polarization towards the M2 macrophage phenotype for the PGG-treated tissues would indicate success in this study. We are aware that PGG plays a significant role in diminishing inflammation; however, another successful output of this study would be to have a fuller understanding of how PGG acts to discourage these deleterious events. It would also be interesting to see how the ADSC's reacted in vivo. These cells have shown to possess anti-inflammatory properties, to confirm this would also be a success. Another measure of success would be to see how the fibrin seeded constructs handled the host response. Fibrin, as mentioned,

has shown to encourage the pro-healing macrophage phenotype, it would be very positive if this was confirmed, especially with the pre-differentiated cells.

6.3.2.2 Evaluation of Remodeling:

In future in vivo studies, whether sub-dermal or even large animal, remodeling of the implanted scaffold should be further evaluated. In our work, we examined the expression of MMPs to compare degradation between PGG and non-treated sample groups. Remodeling of the scaffold however is also imperative for the success of the scaffold. Revitalization of the scaffold with new collagen could be determined using immunochemistry. After implantation for 4 to 8 weeks, explants would be histologically processed and examined. Stainings could be done for HSP-47 and prolyl-4-hydroxylase as before. The difference for this experiment would be to choose antibodies that are species specific. These antibodies would of course be porcine and the species chosen for the implant group. Identification of new, remodeled collagen from the host's infiltrated cells and original collagen present from the scaffold could be determined. This in vitro remodeling of the matrix is imperative for the success of the construct moving forward.

6.3.3 Aim 3:

It is our continued belief that revitalization of the scaffold with appropriate cell types and then preconditioning these seeded scaffolds in a bioreactor is the best approach towards a tissue engineered mitral valve. The first barrier to this success is finding and optimizing a cell seeding process that allows uniform distribution throughout the scaffold. The niche microstructure that our scaffolds provide ideal conditions for cell differentiation, but are meaningless without a cellular presence. As discussed in Chapter 5, there was

marked improvement in our ability to seed scaffolds with cells, however this could be greatly improved. This lack of completion of cell seeding was evident in the bioreactor experiments when very few cells were found to have migrated into the scaffold. Therefore, future pilot studies should be conducted to see what alternative methods should be attempted to yield a more efficient and practical cell seeding. Practicality and translatability are of course key elements here. Many works in literature reference their uniform cell seeding, however many times the cells were statically seeded on the scaffolds and the cells allowed 6 to 8 weeks to migrate through the tissue. In a clinical setting, this timetable is too long for patients in need of a functioning heart valve.

The following are several suggested pilot studies for cell seeding experiments as well as some suggested studies using the newly design mitral valve bioreactor. From these experiments, hopefully future researchers will be able to efficiently seed our ECM scaffold and precondition the heart valve in the bioreactor. To complete these significant steps would undoubtedly complete the tissue engineering paradigm and provide a novel heart valve to all patients.

6.3.3.1 Cell Seeding Pilot Studies:

As mentioned in Aim 5, significant progress was made in encouraging migration of cells into the scaffold. Our group has found that direct injection of cells into the scaffold provides the best means to force cells into the scaffold's interior. Statically seeding cells onto the exterior has not proven an effective method for cell migration. We believe that the incorporation of the fibrin gel as a cell carrier has been beneficial to the cells. As mentioned

previously, the viscosity of the gel allows for a less stressful injection process for the cells and has been shown to facilitate spreading.

Further pilot studies should be used investigate increasing scaffold porosity to allow for greater ease of transport for cells. There are several ways to do this, however scaffold integrity, an accomplishment for Aim 1, must not be sacrificed too much. Our group has used low concentrations of acetic acid as well as various proteases to provide a less dense interstitial barrier for the cells to pass through. Another method for creating pores is through lyophilization. This process naturally creates pores when completed. This may also offer a clinical translatability benefit in that PGG-treated and lyophilized scaffolds would only need to be rehydrated and seeded. Storage and transportation of these "dry" scaffolds is much more feasible than storing and transporting "wet" sterile scaffolds. Taking advantage of this rehydration step may also allow for greater integration of growth factors and other mechanisms for coaxing cell migration.

Growth factors as well as cytokines should be used in further pilot studies to encourage cells to migrate. Fibrin has been shown to bind growth factors[9,10]. We should use this property to attach growth factors and to evaluate their effects on cell seeding. Cytokines such as SDF-1 have also shown to have drastic effects on cell migration[11–13]. We should use cytokines such as this to encourage movement outside of the injection site.

Pilot studies centering on utilization of fibrin, growth factors and cytokines, and slight alteration of the ECM scaffold could very well lead to an optimized cell seeding. This project's design, and our tissue engineering paradigm rely heavily on complete recellularization of the scaffolds and eventually, preconditioning in a bioreactor.

Also imperative would be the need to recellularize the chordae tendinae. As described above, only pre-differentiated endothelial cells were seeded onto the chordae. However as seen in fresh chordae sections, cells do reside in these collagenous chords. Therefore, an attempt to inject these chordae with cells, and an evaluation of this seeding should be completed. If direct injection of these this small, dense tissue proves difficult, recellularization utilizing chemotaxis may be the next best option.

In the seeding studies addressed above, it was apparent that non-treated scaffolds allowed for better cell seeding throughout the construct. Therefore a better understanding of why this would occur is important to understand. However, due the large amount of beneficial effects PGG provides to the scaffold, elimination of this stabilizing agent should be heavily discouraged. A pilot study can be conducted in which non-treated scaffolds are cell seeding using the methods described in Aim 3. PGG treatment can then be applied similarly to how Isenburg et al. treated their tissues with very low doses of PGG so as not to affect cytotoxicity[14]. The efficiency of the seeding and the effects this low dosage of PGG would have on the construct would need to be heavily investigated as this protocol would greatly vary from the methods of stabilization and cell seeding used previously.

6.3.3.2 Bioreactor Studies and Modifications:

One of the bigger accomplishments for this project was the development of a mitral valve bioreactor. As previously mentioned, an aortic valve bioreactor was already developed by our lab, however the complexity of the mitral apparatus left not only our group, but many other research groups without a proper means to test the mitral valve in sterile, physiological conditions.

In the future, we should design a better mounting mechanism for the papillary muscles. During our bioreactor experiments, the springs, which were used to translate tension through the chordae tendinae to the leaflets, would often cut into the papillary muscles. We should develop a method of holding this papillary muscle and attaching this mounting device to the springs to allow for proper force distribution and valve coaptation. Testing should be done for better placement of these papillary muscles and the corresponding chordae to ensure function.

6.3.3.3 The Mitral Valve Bioreactor as a Pathological Model:

After a more optimized cell seeding process is developed, use of the mitral valve bioreactor does not solely need to be defined as a preconditioner for seeded cells. This novel device could also serve as a means for modeling mitral valve pathologies in vitro. Conditions for mitral valve pathologies could readily be created. For example, after recellularization and endothelialization of the scaffold, the living construct could be placed in the bioreactor with a ruptured chordae tendinae. This common issue in degenerating valves could be easily recreated in vitro in the bioreactor. Histological evaluation of how the cells react to this misguided force distribution could provide some insight into the damage done interstitially during this pathology. Another example might be the altering the shape of the annulus. A rounded annulus, as opposed to its natural saddle shape, would disrupt optimal force distribution and could cause regurgitation. The effects of this on the valve could be evaluated. In addition, not many groups have studied the effects of diabetic conditions on mitral valves. By altering media conditions, calcification may build up in the valve, and development of advanced glycation end products (AGES) may occur.

6.3.3.4 Comparison of Non-Treated and PGG-Treated Preconditioned Constructs:

For a large portion of the studies discussed in this dissertation, PGG and non-treated scaffolds and seeded constructs were compared and contrasted. Therefore, recellularization of a non-treated scaffold and placement of into the bioreactor would present an intriguing comparison to our currently PGG-treated scaffold. Treatment with PGG would be the only aspect of the study design that would defer from previously described bioreactor experiments. Analysis of preconditioned, non-treated valves would provide interesting insight into activation of the seeded cells, matrix remodeling, and the mechanical integrity of the construct post-bioreactor. Comparing the activation of seeded fibroblasts with those of PGG-treated scaffolds would also produce interesting results.

6.3.3.5 Evaluation of PGG's Longevity in Scaffold

Treatment with PGG has had many beneficial effects on our decellularized scaffold and recellularized constructs. However, PGG-does not cross-link with the scaffold and will slowly leave the scaffold over time. Therefore it will be important to understand the longevity in which PGG resides in the scaffold and the effect this has on the scaffolds mechanical properties as well as the effect it has on seeded cells. A Phenol-Ferric Chloride stain can be performed on our paraffin sections at different time points post-bioreactor treatment. Time points of 4, 8 and 12 weeks can be completed in the bioreactor. At each of these points, the sections can be stained for PGG and mechanical properties of the construct and be determined. Activation of seeded cells and their behavior and the presence of PGG will be compared. Ideally, by the time that PGG leaves the construct, remodeling by the

seeded cells will be complete and the construct will no longer need the stabilizing effects of PGG.

6.3.3.6 Considerations for Clinical and Commercial Translation:

Clinical collaborators have alluded that some repair methods may be more feasible for both the patient and the surgeon if a tissue engineered solution were available. Therefore, if a recellularization protocol was optimized for leaflets and even chordae tendinae, these parts of the valve could be used to repair damaged or diseased valves. Living and thus self-healing tissues would provide far more benefit than synthetic leaflets or chordae currently used. Also,, current reparative methods could be utilized for the deployment of these tissue engineered repairs.

6.4 References:

1. Benjamin, E. *et al.* Heart Disease and Stroke Statistics — 2017 Update A Report From the American Heart Association. *Circulation* (2017). doi:10.1161/CIR.0000000000000485
2. Levine, R. A. *et al.* Mitral Valve Disease - Morphology and Mechanisms. *Nat. Publ. Gr.* **12,** 689–710 (2015).
3. Mozaffarian, D. *et al. Heart Disease and Stroke Statistics--2015 Update: A Report From the American Heart Association*. *Circulation* **131,** (2014).
4. Roberts, S. *et al.* Pathogenic mechanisms in rheumatic carditis: focus on valvular endothelium. *J. Infect. Dis.* **183,** 507–511 (2001).
5. Hopkins, R. A. *et al.* Calcium and Phosphorus Concentrations in Native and Decellularized Semilunar Valve Tissues Calcium and Phosphorus Concentrations in Native and Decellularized Semilunar Valve Tissues. (2014).
6. Gotoh, Y. & Cooper, J. A. Reactive Oxygen Species- and Dimerization-induced Activation of Apoptosis Signal-regulating Kinase 1 in Tumor Necrosis Factor- ␣ Signal Transduction *. **273,** 17477–17482 (1998).
7. Levi, R., Barbee, K., Golomb, G., Spijler, K. L. & Systems, H. Effects of radical oxygen species and antioxidants on macrophage polarization. 5–6 (2015).
8. Hsieh, J. Y. *et al.* Differential regulation of macrophage inflammatory activation by fibrin and fibrinogen. *Acta Biomater.* **47,** 14–24 (2017).
9. Martino, M. M., Briquez, P. S., Ranga, A., Lutolf, M. P. & Hubbell, J. a. Heparin-

binding domain of fibrin(ogen) binds growth factors and promotes tissue repair when incorporated within a synthetic matrix. *Proc. Natl. Acad. Sci. U. S. A.* **110,** 4563–8 (2013).
10. Whelan, D., Caplice, N. M. & Clover, A. J. P. Fibrin as a delivery system in wound healing tissue engineering applications. *J. Control. Release* **196,** 1–8 (2014).
11. Rybalko, V. Y. *et al.* Controlled delivery of SDF-1α and IGF-1: CXCR4 $^{+}$ cell recruitment and functional skeletal muscle recovery. *Biomater. Sci.* **3,** 1475–1486 (2015).
12. Rø, T. B. *et al.* HGF and IGF-1 synergize with SDF-1α in promoting migration of myeloma cells by cooperative activation of p21-activated kinase. *Exp. Hematol.* **41,** 646–655 (2013).
13. Marquez-Curtis, L. A. & Janowska-Wieczorek, A. Enhancing the migration ability of mesenchymal stromal cells by targeting the SDF-1/CXCR4 axis. *Biomed Res. Int.* **2013,** (2013).
14. Isenburg, J. C., Simionescu, D. T., Starcher, B. C. & Vyavahare, N. R. Elastin stabilization for treatment of abdominal aortic aneurysms. *Circulation* **115,** 1729–37 (2007).

APPENDICES

Appendix A

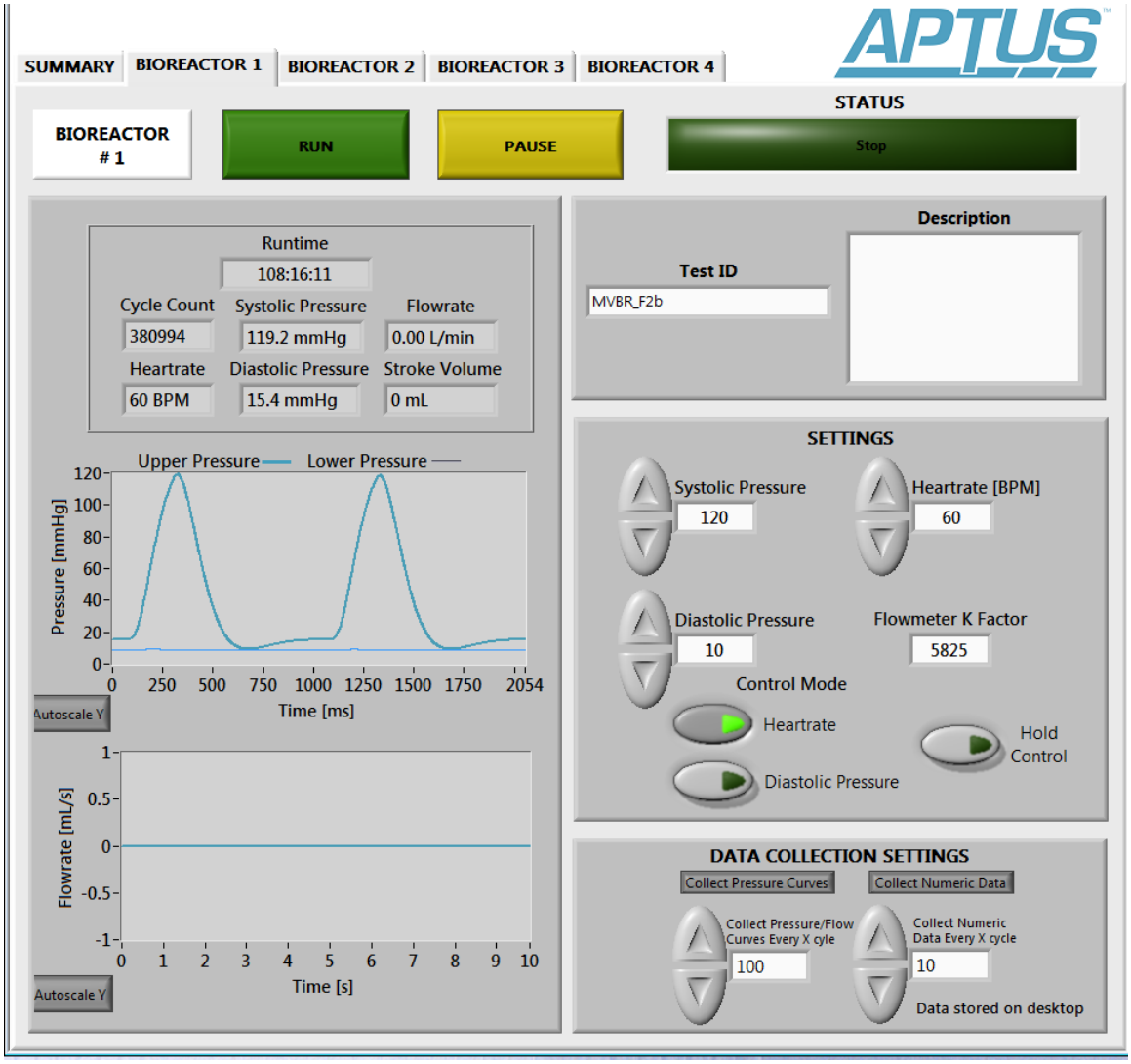

Figure 5.11: Read out for Aptus Bioreactor System. This is the computer read-out provided by the Aptus software. This system allows changing the parameters for pressures, both systolic and diastolic, heartrate, and flow in the settings tab. Pressure and flow outputs are displayed on the left in numerical and graphical format.